SYNTHESIS,CHARACTERIZATION AND NONLINEAR TRANSMISSION STUDIES ON STRONTIUM NANOPARTICLES AND AMINE COATED SILVER NANOPARTICLES

A thesis

Submitted in Partial Fulfillment of the requirements for the award of the Degree of

MASTER OF TECHNOLOGY
IN
NANOSCIENCE & TECHNOLOGY
BY

NARESH SAINI
(ROLL.NO. 0709115)

With the co-operation of
Dr. REJI PHILIP
Associate Professor
RAMAN RESEARCH INSTITUTE
Bangalore

Under the esteemed guidance of

Dr. Neeraj Dilbaghi
Reader
Deptt. Of Bio & Nano Technology
Guru Jambheshwar University of Science &Technology,
Hisar (HARYANA)-125001

DEPARTMENT OF BIO & NANO TECHNOLOGY

GURU JAMBHESHWAR UNIVERSITY OF SCIENCE & TECHNOLOGY

HISAR (HARYANA)-125001

रामन अनुसंधान संस्थान
सी. वी. रामन एवेन्यू, सदाशिवनगर, बेंगलूर - 560 080, भारत
RAMAN RESEARCH INSTITUTE
C. V. Raman Avenue, Sadashivanagar, Bangalore – 560 080, India

Dr. Andal Narayanan
Associate Professor,
LAMP (Light and Matter Physics) Group

June 05, 2009

CERTIFICATE

Certified that the report entitled **'SYNTHESIS, CHARACTERIZATION AND NONLINEAR TRANSMISSION STUDIES ON STRONTIUM NANOPARTICLES AND AMINE COATED SILVER NANOPARTICLES'** is a work carried out by Mr. Naresh Saini using the facilities of the LAMP (Light And Matter Physics) group at the Raman Research Institute, Bangalore during the academic period of January 2009 – June 2009.

Dr. Andal Narayanan.
Coordinator,
LAMP Group,
Raman Research Institute,
Bangalore – 560080.

Phone : Off +91 80 2361 0122, 6547 1500 Fax : 91 80 2361 0492 e-mail : root@rri.res.in

DECLARATION OF THE CANDIDATE

I hereby declare that project entitled "*SYNTHESIS, CHARACTERIZATION AND NONLINEAR TRANSMISSION STUDIES ON STRONTIUM NANOPARTICLES AND AMINE COATED SILVER NANOPARTICLES*" has been carried out at **RAMAN RESEARCH INSTITUTE, BANGLORE** and submitted for the partial fulfillment for the award of degree of M.Tech to **GURU JAMBESHWAR UNIVERSITY OF SCIENCE & TECHNOLOGY (GJU S&T)**. The matter embodied in this report has not been submitted anywhere else for the award of any other degree/diploma.

NARESH SAINI

CERTIFICATE

TO WHOM IT MAY CONCERN

This is to certify that the dissertation entitled "*SYNTHESIS, CHARACTERIZATION AND NONLINEAR TRANSMISSION STUDIES ON STRONTIUM NANOPARTICLES AND AMINE COATED SILVER NANOPARTICLES*" submitted by Mr. Naresh Saini to Guru Jambheshwar University of Science & Technology Hisar, in partial fulfillment of the requirements for the degree of M.Tech, in the subject of Nanoscience & Technology has been approved after an oral examination on the same, in collaboration with an External Examiner.

MAJOR ADVISOR **EXTERNAL EXAMINER**

HEAD OF THE DEAPRTMENT

DEAN, POST-GRADUATE STUDIES

ACKNOWLEDGEMENTS

First and foremost of all, I feel obliged to express my sincere gratitude to Dr. Reji Philip & Ms Sunita Sharma, LAMP Group, RRI, Banglore for giving me an opportunity to carry out this work at Nonlinear and Ultrafast Lab, Raman Research Institute, Bangalore. It is indeed a pleasure to acknowledge my gratitude for his invaluable guidance, support and general discussions.

I gratefully acknowledge to Dr.Andal Narayanan, Associate Professor and Dr. Lakshminarayanan V, Professor, for their valuable help and support.

I am sincerely thankful to Dr.Ravi Subrahmanyan, Director RRI, for providing excellent facilities at this premier Research Institute of India.

I am sincerely grateful to my internal supervisor Dr. Neeraj Dilbaghi, Reader in the Department of Bio & Nanoscience & technology, Guru Jambheshwar University of Science & Technology, Hisar, Haryana for guiding me and helping me in all related problems before and during the project period from such a long part.

I express appreciation to the faculty members of the Department of Bio & Nanotechnology, G.J.University of Science & Technology, Hisar, Haryana. Dr. J.S Rana (Professor &Chairman), for their support and guidance.

Words fall short to express my sense of gratitude to Suchand Sandeep(R.S),Raman Research Institute,Banglore, without whose help and support this project would not have taken this form. A special token of thanks to Sai Krishna(R.S),Jawaharlal Nehru Centre for Advanced Scientific Research,Banglore & Rajkumar Joshi, IIT,Bombay for the valuable suggestions and all those fruitful discussions during my tenure at RRI. I also express a warm note of acknowledgements to Satyam kumar Gupta(R.S),Rakesh Pandey(R.S),Vinita(Assit. Professor) and all others at LAMP group who had been a part of the exciting working environment at the lab. A token of thanks to Tarun Gupta, Kapil Jangra Navneet Singh,Surender Duhan, Simijesh, Laxmi, Sonia, Sunil,Arun, and all those who made my stay at RRI memorable.

And last, but not the least, I express my deep respect and sincere gratitude to my parents for being 'the beacon light' for all the endeavors in my life. I express my note of acknowledgements to my beloved friend Rajesh Dabodhia, who made my life beautiful & give a Motive. Above all, I thank the Almighty GOD, for leading me kindly along the twists and turns of life and for giving me the strength to carry out this work well

Naresh Saini

CONTENTS

CHAPTER-1 INTRODUCTION

1.1 HISTORY OF NANOMATERIALS 1

1.2 FUNDAMENTAL ASPECTS 3

1.3 SIZE CONCERNS 4

1.4 QUANTUM SIZE EFFECT 5

1.5 NANOPARTICLES 6

1.6 CLASSIFICATION OF NANOMATERIALS 6

1.7 METAL NANOPARTICLES 7

1.8 MAGNETIC NANOPARTICLES AND THEIR PROPERTIES 8

1.9 NANOSCALE PROPERTIES AND APPLICATIONS 8

1.9.1 NANOSCALE PROPERTIES: OPTICAL PROPERTIES OF NANOMATERIALS 8

1.9.1.1 APPLICATIONS OF OPTICAL PROPERTES OF NANOMATERIALS 9

1.9.2 NANOSCALE PROPERTIES: MAGNETIC PROPERTIES OF NANOMATERIALS 9

1.9.2.1 APPLICATION OF MAGNETIC PROPERTIES OF NANOMATERIALS 10

1.9.3 ELECTRICAL PROPERTIES OF NANOMATERIALS 10

1.9.3.1 APPLICATIONS OF ELECTRICAL PROPERTIES OF NANOMATERIALS 10

1.9.3.1.1 HIGH ENERGY DENSITY BATTERIES 10

1.9.3.1.2 LARGE ELECTROCHROMIC DISPLAY DEVICES 10

1.9.4 NANOSCALE PROPERTIES: CHEMICAL PROPERTIES OF NANOMATERIALS 11

1.9.4.1APPLICATIONS OF CHEMICAL PROPERTIES OF NANOMATERIALS 11

1.9.5 NANOSCALE PROPERTIES: MECHANICAL PROPERTIES OF NANOMATERIALS 11

1.9.5.1 APPLICATIONS OF MACHANICAL PROPERTIES OF NANOMATERIALS 12

1.9.5.1.1 TOUGHER AND HARDER CUTTING TOOLS 12

1.9.5.1.2 AUTOMOBILES WITH GREATER FUEL EFFICIENCY 12

1.9.5.1.3 AEROSPACE COMPONENTS WITH ENHANCED PERFORMANCE CHARACTERISTICS 12

1.9.5.1.4 DUCTILE CERAMICS 13

1.9.5.1.5 BETTER INSULATION MATERIALS 13
1.10 MATTER-LASER INTERACTION 13
1.10.1 NONLINEAR RESPONSE OF MATTER IN STRONG RADIATION FIELD 13
1.10.2 LASER INTENSITY REGIMES 15
1.10.3 MODERATE ENERGY NONLINEAR EFFECTS 16
1.10.4 OPTICAL FIELD IONIZATION OF ATOMS 17
1.11 OUTLINE OF THE THESIS 21

CHAPTER-2 MATERIALS AND PREPARATION TECHNIQUE OF NANOMATERIALS: WET CHEMICAL ROUTE

2.1 INTRODUCTION 23
2.2 NUCLETION AND GROWTH FROM SOLUTIONS 25
2.3 STABILIZATION OF FINE PARTICLES AGAINST AGGLOMERATION 26
2.4 SOL-GEL METHOD FOR NANOPARTICLE SYNTHESYS 30
2.4.1 HISTORICAL DEVELOPMENT OF SOL-GEL PROCESSING 30
2.4.1.1 ORIGINS 30
2.4.1.2 THE BEGINNING OF SOL-GEL SCIENCE 32
2.4.1.3 THE EXPLOSION OF SOL-GEL TECHNOLOGY 32
2.4.2 INTRODUCTION TO SOL-GEL PROCESS 33
2.4.3 DISCRETE PARTICLES VS NETWORK POLYMER 35
2.4.4 POLYMERIZATION OF METAL ALKOXIDES 37
2.5 SOL-GEL METHOD 38
2.5.1 HYDROLYSIS 38
2.5.1.1 PRECURSOR SUBSTITUENT EFFECTS 40
2.5.1.2 HYDROPHOBIC EFFECTS AND CO-SOLVANTS 40
2.5.1.3 EFFECT OF WATER: ALKOXIDE RATIO (R) 41
2.5.2 CONDENSATION 42
2.5.2.1 PRECURSOR SUBSTITUENT EFFECTS 43
2.5.3 GELATIN 43
2.5.4 AGEING 44

2.5.4.1 CROSS-LINKING AND SYNERESIS 44
2.5.4.2 COARSENING AND RIPENING 44
2.5.4.3 SIGNIFICANCE OF AGEING 45
2.5.5 DRYING 45
2.5.5.1 THE CONSTANT RATE PERIOD 45
2.5.5.2 THE CRITICAL POINT 45
2.5.5.3 CONSEQUENCES OF DRYING 46
2.5.5.4 AVOIDING CRACKING 46
2.5.6 DENSIFICATION 47
2.5.6.1 STAGES OF DENSIFICATION 47
2.6 ADVANTAGES OF SOL-GEL TECHNIQUE 49
2.7 LIMITATIONS OF SOL-GEL TECHNIQUE 50
2.8 ADVANTAGES OF POLYMER COMPONENTS IN SOL-GEL IN SOL GEL CERAMIC 50
2.9 APPLICATIONS 52

CHAPTER-3 NONLINEARITY

3.1 INTRODUCTION 53
3.1.1 LINEAR OPTICS 53
3.1.2 NONLINEAR OPTICS 53
3.2 ORIGIN OF THE TERM NON-LINEAR OPTICS 54
3.2.1 NON-LINEAR POLARIZATION OF THE MEDIUM ALLOWS MIXING OF FREQUENCY 55
3.2.2 PHYSICS OF NONLINEAR LIGHT TRANSMISSION 56
3.3 SECOND AND THIRD ORDER NONLINEAR POLARIZATION 56
3.4 NONLINEAR ABSORPTION 57
3.4.1 TWO-PHOTON ABSORPTION 57
3.4.2 THREE-PHOTON ABSORPTION 58
3.5 NONLINEAR MEASUREMENTS- Z SCAN TECHNIQUE 59

3.5.1 OPEN APERTURE Z-SCAN SETUP 59
3.6 APPLICATION OF NONLINEARITY: OPTICAL LIMITING 60
3.6.1 INTRODUCTION 60
3.6.2 PASSIVE OPTICAL LIMIT
3.6.2.1 TWO PHOTON ABSORPTION 60
3.6.2.2 REVERSE SATURABLE ABSORPTION 61
3.6.2.3 FREE CARRIER ABSORPTION 61
3.6.2.4 NONLINEAR REFRACTION 61
3.6.2.5 INDUCED SCATTERING 61
3.6.3 APPLICATION OF OPTICAL LIMITERS 62

CHAPTER-4 SAMPLE CHARACTERIZATION 63

4.1 ATOMIC FORCE MICROSCOPY 63
4.1.1 BASIC PRINCIPLE 64
4.1.2 IMAGING MODES 65
4.1.2.1 TRAPPING MODE 66
4.2.1.2 NON-CONTACT MODE 67
4.1.3 AFM -BEAM DEFLECTION DETECTION 67
4.1.4 FORCE SPECTROSCOPY 68
4.1.5 IDENTIFICATION OF INDIVIDUAL SURFACE ATOMS 68
4.1.6 PIEZOELECTRIC SCANNERS 68
4.1.7 ADVANTAGES AND DISADVANTAGES 70
4.2 SCANNING ELECTRON MICROSCOPE (SEM) 71
4.2.1 SCANNING PROCESS AND IMAGE FORMATION 72
4.2.2 MAGNIFICATION 73
4.2.3 SAMPLE PREPARATION: 74
4.2.4 BIOLOGICAL SAMPLES 75
4.2.5 MATERIALS 77
4.2.5.1 SPUTTER COATER: 77
4.3 FOURIER INFRARED SPECTROSCOPY 78

4.3.1 PRINCIPLE 78
4.3.2 SAMPLE PREPARATION 78
4.4 Z- SCAN MEASURMENT 79
4.4.1 EXPERIMENTAL SETUP 79
4.4.2 CLOSED APERTURE Z-SCAN 80
4.4.3 WORKING 80
4.4.4 OPEN APERTURE Z-SCAN 81
4.4.5: CURVE FITTING EQUATION 83
4.4.6 FLUENCE CALCULATION 84
4.5 X-RAY DIFFRACTION 84
4.5.1 PRINCIPLE 84
4.5.2 POWDER AND SMALL ANGLE X-RAY DIFFRACTION 85
4.5.3 GRAPH 85
4.6 UV- VISIBLE SPECTROMETER 85

CHAPTER-5 EXPERIMENTAL PROCEDURE 85

INTRODUCTION (PART A) 88
5.1 STRONTIUM
5.2 CHARACTERISTICS 88
5.3 SAMPLE PREPARATION OF STRONTIUM FERRITE 90

INTRODUCTION (PART- B) 91
5.4 SILVER 91

5.5 CHARACTERISTICS 91
5.6 APPLICATIONS 92
5.6.1 PRECIOUS METAL 92
5.6.2 DENTISTRY 93
5.6.3 PHOTOGRAPHY AND ELECTRONICS 93
5.6.4 SOLDER AND BRAZING 94
5.6.5 MIRRORS AND OPTICS 94
5.6.6 NUCLEAR REACTORS 94
5.6.7 CATALYST 94
5.6.8 MEDICINE 95
5.6.9 MEDICATION 96
5.6.10 FOOD 96
5.6.11 CLOTHING 96
5.7 Ag NPs 97
5.8 SAMPLE PREPARATION FOR Ag NANOPARTICLE 98

CHAPTER 6 RESULTS AND DISCUSSION 100

6.1 AFM STUDIES ON AMINE COATED AG NANOPARTICLES 100
6.2 SEM STUDIES FOR $SrFe_{12}O_{19}$ 101
6.3 FTIR ANALYSIS FOR Ag 104
6.4 FTIR ANALYSIS FOR $SRFe_{12}O_{19}$ 105
6.5 UV-VIS ABSORPTION MEASUREMENTS OF AG NANOPARTICLES 108
6.6 UV-VIS ABSORPTION MEASUREMENTS OF STRONTIUM NANOPARTICLES 109
6.7 NONLINEAR OPTICAL PROPERTIES 112
6.8 CONCLUSIONS 117

REFERENCES

Preface

Over the past decade, nanomaterials have been the subject of enormous interest. These materials, notable for their extremely small feature size, have the potential for wide-ranging industrial, biomedical, and electronic applications. As a result of recent improvement in technologies to see and manipulate these materials, the nanomaterials field has seen a huge increase in funding from private enterprises and government, and academic researchers within the field have formed many partnerships.Nanomaterials can be metals, ceramics, polymeric materials, or composite materials. Their defining characteristic is a very small feature size in the range of 1-100 nanometers (nm). The unit of nanometer derives its prefix nano from a Greek word meaning dwarf or extremely small. One nanometer spans 3-5 atoms lined up in a row. By comparison, the diameter of a human hair is about 5 orders of magnitude larger than a nanoscale particle. Nanomaterials are not simply another step in miniaturization, but a different arena entirely; the nanoworld lies midway between the scale of atomic and quantum phenomena, and the scale of bulk materials. At the nanomaterial level, some material properties are affected by the laws of atomic physics, rather than behaving as traditional bulk materials do.Although widespread interest in nanomaterials is recent, the concept was raised over 40 years ago. Physicist Richard Feynman delivered a talk in 1959 entitled *"There's Plenty of Room at the Bottom"*, in which he commented that there were no fundamental physical reasons that materials could not be fabricated by maneuvering individual atoms. Nanomaterials have actually been produced and used by humans for hundreds of years - the beautiful ruby red color of some glass is due to gold nanoparticles trapped in the glass matrix. The decorative glaze known as luster, found on some medieval pottery, contains metallic spherical nanoparticles dispersed in a complex way in the glaze, which give rise to its special optical properties. The techniques used to produce these materials were considered trade secrets at the time, and are not wholly understood even now.Development of nanotechnology has been spurred by refinement of tools to see the nanoworld, such as more sophisticated electron microscopy and scanning tunneling microscopy. By 1990, scientists at IBM had managed to position individual xenon atoms on a nickel surface to spell out the company logo, using scanning tunneling microscopy probes, as a demonstration of the extraordinary new technology being developed. In the mid-1980s a new class of

material - hollow carbon spheres - was discovered. These spheres were called buckyballs or fullerenes, in honor of architect and futurist Buckminster Fuller, who designed a geodesic dome with geometry similar to that found on the molecular level in fullerenes. The C_{60} (60 carbon atoms chemically bonded together in a ball-shaped molecule) buckyballs inspired research that led to fabrication of carbon nanofibers, with diameters under 100 nm. In 1991 S. Iijima of NEC in Japan reported the first observation of carbon nanotubes, which are now produced by a number of companies in commercial quantities. The world market for nanocomposites (one of many types of nanomaterials) grew to millions of pounds by 1999 and is still growing fast.The variety of nanomaterials is great, and their range of properties and possible applications appear to be enormous, from extraordinarily tiny electronic devices, including miniature batteries, to biomedical uses, and as packaging films, superabsorbants, components of armor, and parts of automobiles.What makes these nanomaterials so different and so intriguing? Their extremely small feature size is of the same scale as the critical size for physical phenomena - for example, the radius of the tip of a crack in a material may be in the range 1-100 nm. The way a crack grows in a larger-scale, bulk material is likely to be different from crack propagation in a nanomaterial where crack and particle size are comparable. Fundamental electronic, magnetic, optical, chemical, and biological processes are also different at this level. Where proteins are 10-1000 nm in size, and cell walls 1-100 nm thick, their behavior on encountering a nanomaterial may be quite different from that seen in relation to larger-scale materials. Nanocapsules and nanodevices may present new possibilities for drug delivery, gene therapy, and medical diagnostics.Surfaces and interfaces are also important in explaining nanomaterial behavior. In bulk materials, only a relatively small percentage of atoms will be at or near a surface or interface (like a crystal grain boundary). In nanomaterials, the small feature size ensures that many atoms, perhaps half or more in some cases, will be near interfaces. Surface properties such as energy levels, electronic structure, and reactivity can be quite different from interior states, and give rise to quite different material properties.It is not so amazing, then, that government bodies, companies, and university researchers are joining forces or competing to synthesize, investigate, produce, and apply these amazing nanomaterial .

CHAPTER-1

INTRODUCTION

1.1 HISTORY OF NANOMATERIALS

Although generally nanoparticles are considered an invention of modern science, they actually have a very long history. Specifically, nanoparticles were used by artisans as far back as the 9th century in Mesopotamia for generating a glittering effect on the surface of pots. Even these days pottery from the Middle Ages and Renaissance often retain a distinct gold or copper colored metallic glitter. This so called lustre is caused by a metallic film that was applied to the transparent surface of a glazing. The lustre can still be visible if the film has resisted atmospheric oxidation and other weathering. The lustre originates within the film itself, which contains silver and copper nanoparticles, dispersed homogeneously in the glassy matrix of the ceramic glaze. These nanoparticles were created by the artisans by adding copper and silver salts and oxides together with vinegar, ochre, and clay, on the surface of previously-glazed pottery. The object was then placed to a kiln and heated to about 600 °C in a reducing atmosphere. In the heat the glaze would soften, causing the copper and silver ions to migrate into the outer layers of the glaze. There the reducing atmosphere reduced the ions back to metals, which then came together forming the nanoparticles that give the colour and optical effects. Lustre technique shows that craftsmen had a rather sophisticated empirical knowledge of materials. The technique originated in the islamic world. As Muslims were not allowed to use gold in artistic representations, they had to find a way to create a similar effect without using real gold. The solution they found was using lustre.

Michael Faraday provided the first description, in scientific terms, of the optical properties of nanometer-scale metals in his classic 1857 paper "Experimental relations of gold (and other metals) to light". Several techniques were used to characterize the chemical and physical properties of these lustre, such as Rutherford Backscattering Spectrometry (RBS), optical absorption in the visible-ultraviolet region, electron microscopy (TEM and SEM etc. Nanoparticles are of great scientific interest as they are effectively a bridge between bulk materials and atomic or molecular structures. A bulk material should have constant physical properties regardless of its size, but at the nano-

scale this is often not the case. Size-dependent properties are observed such as quantum confinement in semiconductor particles, surface plasmon resonance in some metal particles and superparamagnetism in magnetic materials. The properties of materials change as their size approaches the nanoscale and as the percentage of atoms at the surface of a material becomes significant. For bulk materials larger than one micrometer, the percentage of atoms at the surface is minuscule relative to the total number of atoms of the material. The interesting and sometimes unexpected properties of nanoparticles are partly due to the aspects of the surface of the material dominating the properties in lieu of the bulk properties. Nanoparticles exhibit a number of special properties relative to bulk material. For example, the bending of bulk copper (wire, ribbon, etc.) occurs with movement of copper atoms/clusters at about the 50 nm scale. Copper nanoparticles smaller than 50 nm are considered super hard materials that do not exhibit the same malleability and ductility as bulk copper. The change in properties is not always desirable. Ferroelectric materials smaller than 10 nm can switch their magnetisation direction using room temperature thermal energy, thus making them useless for memory storage.

Suspensions of nanoparticles are possible because the interaction of the particle surface with the solvent is strong enough to overcome differences in density, which usually result in a material either sinking or floating in a liquid. Nanoparticles often have unexpected visible properties because they are small enough to confine their electrons and produce quantum effects. For example gold nanoparticles appear deep red to black in solution, depending on their size. Nanoparticles have a very high surface area to volume ratio. This provides a tremendous driving force for diffusion, especially at elevated temperatures. Sintering can take place at lower temperatures, over shorter time scales than for larger particles. This theoretically does not affect the density of the final product, though flow difficulties and the tendency of nanoparticles to agglomerate complicates matters. The large surface area to volume ratio also reduces the incipient melting temperature of nanoparticles. Moreover nanoparticles have been found to impart some extra properties to various day to day products, like the presence of titanium dioxide nanoparticles impart what we call as the self-cleaning effect, and the size being in the nanorange, the particles can't be seen with naked eyes. Nano Zinc Oxide particles have

been found to have superior UV blocking properties compared to its bulk substitute. This is one of the reasons why it is often used in the sunscreen lotions. Clay nanoparticles when incorporated into polymer matrices increase re-inforcement, leading to stronger plastics, verified by a higher glass transition temperature and other mechanical property tests. These nanoparticles are hard, and impart their properties to the polymer (plastic). Nanoparticles have also been attached to textile fibers in order to create smart and functional clothing.

To summerise, *nanomaterials* are materials with morphological features smaller than a one tenth of a micrometre in at least one dimension. Despite the fact that there is no consensus upon the minimum or maximum size of nanomaterials, with some authors restricting their size to as low as 1 to ~30 nm, a logical definition would situate the nanoscale between microscale (0.1 micrometre) and atomic/molecular scale (about 0.2 nanometers).

1.2 FUNDAMENTAL ASPECTS

An aspect of nanotechnology is the vastly increased ratio of surface area to volume present in many nanoscale materials, which makes possible new quantum mechanical effects, for example the "quantum size effect" where the electronic properties of solids are altered with great reductions in particle size. This effect does not come into play by going from macro to micro dimensions. However, it becomes pronounced when the nanometer size range is reached. A certain number of physical properties also alter with the change from macroscopic systems. Novel mechanical properties of nanomaterials are a subject of nanomechanics research. Catalytic activities also reveal new behaviour in the interaction with biomaterials. Nanotechnology can be thought of as extensions of traditional disciplines towards the explicit consideration of these properties. Additionally, traditional disciplines can be re-interpreted as specific applications of nanotechnology. This dynamic reciprocation of ideas and concepts contributes to the modern understanding of the field. Broadly speaking, nanotechnology is the synthesis and application of ideas from science and engineering towards the understanding and production of novel materials and devices. These products generally make copious use of physical properties associated with small scales. As mentioned above, materials reduced to the nanoscale can suddenly show very different properties compared to what they

exhibit on a macroscale, enabling unique applications. For instance, opaque substances become transparent (copper); inert materials attain catalytic properties (platinum); stable materials turn combustible (aluminum); solids turn into liquids at room temperature (gold); insulators become conductors (silicon). Materials such as gold, which is chemically inert at normal scales, can serve as a potent chemical catalyst at nanoscales. Much of the fascination with nanotechnology stems from these unique quantum and surface phenomena that matter exhibits at the nanoscale. Nanosize powder particles (a few nanometres in diameter, also called nanoparticles) are potentially important in ceramics, powder metallurgy and similar applications. The strong tendency of small particles to form clumps ("agglomerates") is a serious technological problem that impedes such applications. However, a number of dispersants such as ammonium citrate (aqueous) and imidazoline or oleyl alcohol (nonaqueous) are promising solutions as possible additives for deagglomeration.

1.3 SIZE CONCERNS

Another concern is that the volume of an object decreases as the third power of its linear dimensions, but the surface area only decreases as its second power. This somewhat subtle and unavoidable principle has huge ramifications. For example the power of a drill (or any other machine) is proportional to the volume, while the friction of the drill's bearings and gears is proportional to their surface area. For a normal-sized drill, the power of the device is enough to handily overcome any friction. However, scaling its length down by a factor of 1000, for example, decreases its power by 1000^3 (a factor of a billion) while reducing the friction by only 1000^2 (a factor of "only" a million). Proportionally it has 1000 times less power per unit friction than the original drill. If the original friction-to-power ratio was, say, 1%, that implies the smaller drill will have 10 times as much friction as power. The drill is useless.

For this reason, while super-miniature electronic integrated circuits are fully functional, the same technology cannot be used to make working mechanical devices beyond the scales where frictional forces start to exceed the available power. So even though you may see microphotographs of delicately etched silicon gears, such devices are currently little more than curiosities with limited real world applications, for example in

moving mirrors and shutters. Surface tension increases in much the same way, thus magnifying the tendency for very small objects to stick together.

This could possibly make any kind of "micro factory" impractical: even if robotic arms and hands could be scaled down, anything they pick up will tend to be impossible to put down. The above being said, molecular evolution has resulted in working cilia, flagella, muscle fibers and rotary motors in aqueous environments, all on the nanoscale. These machines exploit the increased frictional forces found at the micro or nanoscale. Unlike a paddle or a propeller, which depends on normal frictional forces (the frictional forces perpendicular to the surface) to achieve propulsion, cilia develop motion from the exaggerated drag or laminar forces (frictional forces parallel to the surface) present at micro and nano dimensions. To build meaningful "machines" at the nanoscale, the relevant forces need to be considered. We are faced with the development and design of intrinsically pertinent machines rather than the simple reproductions of macroscopic ones. All scaling issues therefore need to be assessed thoroughly when evaluating nanotechnology for practical applications.

1.4 QUANTUM SIZE EFFECT

As a result of geometrical constraint, the electron feels the presence of the particle boundaries and responds to the changes in particle size by adjusting its energy levels. This phenomenon is called quantum confinement. The quantum confinement leads to the collapse of the continuous energy band of bulk material into discrete atomic like energy levels this discrete structure of energy states leads to a discrete absorption spectrum of quantum dots which is in contrast to continuous absorption spectrum of bulk semiconductor.

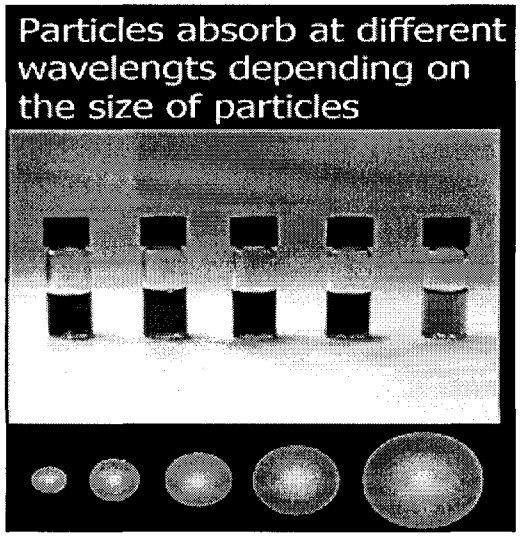

Fig 1.1 Particles absorb at different wavelengths depending on the size of particles

Changing the geometry of the surface of quantum dots changes the band gap energy. In case of small sized quantum dots the band gap will be energetically larger. So, we refer such a quantum dot to be blue shifted reflecting the fact that electron should fall to a greater distance in terms of energy thus producing a radiation of shorter wavelength. But, in case of larger sized quantum dots they are red shifted. Quantum dots of same material but different size have different band gap, which absorbs and emits different frequencies. Thus the material property changes dramatically because of quantum sized effect.

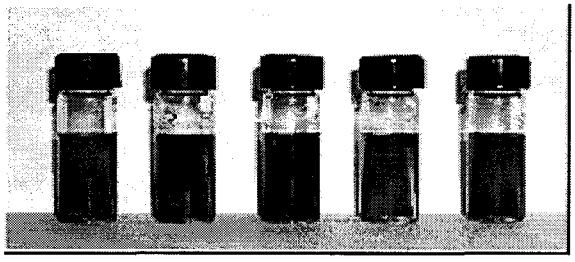

Fig 1.2 Same material of different nano size emits different colors

1.5 Nanoparticles

In nanotechnology, a particle is defined as a small object that behaves as a whole unit in terms of its transport and properties. It is further classified according to size: In terms of diameter, fine particles cover a range between 100 and 2500 nanometers, while

ultrafine particles, on the other hand, are sized between 1 and 100 nanometers. Similarly to ultrafine particles, nanoparticles are sized between 1 and 100 nanometers, though the size limitation can be restricted to two dimensions. Nanoparticles may or may not exhibit size-related properties that differ significantly from those observed in fine particles or bulk materials. Nanoclusters have at least one dimension between 1 and 10 nanometers and a narrow size distribution. Nanopowders are agglomerates of ultrafine particles, nanoparticles, or nanoclusters. Nanometer sized single crystals, or single-domain ultrafine particles, are often referred to as nanocrystals. The term NanoCrystal is a registered trademark of Elan Pharma International (EPIL) used in relation to EPIL's proprietary milling process and nanoparticulate drug formulations. Nanoparticle research is currently an area of intense scientific research, due to a wide variety of potential applications in biomedical, optical, and electronic fields.

1.6 CLASSIFICATION OF NANOMATERIALS

For the purpose of this article, most current nanomaterials could be organized into four types.

1. Carbon Based Materials
2. Metal Based Materials
3. Dendrimers
4. Composites

Carbon Based Materials: These nanomaterials are composed mostly of carbon, most commonly taking the form of hollow spheres, ellipsoids, or tubes. Spherical and ellipsoidal carbon nanomaterials are referred to as fullerenes, while cylindrical ones are called nanotubes. These particles have many potential applications, including improved films and coatings, stronger and lighter materials, and applications in electronics.

Metal Based Material: These nanomaterials include quantum dots, nano gold, nano silver and metal oxides, such as titanium dioxide. A quantum dot is a closely packed semiconductor crystal comprised of hundreds or thousands of atoms, and whose size is on the order of a few nanometers to a few hundred nanometers. Changing the size of quantum dots changes their optical properties.

Dendrimers: These nanomaterials are nanosized polymers built from branched units. The surface of a dendrimer has numerous chain ends, which can be tailored to perform

specific chemical functions. This property could also be useful for catalysis. Also, because three-dimensional dendrimers contain interior cavities into which other molecules could be placed, they may be useful for drug delivery.

Composites: Composites combine nanoparticles with other nanoparticles or with larger, bulk-type materials. Nanoparticles, such as nanosized clays, are already being added to products ranging from auto parts to packaging materials, to enhance mechanical, thermal, barrier, and flame-retardant properties.

1.7 METAL NANOPARTICLES

Metal nanoparticles are of great interest for researchers from a broad spectrum of disciplines including biotechnology, medicine data storage, catalysis, environmental preservation and improvement. Their application comes about because one of its dimension typically is in the range 4-20 nm which invokes many novel properties that helps in the various fields. Scientists, for the past decades, have been trying to synthesize them and study them and find out applications for them and the area is still in the pioneering stage. However most of syntheses are not easy and have many obstacles in a stable and working nanoparticles. Many of them are still very difficult to prepare in terms of requirement of unsafe chemicals, or advanced and expensive processes and still many of them are underway of alternatives that are easier and economical. Furthermore, they also require to be stable for longer periods as many of them tend to form agglomerates, increasing in size within weeks or even hours. For this many of them are protected by a cover using inorganic or organic molecules or polymers which form the surfactants to prevent it to crumble together. The dramatical increase in surface atoms to total atoms ratio of such nanoparticles are of particular interest. As the size of the particle decreases, the number of atoms at the surface decreases but the bulk atoms decrease by a far more than in the proportion of the ratio. This property is one of the fundamental factors for elevating a catalyst's performance.

1.8 MAGNETIC NANOPARTICLES AND THEIR PROPERTIES

Magnetic nanoparticles are a class of nanoparticles, which can be manipulated using a magnetic field. Such particles commonly consist of magnetic elements such as iron, nickel and cobalt and their chemical compounds. These particles have been the focus of much research recently because they possess attractive properties which could

see potential use in catalysis, biomedicine, magnetic resonance imaging, data storage and environmental remediation. The physical and chemical properties of magnetic nanoparticles largely depend on the synthesis method and chemical structure. In most cases, the particles range from 1 to 100 nm in size, and display super paramagnetism.

1.9 NANOSCALE PROPERTIES AND APPLICATIONS

1.9.1 NANOSCALE PROPERTIES: OPTICAL PROPERTIES OF NANOMATERIALS

Nanocrystalline systems have attracted much interest for their novel optical properties, which differ remarkably from bulk crystals. Key contributory factors include quantum confinement of electrical carriers within nanoparticles, efficient energy and charge transfer over nanoscale distances and in many systems a highly enhanced role of interfaces. With the growing technology of these materials, it is increasingly necessary to understand the detailed basis for nanophotonic properties. The linear and nonlinear optical properties of such materials can be finely tailored by controlling the crystal dimensions, and the chemistry of their surfaces, fabrication technology becomes a key factor for the applications Surface Plasmons (SP) are the origin of the color of nanomaterials. A surface plasmon is a natural oscillation of the electron gas inside a given nanosphere. If the sphere is small compared to a wavelength of light, and the light has a frequency close to that of the SP, then the SP will absorb energy. The frequency of the SP depends on the dielectric function of the nanomaterial, and the shape of the nanoparticle.

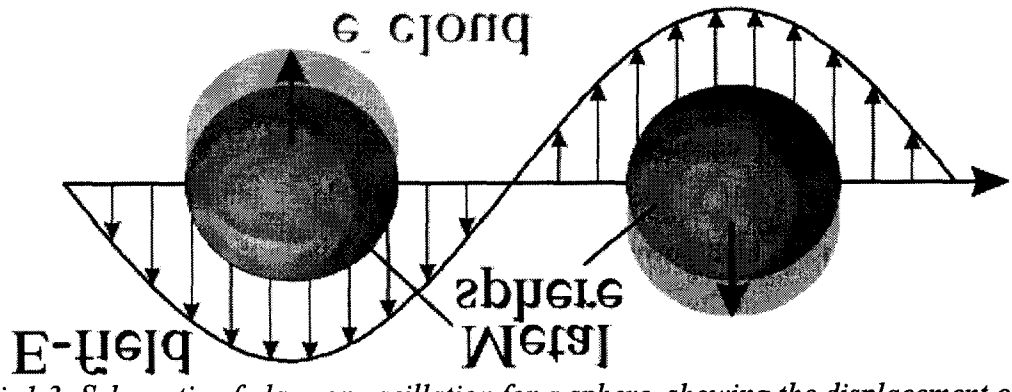

Fig1.3: Schematic of plasmon oscillation for a sphere, showing the displacement of the conduction electron charge cloud relative to the nuclei.

For a gold spherical particle, the frequency is about 0.58 of the bulk plasma frequency. Thus, although the bulk plasma frequency is in the UV, the SP frequency is in the visible (close to 520 nm). Suppose we have a suspension of nanoparticles in a host. If a wave of light is applied, the local electric field may be hugely enhanced near an SP resonance. If so, one expects various nonlinear susceptibilities, which depend on higher powers of the electric field, to be enhanced even more.

1.9.1.1 APPLICATIONS OF OPTICAL PROPERTES OF NANOMATERIALS

Glues containing nanoparticles have optical properties that give rise to uses in optoelectronics. Casings, containing nanoparticles used in electronic devices, such as computers, offer improved shielding against electromagnetic interference. Electrochromic, devices are similar to liquid-crystal displays (LCD), are been developed with nanomaterials. The incorporation of nanomaterials in surface coatings can provide long-term abrasion resistance without significantly effecting optical clarity, gloss, color or physical properties.

1.9.2 NANOSCALE PROPERTIES: MAGNETIC PROPERTIES OF NANOMATERIALS

The strength of a magnet is measured in terms of coercivity and saturation magnetization values. These values increase with a decrease in the grain size and an increase in the specific surface area (surface area per unit volume) of the grains. Therefore nanomaterials present also good properties in this field.

1.9.2.1 APPLICATION OF MAGNETIC PROPERTIES OF NANOMATERIALS

Magnets made of nanocrystalline yttrium-samarium-cobalt grains possess very unusual magnetic properties due to their extremely large surface area. Typical applications for these high-power rare-earth magnets include quieter submarines, automobile alternators, land-based power generators, and motors for ships, ultra-sensitive analytical instruments, and magnetic resonance imaging (MRI) in medical diagnostics.

1.9.3 ELECTRICAL PROPERTIES OF NANOMATERIALS

Nanomaterials can hold considerably more energy than conventional because of their large grain boundary (surface) area. They are materials in which an optical absorption band can be introduced, or an existing band can be altered by the passage of current through these materials, or by the application of an electric field.

1.9.3.1 APPLICATIONS OF ELECTRICAL PROPERTIES OF NANOMATERIALS

1.9.3.1.1 HIGH ENERGY DENSITY BATTERIES

Conventional and rechargeable batteries are used in almost all applications that require electric power. The energy density (storage capacity) of these batteries is quite low requiring frequent recharging. Nanocrystalline materials are good candidates for separator plates in batteries because they can hold considerably more energy than conventional ones. Nickel-metal hydride batteries made of nanocrystalline nickel and metal hydrides are envisioned to require far less frequent recharging and to last much longer.

1.9.3.1.2 LARGE ELECTROCHROMIC DISPLAY DEVICES

An electrochromic device consists of materials in which an optical absorption band can be introduced, or an existing band can be altered by the passage of current through the materials, or by the application of an electric field. They are similar to liquid-crystal displays (LCD) commonly used in calculators and watches and are primarily used in public billboards and ticker boards to convey information. The resolution, brightness, and contrast of these devices depend on the tungstic acid gel's grain size. Hence, nanomaterials, such as tungstic oxide gel, are being explored for this purpose.

1.9.4 NANOSCALE PROPERTIES: CHEMICAL PROPERTIES OF NANOMATERIALS

One of the important factors for the chemical applications of nanomaterials is the increment of their surface area, which increases the chemical activity of the material.

1.9.4.1APPLICATIONS OF CHEMICAL PROPERTIES OF NANOMATERIALS

Due to their enhanced chemical activity, nanostructural materials can be used as catalysts to react with such noxious and toxic gases as carbon monoxide and nitrogen

oxide in automobile catalytic converters and power generation equipment to prevent environmental pollution arising from burning gasoline and coal. Fuel cell technology is another important application of the noble metal nanoparticles relating the catalysis of the reactions. In the present, the fuel cell catalysts are based on platinum group metals (PGM). Pt and Pt-Ru alloys are some of the most frequently used catalysts from this group. In fact, the use of these metals is one major factor for cell costs, which has been one of the major drawbacks preventing it from growing into a more important technology. One possibility to produce economical catalysts is the use of bimetallic nanoparticles.

1.9.5 NANOSCALE PROPERTIES: MECHANICAL PROPERTIES OF NANOMATERIALS

Scientific challenges in nanoscience and nanotechnology include the development of nanomaterials with novel mechanical properties. The need for scratch, and abrasion resistance is well established in various markets, including fingernail polishes, flooring, plastic glazing, headlamp covers and other automotive parts, transportation windows and optical lenses, where clear scratch-resistant coatings are used. Because the nanosize, many of their mechanical properties of the materials is modified, among others, hardness and elastic modulus, fracture toughness, scratch resistance, fatigue strength, and hardness. Energy dissipation, mechanical coupling within arrays of components, and mechanical nonlinearities are influenced by structuring components at the nanometer scale. This includes also the interpretation of unusual mechanical behavior (e.g., strengths approaching the theoretical limit) and the exploration of new ways to integrate diverse classes of mechanically functional materials on the nano-size.

1.9.5.1 APPLICATIONS OF MACHANICAL PROPERTIES OF NANOMATERIALS

1.9.5.1.1 TOUGHER AND HARDER CUTTING TOOLS

Cutting tools made of nanomaterials, such as tungsten carbide, tantalum carbide, and titanium carbide, are much harder, much more wear-resistant, erosion-resistant, and last longer than their conventional (large-grained) counterparts. Also, for the miniaturization of microelectronic circuits, the industry needs micro drills (drill bits with

diameter less than the thickness of an average human hair or 100 μm) with enhanced edge retention and far better wear resistance. Since nanocrystalline carbides are much stronger, harder, and wear-resistant, they are currently being used in these micro drill.

1.9.5.1.2 AUTOMOBILES WITH GREATER FUEL EFFICIENCY

In automobiles, since nanomaterials are stronger, harder, and much more wear-resistant and erosion-resistant, they are envisioned to be used in spark plugs. Also, automobiles waste significant amounts of energy by losing the thermal energy generated by the engine. So, the engine cylinders are envisioned to be coated with nanocrystalline ceramics, such as zirconia and alumina, which retain heat much more efficiently that result in complete and efficient combustion of the fuel.

1.9.5.1.3 AEROSPACE COMPONENTS WITH ENHANCED PERFORMANCE CHARACTERISTICS

One of the key properties required of the aircraft components is the fatigue strength, which decreases with the component's age. The fatigue strength increases with a reduction in the grain size of the material. Nanomaterials provide such a significant reduction in the grain size over conventional materials that the fatigue life is increased by an average of 200-300%. In spacecrafts, elevated-temperature strength of the material is crucial because the components (such as rocket engines, thrusters, and vectoring nozzles) operate at much higher temperatures than aircrafts and higher speeds. Nanomaterials are perfect candidates for spacecraft applications, as well.

1.9.5.1.4 DUCTILE CERAMICS

Ceramics are very hard, brittle, and hard to machine even at high temperatures. However, with a reduction in grain size, their properties change drastically. Nanocrystalline ceramics can be pressed and sintered into various shapes at significantly lower temperatures. Zirconia, for example, is a hard, brittle ceramic, has even been rendered superplastic, i. e., it can deformed to great lengths (up to 300% of its original length). However, these ceramics must possess nanocrystalline grains to be superplastic. Ceramics based on silicon nitride (Si3N4) and silicon carbide (SiC), have been used in automotive applications as high-strength springs, ball bearings, and valve lifters, and because they possess good formability and machinabilty combined with excellent

physical, chemical, and mechanical properties. They are also used as components in high-temperature furnaces.

1.9.5.1.5 BETTER INSULATION MATERIALS

Aerogels are nanocrystalline porous and extremely lightweight materials and can withstand 100 times their weight. They are currently being used for insulation in offices, homes, etc. They are also being used as materials for "smart" windows, which darken when the sun is too bright and they lighten themselves otherwise.

1.10 MATTER-LASER INTERACTION

1.10.1 NONLINEAR RESPONSE OF MATTER IN STRONG RADIATION FIELD

Study of phenomena that occur due to the modification of the optical properties of a material by the presence of an optical field is termed as nonlinear optics. They are '*nonlinear*' in the sense that they occur when the response of the material to the applied optical field depends in a nonlinear manner upon the strength of the electric field. A laser is a typical source that is strong enough to induce nonlinear phenomena in even weakly nonlinear materials. The electric polarization (dipole moment per unit volume) plays a key role in the description of nonlinear optical phenomena, as the time varying polarization can act as a source of new components of the electromagnetic field. Hence the optical response of a material is generally expressed in terms of the polarization, given as a power series in the applied electric field as,

$$\widetilde{P}(t) = \varepsilon_0\left[\chi^{(1)}\widetilde{E}(t) + \chi^{(2)}\widetilde{E}^2(t) + \chi^{(3)}\widetilde{E}^3(t) + \ldots\ldots\ldots\ldots\right]$$

where the tilde denote a quantity that rapidly varies with time. $\chi^{(1)}$ is the linear susceptibility of the material, and $\chi^{(2)}$ and $\chi^{(3)}$ represent the second and third order nonlinear susceptibilities of the material respectively. This expression is valid for a lossless and dispersionless medium. Here the fields have been taken as scalar for simplicity [Boyd, R.W.]. It is implicit in the above expression that the atomic polarization follows the changes of the driving electric field instantaneously. This relation between the material response and the applied optical field will break down under conditions like '*resonant excitation*' of the system [Boyd, R.W.], and in the presence of a '*super intense laser field*', where the applied laser field becomes comparable to the characteristic atomic

field strength. Depending on the initial and final quantum states of the system, the nonlinear optical processes can be categorized as *parametric* and *nonparametric* processes. In parametric processes such as Sum and Difference Frequency Generation, Second Harmonic Generation, Optical Parametric Oscillation etc. the initial and final quantum mechanical states of the system are identical. Or in other words, the population from the ground state can be removed only for a very shot interval in which the system exists in a *virtual level*, which is not an energy eigenstate of the free system but the combined energy state of one of the energy eigenstates and one or more of photons of the radiation field. According to the uncertainty principle, the population will reside in the virtual level for a time duration of $\hbar/\Delta E$ where ΔE is the difference in energy between the virtual level and the nearby energy eigenstate. In nonparametric processes such as Saturable Absorption, Two-photon Absorption, Stimulated Raman Scattering etc. the population will be transferred from one real level to another real level. These two processes differ in that the parametric processes are described by a real susceptibility whereas the nonparametric processes are described by a complex susceptibility. Photon energy is conserved in a parametric process but in a nonparametric process photon energy need not be conserved as energy exchange with the medium can take place. The light-matter interaction can be considered by a semi-classical picture (in which the matter is quantized and the field is classical) so long as the number of photons in each mode of the electromagnetic radiation is much larger than one. For a typical pulsed laser the number of photons per mode is of the order of 10^{19}. Hence for the interaction involving pulsed lasers always a semi-classical treatment is adequate even though the quantized field theory also can lead to the same explanation to the related phenomena in the limit of the number of photons per mode tending to larger values. Quantization of field becomes necessary when the number of photons per mode of electromagnetic radiation is of the order of one. The dependence of the dielectric constant and the magnetic permeability of matter on the field strength inherently suggests the nonlinear properties of Maxwell's equations for the interaction of electromagnetic radiation with matter. This manifests through the nonlinear polarization that depends on the electric field strength as a power series as given in equation. This nonlinear response was theoretically investigated by Goeppert-Mayer in 1931 in the earlier years of quantum mechanics. But as the intensities

of the optical field required to observe the effect of nonlinear polarization is of the order of 1MW/cm^2, which is far unattainable by the classical sources of optical radiation, the experimental observation of the nonlinear phenomena had to wait till 1961 [Kaiser and Garrett], until the invention of lasers. The charm of these high intensity interactions is that ionization of matter is done with photons of frequency far below the frequency corresponding to their ionization potential, which is in contradiction to the linear photoelectric effect. Many effects, which were too weak to be detected by the conventional sources of light existing in the pre-laser era, became observable by the use of high intense laser pulses.

1.10.2 LASER INTENSITY REGIMES

At low input intensities, the external field of the laser to the material system is much weaker than the static atomic Coulomb field. Under such a situation, the influence of the laser field is only to slightly perturb the atomic quantum states, when the interaction is non-resonant. For visible and near infrared input laser radiations, an intensity less than 10^{13} W/cm^2 corresponds to the perturbative regime for non-resonant interaction. $\chi^{(2)}$, $\chi^{(3)}$, $\chi^{(5)}$ etc. processes take place in this intensity region, where bound-bound transition is the prevailing mechanism. The valence electrons are still bound to the core in these interactions. For intensities from 10^{13} W/cm^2 to 10^{14} W/cm^2 multiphoton ionization by the simultaneous absorption of many photons becomes significant. This is the intensity regime between the perturbative and strong field regimes of light-matter interaction. In this process, free electrons are generated with a kinetic energy that is a fraction of the photon energy. Any energy in excess to the ionization becomes the kinetic energy of the liberated electron. If the ionization energy matches exactly with the energy of an integer number of photons in the electromagnetic radiation, then the resultant electron in the continuum will not possess any kinetic energy. This is the nonlinear counter part of photoelectric effect in the linear regime of electromagnetic excitation. This is the intensity regime where the contribution of the freed electrons and that from the induced atomic dipoles in the bound-bound transition in a system, subjected to the laser field, becomes comparable. A physical example is the self-channeling of intense nanosecond pulses over large distances. Here the self-focusing due to optical Kerr effect (contribution from the induced atomic dipole) and self-defocusing due to free electrons

tend to balance. If the strength of the applied laser electric field is comparable to or greater than the binding atomic Coulomb field experienced by the valence electrons, there is a good probability for a valence electron to escape from its bound state via tunneling or above-barrier ionization, before the laser electric field reverses its sign. This electron subsequently wiggles in the linearly polarized laser field and the cycle-averaged kinetic energy of the electron exceeds the binding energy. This regime, in which the ionization process dominates the atomic polarization response, is termed as strong-field regime of nonlinear optics. The nonlinear polarization in this optical ionization regime is mainly governed by the wiggle of the liberated electrons in the proximity of the parent ion. Once the electron is set completely free from the vicinity of the parent ion, it gives only linear response to the applied laser field yielding results corresponding to classical motion of a free electron in an applied electric field. In the intensity regime of 10^{14} W/cm^2 to 10^{15} W/cm^2 tunnel ionization predominates. For intensities greater than 10^{15} W/cm^2 above-barrier ionization takes over. When the input laser intensity is extremely high so that the optical ionization leads to the ionization of the inner-shell electrons and gives a higher wiggling energy (comparable to the electron rest mass energy) to the electrons, the interaction regime is termed as relativistic nonlinear optics. For the visible and near infrared spectral ranges, intensities of the order and above of 10^{18} W/cm^2 is in the relativistic regime.

1.10.3 MODERATE ENERGY NONLINEAR EFFECTS

For laser intensities up to 10^{13} W/cm^2, the response of the medium to the laser field is in the perturbative nonlinear regime, once the intensity level is higher than that required for a linear response. The nonlinear dependence of the susceptibility of a medium on the driving electric field of the exciting laser will give rise to phenomena like two photon absorption, three photon absorption, second harmonic generation, sum frequency generation etc. When the intensity of the interacting electromagnetic field is moderate, the velocity of the electrons is not in the relativistic regime, and hence the magnetic field component will not give any observable effects. Under higher laser intensities of this regime, a nonlinear electron oscillator model can hence represent the atom. By solving the Maxwell's equations with the time variation of the polarization as the source term, the output from the medium can be found to contain higher harmonics of

the fundamental electromagnetic radiation due to nonlinear response of the medium. As described above, non-parametric effects like two-photon absorption, three-photon absorption and saturable absorption usually lead to a reduction of energy transmission through the medium at high input laser fields. This nonlinear absorption of laser light can form the basis of novel devices like optical limiters and non-reciprocal light transmitters. In optical limiting, the intensity dependent absorption of laser light is such that at high intensities the material will show a reduced transmission. Optical limiters are passive devices that use the nonlinear absorption properties of materials. As part of the present work, we investigated nanoparticles of gold and silver for their nonlinear transmission properties. We also studied the nonreciprocal transmission of laser light through materials possessing an axially asymmetric nonlinear absorption coefficient. From the latter studies we found that in general, a saturable absorber and a two-photon absorber (or any material with the property of reduced light transmission at higher laser intensities) placed in tandem will transmit light in one direction and prevent transmission in the opposite direction, thereby providing an optical diode action.

1.10.4 OPTICAL FIELD IONIZATION OF ATOMS

Traditional optics deals with phenomena in the eV regime, where photon energies fall approximately between 1.77eV (700nm) and 3.11eV (400nm). The process by which an electron in the outermost shells gets excited to a continuum is named as ionization. In the traditional optical regime ionization happens only when the energy of the incident photon matches the binding energy of the electron in its shell. Hence electromagnetic radiation with higher photon energy ionizes matter with grater probability. As we move towards the high frequency side of the electromagnetic spectrum, the ionization probability increases with γ-rays as the highest ionizing radiation. Here it is the energy of the individual photon that determines the ionization of a single atom, rather than the intensity of the incident radiation (intensity helps only in ionizing a larger number of atoms). But with the advent of high power lasers, the electric field strength associated with the emission is so high that the radiation intensity has a deciding role in the ionization of a single atom. Thus ionization of atoms or molecules with non-resonant light frequencies becomes possible. The intensity of a light field can be related to its electric field strength through

$$I = \frac{1}{2}\sqrt{\frac{\varepsilon_0}{\mu_0}}E_0^2 \equiv \frac{1}{2}\varepsilon_0 c E_0^2$$

where c (the velocity of electromagnetic radiation in free space) is given by

$$c = \frac{1}{\sqrt{\varepsilon_0 \mu_0}}$$

The behaviour of atom in high laser intensities (>10^{13} W/cm^2) is usually analyzed on the basis of 'keldysh parameter' given as:

$$\gamma = \frac{\omega_0 \sqrt{2mI_0}}{eE_a}$$

where ω_0 is the laser carrier frequency, m the electron rest mass, I_0 the ionization potential of the atom (i.e. the binding energy of the most weakly bound electron), E_a the time dependent amplitude of the linearly polarized laser field, and e the electron charge , For high frequencies and not very high intensities $\gamma>1$ and multiphoton ionization (MPI) dominates. For very high intensities (>10^{14} W/cm^2) and low frequencies $\gamma<1$ and the laser field significantly modifies the Coulomb potential.

For the range of laser intensities 10^{13} W/cm^2 to 10^{17} W/cm^2 that are readily available from the present day high power lasers, the corresponding electric field strength is in the range of 10^{10} V/m to 10^{12} V/m. Here the electric field strength is comparable to the Coulomb field that binds electrons in the atoms or in the valence shell for the molecular bonding. As an extension of the linear photoelectric effect, the nonlinear photoelectric effect, i.e., the multiphoton ionization should absorb N number of photons sufficient to ionize the matter, and the kinetic energy of the ejected electron should possess a kinetic energy not more than the energy of one photon of the exciting laser field. But it is being observed that often the kinetic energy of the ejected electron far exceeds the energy of a photon of the exciting laser-field, which calls for a modified explanation of the multiphoton ionization rather than a direct extension of the linear photoelectric effect to a nonlinear photoelectric effect. This leads to the mechanism of Above Threshold Ionization (ATI), which was first discovered in 1979. Here the electron absorbs more number of photons than that is sufficient for multiphoton ionization. This excess absorption of photons can be explained by inverse Bremsstrahlung absorption if

the matter is dense enough to cause sufficient collision leading to the absorption of photons from the laser field by the accelerating electrons during their scattering with neutral atoms or ions. This phenomenon was observed in 1977 in which the electrons are produced by standard multiphoton ionization but the excess of energy is attained by inverse Bremsstrahlung absorption. But this consideration cannot be applied to the case of low density matter - short laser pulse interaction, as the electron-ion collision probability is very less in such a system. Under such situation multiphoton ionization of atoms cannot explain the absorption of the excess number of photons.

Laser field interaction with low-density matter ATI is the proposed mechanism where each electron in the continuum interacts only with its own parent ion or atom and does not undergo any collision with the neighbouring atom or ion. When an electron gains an energy equal to the ionization potential of the atom, the electron is moved to a distance where the coulomb potential of the nucleus is not significant, and hence it behaves as a free electron. If the density of the material is low enough then the electron will not see the potential of any neighbouring nucleus. If the material is dense then the released electron may come into the potential of the neighboring nuclei as in the case of liquids and solids other than diffuse gases. Hence in the case of ATI the electrons absorb more photon from the laser field while the liberated electron is still in the vicinity of the parent nucleus. Therefore the absorption of larger number of photons by low-density materials for multiphoton ionization in an intense field is being described by. For experiments at moderately high intensity, where the bound-state energies of the atom remain un-shifted by the electromagnetic radiation, the perturbative theory of ATI holds. The perturbation theory of ATI breaks down at higher laser intensities and for longer wavelengths. Phenomena like the absence of the low energy peaks of the photoelectron etc. start at this condition. The photoemissions under this condition are analyzed using the non-perturbative approach. Ionization using laser pulses with only a few cycles, depends on the initial phase of the field. For higher intensities of the excitation laser field corresponding to a regime of $\gamma<1$, the Coulomb barrier becomes narrow allowing Tunnel Ionization (TI). The γ value decides whether the ionization process is MPI or TI. At still higher intensities ($>10^{15}$ W/cm^2) the electric field amplitude of the laser is so prominent that it suppresses the Coulomb barrier below the energy level of the ground state leading

to Above the Barrier Ionization (ABI). The minimum value of the exciting laser field that is required to induce ABI can be obtained by equating the maximum value of the resultant atomic potential, in the presence of the laser field, to the binding energy of the electron. Different routes of ionization of an atom in the presence of an intense laser field are shown in figure 1.4.

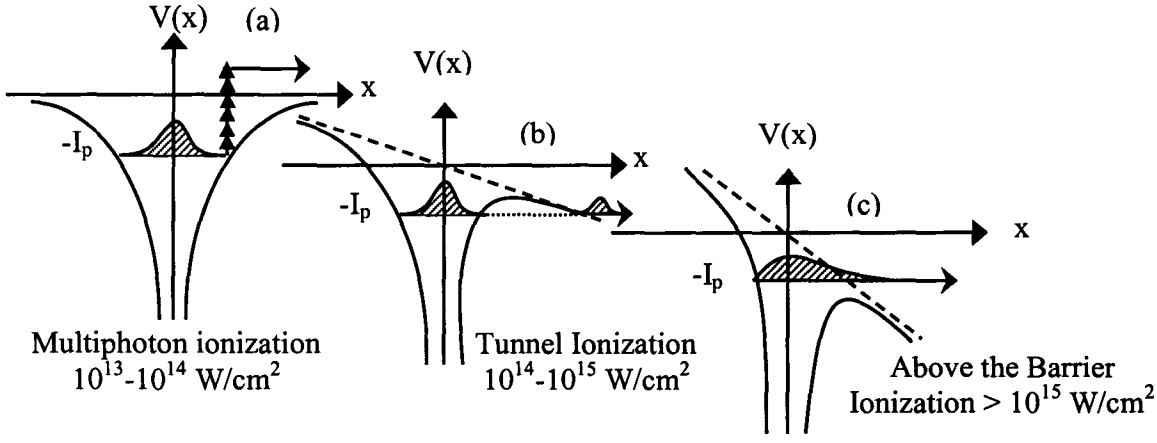

Figure 1.4: Schematic diagram of the three possible ionization mechanisms in the high intensity laser field – atom interaction

The electron, once freed from the Coulomb potential by any of the above three mechanisms, is released into a strong electromagnetic field provided by the focused excitation laser. Light being a combination of transverse electric and magnetic fields, the released electron sees the two fields and is subjected to the Lorentz force. Since the force exerted by the magnetic field is v/c times less than that of the electric field in the non-relativistic regime, the electron follows the electric field of the laser pulse. Hence the electron will undergo an oscillatory motion in the laser electric field. The oscillatory energy possessed by the free electron in the laser field is named as the electron quiver energy. The electron follows the laser electric field in direction and frequency in the non-relativistic regime. In the relativistic regime, the magnetic field will also start to exert significant force on the electron so that the resultant trajectory of the electron in the laser field will be governed by both the electric and the magnetic fields. Apart from the electron quiver energy due to the oscillation of the electron in the laser field, there is

$$E_{osc} = \frac{e^2 E^2}{4m\omega^2}$$

energy that is acquired by the free electron subjected to an inhomogeneous laser field. This is named as ponderomotive energy. The concept of ponderomotive force is well known in the electrodynamics of condensed media owing to the inhomogeneity of the medium or that of the field. For a less dense medium the origin is the inhomogeneity of the field itself. In the case of a pulsed Gaussian laser beam, there is an inhomogeneity in the laser field in space and time. The electron motion in an inhomogeneous electric field when averaged over fast oscillations in the field gives the averaged trajectory of the electron in the inhomogeneous field, and is interpreted as the motion under the ponderomotive force.

This gives the way in which the electron decouples from the laser focal volume.The ponderomotive force, which pushes the electrons away from the region of high field pressure, is given as

$$\vec{F}_p = -\frac{e^2}{4m\omega^2}\vec{\nabla}\vec{E}^2(x) = -\vec{\nabla}U_p$$

for a linearly polarized laser field oscillating with an angular frequency ω. U_p, the ponderomotive energy is the cycle averaged quiver energy of the electron in the oscillating laser electric field. So far we discussed the optical ionization processes mainly involving diffuse atomic systems. For molecular states the ionization mechanisms remain the same. The only difference is the relevant change in the energy levels and ionization potentials of the system. One qualitative difference is that, in intense field molecular ionization, the ionization rate sensitively depends on the molecular configuration, i.e., inter nuclear distance. Hence the ionization can act as a sensitive probe for the molecular structure and motion.

1.11 OUTLINE OF THE THESIS

This report contains experimental work involving the interaction of moderate laser pulses with metal nano particles. An introduction of nanomaterials and their nonlinear response of matter to large electric fields present in intense laser pulses is outlined in the first part of this chapter, followed by a discussion of the different mechanisms in the laser matter interaction in different regimes of laser intensity. The nonlinear effects in the moderate energy regime are discussed in brief. The optical field ionization mechanisms are outlined. Chapter 2 discusses materials and their preparation

technique. Chapter 3 considers nonlinearity. Chapter 4 & 5 contains optical limiting and experimental procedure. And chapter 6 contains the results & discussion. Results from the moderate intensity Matter-Laser Interaction studies and with nonlinear light transmission studies in nano particles of different size, dispersed in different host materials are discussed. Both experiments and numerical analysis are presented. The materials studied are found to be potential candidates for application as fast passive optical limiters to protect eyes and sensitive sensors.

CHAPTER-2

MATERIALS AND PREPARATION TECHNIQUE OF NANOMATERIALS: WET CHEMICAL ROUTE

2.1 INTRODUCTION

In the chemical preparation of nanoscale particles with desired properties the structural properties (crystalline or amorphous structure, size, shape, morphology), and chemical properties (composition of the bulk, interface, and surface) important factor to be considered. Because of its advantages, the role of chemistry in materials, the role of chemistry in the materials science has been rapidly growing. The strength of chemistry in materials science is its versatility in designing and synthesizing new materials, which can be processed and fabricated into final component. Chemical synthesis permits the manipulation of matter at the molecular level; good chemical homogeneity can be achieved. Also, by understanding the relationship between how matter is assembled on an atomic and molecular level and the material macroscopic properties, molecular synthetic chemistry can be tailor designed to prepare novel starting components. Better control of the particle size, shape, and size distribution can be achieved in particle synthesis. To benefit from the advantages of chemical processing, an understanding of principles of crystal chemistry, thermodynamics, phase equilibrium, and reaction kinetics is required. There are also potential difficulties in chemical processing. In some preparations, the chemistry is complex and hazardous. Entrapment of impurities in the final product needs to be avoided or minimized to obtain desired properties. Scaling up for the economical production of a large quantity of material may be relatively easy for some but not all system. Another problem is that undesirable agglomeration at any stage of the synthesis process can change the properties. Many liquid phase chemistry methods exist for synthesizing nanoscale or ultrafine particles. The scope of this chapter is limited to describing some selected examples of these methods for making nanoscale particles or powder, and is not intended to provide a comprehensive review. Chemical techniques for making film and modifying surfaces with nanoscale structures, such as electrochemical methods, are not discussed here. The examples include both conventional and more recent methods. In some examples, liquid phase chemistry is used to prepare the precursor, which is subsequently converted to nanoscale particles by non-liquid phase chemical reactions. In the following, the size of a powder refers

to the particles dimension as observed by imaging techniques such as scanning electron microscopy **(SEM).** The particles may be a single unit, e.g. a single crystal, or it may consist of subunits. The small subunits are defined as the primary particles and the agglomerates of these primary particles are called secondary particles (figure 2.1).

Fig 2.1 a schematic diagram showing the primary and secondary particles

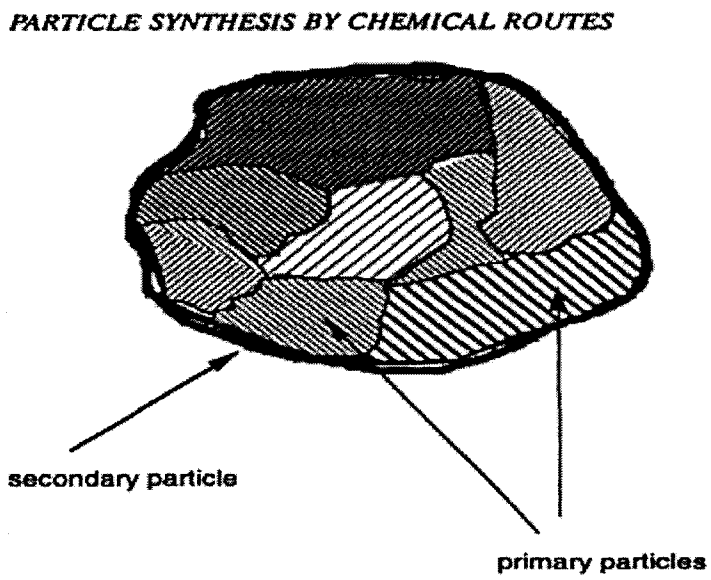

The measurements of particles size by **SEM** often can only determine the size of secondary nanoparticles. For crystalline materials, the size of primary nanoparticles can be estimated by the amount by which the x-ray line is broadened, or determines from dark-field imaging by transmission electron microscopy **(TEM)** or from lattice imaging by high-resolution transmission electron microscopy **(HRTEM).** Use of dark-field **TEM** and **HRTEM** for determining the primary particles size is preferred over x-ray line broadening. These techniques are more direct and less likely to be affected by experimental errors and/or other properties of the particles such as strain or a distribution in the size of the lattice parameter. For amorphous particles, the size of primary particles can also be estimated by bright-field imaging using **TEM** or **HRTEM.**

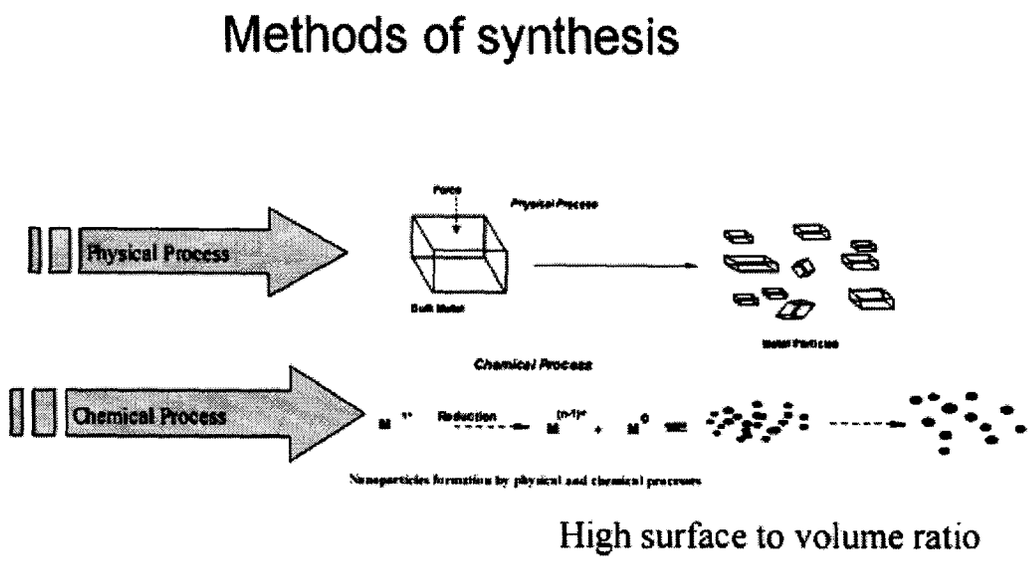

Fig 2.2 Top down and bottom up approach

2.2 NUCLETION AND GROWTH FROM SOLUTIONS

Precipitation of a solid from a solution is a common technique for the synthesis of fine particles. The general procedure involves in aqueous or non-aqueous solution containing the soluble or suspended salts. Once the solutions become supersaturated with the product, a precipitate is formed by either homogeneous or heterogeneous nucleation. Homogeneous and heterogeneous nucleation refer to the formation of stable nuclei with or without foreign species respectively. After the nuclei are formed, their growth usually proceeds by diffusion. In diffusion controlled growth, concentration gradients and the temperature are important in determining the growth rate. To form monodispersed particles, i.e. unagglomerated particles with a very narrow size distribution, all the nuclei must form at nearly the same time, and subsequent growth must occur without further nucleation or agglomeration of the particles.

In general, the particles size and particles-size distribution, the amount of crystallinity, the crystal structure, and the degree of dispersion can be affected by reaction kinetics. Factors influencing the rate of reactions include the concentration of reactants, the reaction temperature, the pH, and the order in which the reagents are added to the solution. A multi-element material is often made by co-precipitation of batched ions. However, it is not always easy to simultaneously co-precipitate all the desired ions, since different species may only precipitate at different pH. Thus, special attention is required to control chemical homogeneity and stoichiometry. Phase

separation may be avoided during liquid precipitation and the homogeneity at the molecular level improved by converting the precursor to powder form by using spray drying and freeze-drying.

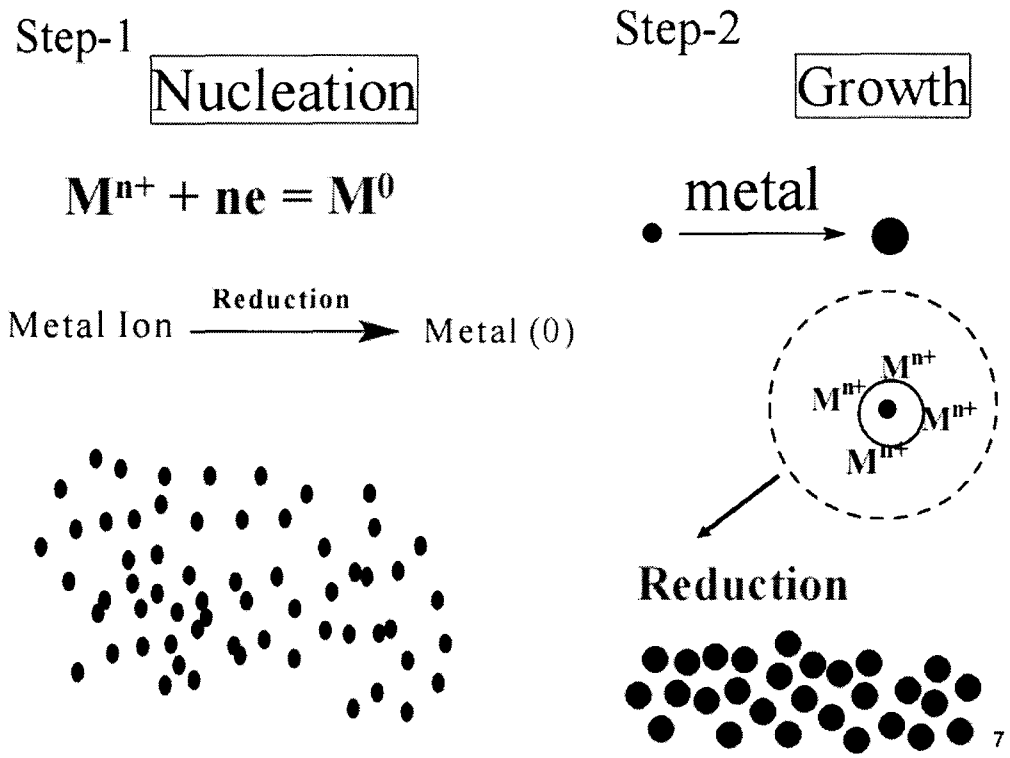

Fig 2.3 The nucleation and growth of NPs

2.3 STABILIZATION OF FINE PARTICLES AGAINST AGGLOMERATION

Fine particles, particularly nanoscale particles, since they have large surface areas, often agglomerates to form either lumps or secondary particles to minimize the total surface or interfacial energy of the system. When the particles are strongly stuck together, these hard agglomerates are called aggregates. Many materials containing fine particles, some examples including paints, pigments, electronic inks, and ferrofluids, are useful if the particles in the fluid suspension remains unagglomearated or dispersed. For instance, the desirable magnetic properties caused by single-magnetic-domain behavior cannot be realized if the ferromagnetic nanoscale particles are not isolated from each other. In the processing of ceramic materials, if the starting powders are adversely agglomerated with entrapped large pores, the green body will fail to shrink and density during sintering for pores above a certain size. Further

details regarding the adverse effect of agglomeration of powders on consolidation may be found in the further literature. Agglomeration of fine particles can occur at the synthesis stage, during drying and subsequent processing of the particles. Thus it is very important to stabilize the particles against adverse agglomeration at each step of particle production and powder processing. Surfactants are used to produce dispersed particles in the synthesis processor disperse as-synthesized agglomerated fine particles. The dispersion of fine particles in liquid media by surfactants has been studied intensively. Many technologies use surfactants. A surfactant is a surface-active agent that has an amphipathic structure in that solvent, i.e. a lyophobic (solvent repulsive) and lyophilic group (solvent attractive). Depending on the charges at the surface-active portions, surfactants are classified as either anionic, cationic, zwitterionic (bearing both positive and negative charges), or non-ionic (no chares). At low concentrations, the surfactant molecules adsorb on the surfaces or interfaces in the system, and can significantly alter the interfacial energies Agglomeration of fine particles is caused by the attractive van der Waals forces and/or the driving forces that tends to minimize the total surface energy of the system. Repulsive interparticle forces are required to prevent the agglomeration of these particles. Two methods are commonly used. The first method provides the dispersion by electrostatic repulsion. This repulsion results from the interactions between the electric double layer surrounding the particles. An unequal charge distribution always exists between a particle surface and the solvent. Electrostatic stabilization of a dispersion occurs when the electrostatic repulsive force overcomes the attractive van der Waals forces between the particles. This stabilization method is generally effective in dilute system of aqueous or polar organic media. This method is very sensitive to the electrolyte concentration since a change in the concentration may destroy the electric double layer, which will result in particles agglomeration.

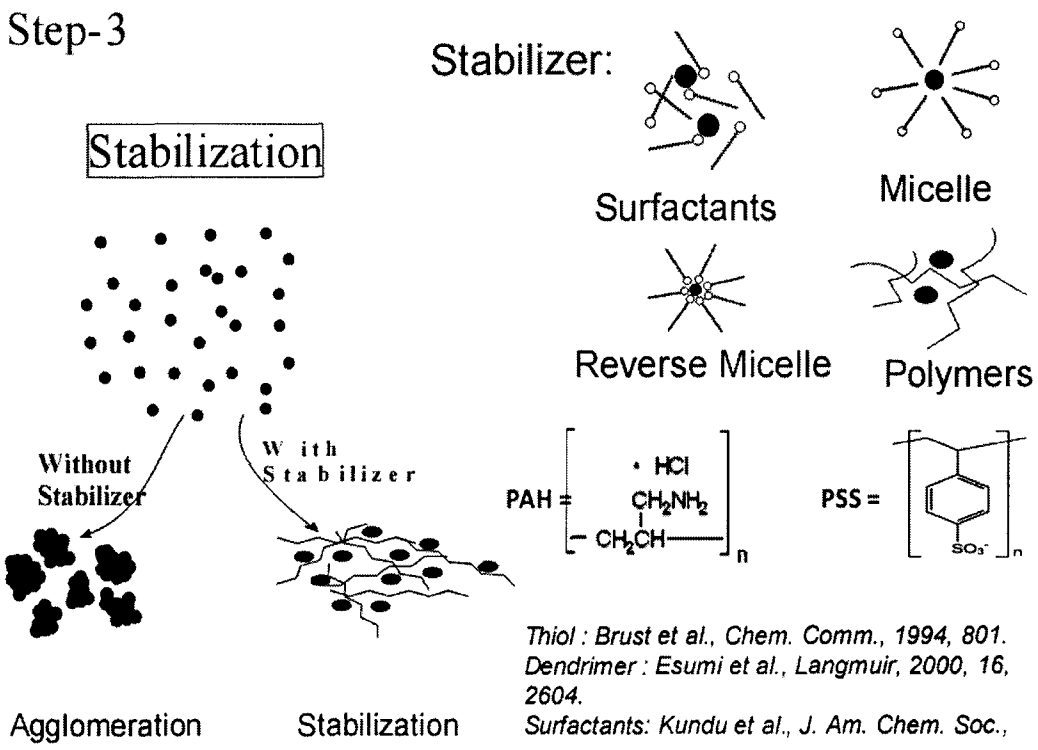

Fig 2.4 Stabilization process of NPs

The second method of stabilization involves the steric forces. Surfactant molecules can adsorb onto the surfaces of particles and their lyophillic chains will then extend into the solvent and interact with each other. The solvent-chain interaction, which is a mixing effect, increases the free energy of the system and produces an energy barrier to the closer approach of particles. When the particles come into closer contact with each other, the motion of the chains extending into the solvent become restricted and produce an entropic effect. Steric stabilization can occur in the absence of the electric barriers. Steric stabilization is effective in both aqueous and non-aqueous media, and is less sensitive to impurities or trace additives than electric stabilization. The stabilization method is repulsion, thus preventing agglomeration. Monodispersed pure or coated iron submicron particles consisting of nanocrystallites were obtained by reducing the colloidal α-Fe_2O_3(uncoated or with silica or cobalt oxide) in a hydrogen atmosphere. The size of iron crystallites increased with increasing reduction temperature and was approximately 80 nm at 450 C.

RAMAN RESEARCH INSTITUTE
BANGALORE - 560 080
LIBRARY
CLASS No.
DNACCI SOLUTIONS

Thermal reduction of inorganic metallic compound in a polyol such as ethylene glycol or diethylene glycol was used to produce monodispersed particle of Co, Ni, Cu, and precious metals. Reaction temperatures as high as the boiling point of the polyol can be used for metals that are not reduced easily. The polyol acts as a solvent for the starting metallic compound and, subsequently, is also used to reduce them to metals. The reaction is a dissolution process and not a solid-state phase transformation. The number of nuclei formed and the rate of reduction increases with increasing the temperature, resulting in a decrease in the particle size. Although micron-sized particles usually results from the homogeneous nucleation in this process, nanoscale particles can be synthesized by addition of impurities to promote heterogeneous nucleation. The particles size decreases as the concentration of foreign nuclei is increased. Bimetallic PdCu colloids have been prepared by the thermal decomposition of copper acetate and palladium acetate in high-boiling-piont organic solvents such as bromobenzene and xylenes. An alternative method for producing PdCu colloids is by reducing the palladium acetate and copper acetate in a boiling alcohol such as 2-ethoxyethanol. It was postulated that the boiling alcohol rapidly reduced Pd(II) to Pd(0), which then reduced Cu(II) at the surface of the growing Pd particles. Poly(vinylpyrrolidone) was added to the solutions to stabilize the colloidal particles with sizes in the range of 3-5 nm. The preparation of finely divided metal and alloy particles has been reported via the reduction of metal salts of groups 6-12 and 14 in organic phases using hydroorganoborates of the general formal $M'H_v(BR_3)$ or $M'H_v[BR_n(OR')_{3-n}]_v$ (where M'=alkali or alkaline earth metal,v=I,2, R, R'=alkyl or aryl) at low temperature (23-67^{0}C). The particle size, as determined by SEM, was between 10 and 100 nm, and the structure of powders was found to be either microcrystalline or amorphous. The impurity content of boron was less than 1.5%. A simple co-reduction of different metal salts (metal of groups 6-12) can be used to prepare metallic alloys. For examples, co-reduction of $FeCl_3$ and $CoCl_2$ using $LiBEt_3H$ in THF, where BEt_3 is triethyl boron and THF is tetrahydrofuron, yielded a boron free Fe/Co alloy powder with a particle size of approximately 100 nm. Stable metal colloids of elements of group 6-11 have also been synthesized in an organic phase by treating metal salts with tetraalkylammonium hydridoorganoborates.

$$MX_n + nNR_4BEt_3H \rightarrow M_{colloid} + nNR_4X + nBEt_3 + n/2H_2\uparrow$$

M: metal of groups 6-11 ; X: Cl, Br; n: 2,3; R: alkyl C_4-C_{20}

A TEM study of these particles indicated a particle size of about 6 nm. An analogous study was conducted of the room-temperature reduction of group six metal chlorides $CrCl_3$, $MoCl_3$, $MoCl_4$, and WCl_4 in toluene with $NaBEt_3H$ to prepare agglomerates of 1-5 nm metallic crystallites. Other approaches for the synthesis of highly reactive metal powder from the reduction of metal salts by reducing agents include the following: (i) alkali metals in ethereal or hydrocarbon solvents; (ii) alkali metals in the presence of an electron carrier such as naphthalene; (iii) stoichiometric amounts of lithium naphthalide. An alternative approach is to rapidly reduce soluble compound of transition metals and post-transition metals and post-transition metals in dimethyl ether or electrides (is an ionic compound in which an electron is the anion) to produce metal particles with crystallite size from 3 to 15 nm. This method can also be applied to the formation of finely dispersed metal particles on oxide supports. The interest in intermetallic compound arises from their attractive properties such as their high melting temperature, high-temperature strength, corrosion resistance, and low density. Powders of NiAl and Ni3Al were prepared by heat treatment of the organometallic precursors synthesized by coprecipitation of constituent metallic salts in ammonium benzoate and hydradinium monochloride . However, the particle size of these powders was quite large (1 to 3 microns). Nanoscale TiB2 particles have been synthesized from the thermal conversion of the amorphous precursor Ti(BH4)3(solvent)n obtained by a wet chemical reaction of TiCl4 with sodium borohydride. The precipitated precursors were converted to a mixture of TiB2 and TiBO3 by heating them in a vacuum at 9500C. The TiB2 phase existed both as rods with diameters ranging from 20 to 40 nm and with an aspect ratio of nine, and as equiaxed particles with diameters less than 300 nm.

2.4 SOL-GEL METHOD FOR NANOPARTICLE SYNTHESYS

2.4.1 HISTORICAL DEVELOPMENT OF SOL-GEL PROCESSING

2.4.1.1 ORIGINS

The earliest use of colloids o prepare functional materials is seen in the cave paintings at lascaux in France, dating back 17000 years the pigments used were based on iron oxide, Carbon and clays, ground into fine powders graded by sedimentation and dispersed in water using natural oils as surface active stabilizers. It is interesting that the decorative use of a technology closely related to much more reason ceramic

decoration methods substantially pre-dates the use of ceramics in construction or other more practical applications. The next major development was the use of firing techniques in addition to simple grinding to alter the chemistry of the mineral precursors. Some 8000 years ago early examples of the use of plaster and brick occurred. Neolithic sites often contain polished plaster floors. At Yiftah El in Israel a $180m^2$ example would have needed over 10 tons of wood to fire kiln. IN these examples we see the beginnings of the solegel ideas, in that fine powdered colloidal material in suspension was molded and then dried and densified by chemical a action or by firing at high temperature. Next glazing methods were developed to seal the surfaces of porous clay vessels. In china by 2000 BC silicate glasses with high calcium content fired at high temperatures were in use. In Mesopotamia by the 2nd century the glazing chemistry had already become quite sophisticated; a very fine Hematite rich illitic clay fraction made by sedimentation was paitered(type of drawing) on to the vessels and fired in a reducing atmosphere to reduce the iron to black magnetite. After sintering of the glaze the atmosphere was made oxidizing by admission of air, oxidizing the iron in the non glazed areas to add color and producing a shiny black glazed decorative pattern on a matt red base. Even earlier (4000 BC) in Egypt an aqueous paste of crushed sand and a sodium salt flux and binder was molded and fired to produce faience by binding the silica particles together with molten flux. Addition of copper salt to the paste led to migration to these mobile salt to the surface during firing, with formation of a translucent blue glaze. The idea of using chemically-linked particles as a matrix for a composite of other particulates materials led to the development of concrete in about 700 BC, eg: in the 260m aqueduct bridge at Jerwan in Iraq. Stones of graded sizes mixed with sand and a binding paste of a quicklime (CaO) and water formed the first concrete, but required an asphalt lining as the lime cement tended to crumble in water. In fact the ash contained oxides of aluminium, silicon and iron and the product was similar to the modern Portland cement proving more durable in under water conditions than recently-laid modern concrete in the same locations. Much the same material was rediscovered by the British engineer John Smeaton in his search for reliable hydraulic cement for building the fourth Eddystone light house in the English channel in 1756-9. He found that the best hydraulic cement was produced by burning limestone with some clay content. His work was continued by Louis Joseph Vicat who examined thousands of different lime stones in France for 30 years and by John Friedrich John in Germany.

2.4.1.2 THE BEGINNING OF SOL-GEL SCIENCE

Strangely, many of these early technologies became in the Dark Ages after the decline of Roman Empire, and probably the next significant development was the discovery of "water glass" by von Helmont in 1644. He dissolved silicate materials (stones, sand, flint etc.) in alkali and found that on acidification a precipitate of silica equal in weight to the original silicate materials was obtained. In 1799 Bergman reported that if the correct amount of dilute acid was used the mixture gelled on acidification. This preparation of a silica gel led to a series of applications remarkably similar to those of today's sol-gel chemistry. In 1840-1860 it was shown to be useful as a glazing solution, as a binder for ceramic precursor powder to make porcelain and special bricks, as a mixture with sand for improving glass-making, as a method for impregnating and hardening soft porous stone, and for making, as a method for impregnating and hardening soft porous stone, and for making "synthetic stone" using a patented process with water glass, lime or chalk, used (and are still used today) for polishing marble floors, in a hydraulic process leading to scratch resistant amorphous silica layers containing fine crystals of calcium and magnesium fluorides. Also in the 19th century many oxide materials were prepared from hydroxide gels. Following the preparation of zirconia by firing zirconium hydroxide gels (Vauqelin 1797) Berthier (1832) used mixed cupric and zirconyl salts treated with ammonia and then fired to produce a green copper zirconate, in 1842 Ebelmen reported the synthesis of uranium oxide by heating the hydroxide, and in 1892 von Chroustchoff heated mixed gels of zirconium hydroxide, silica and alumina in a sealed tube to obtain a zirconopyrophyllite. Meanwhile, two major developments were occurring which were to prove foundation stones for sol-gel processing: the physical properties of colloids came under intensive study by such giants as Becquerel, Faraday, Tyndall, Graham and Schulze; and in1846 Ebelmen prepared the first silicon alkoxide by the reaction between silicon tetrachloride and alcohol, observing that the product gelled on prolonged exposure to atmospheres with normal humidity. In 1876 Troost and Hautefeuille made hydrolysed derivatives of silicon alkoxide. In 1884 Grimaux hydrolyzed tetramethoxysilane to prepare silicic acid sols, and made colloidal iron oxide from iron alkoxide. However, for the next 50 years these developments had little scientific impact for the development of the sol-gel materials field.

2.4.1.3 THE EXPLOSION OF SOL-GEL TECHNOLOGY

The one notable exception in this period was W.A. Patrick, who pioneered the field of silica gel desiccants, catalysts and absorbent materials, starting with the drying and firing of a homogeneous silica gel at up to 700^0C to produce a very porous form of silica. In 1923 he went on to show that impregnation of the partially dried materials with metal salts led to the formation of supported catalyzed, and by 1930 he had filed many patents for supported catalysts, including the use of sol-gel methods. This signaled the beginning of an intensive periods of technological development using sol-gel methods, which produced a very large number of patents, many useful materials, and a large body of data and experience. Only later, with the advent of modern characterization methods, could a set of firmly-based theoretical principles begin to be established to interpret all these data. Indeed it could be said that despite the new methods now available, the subject is still strongly influenced by this empirical approach. It is therefore important that the large amount of early work in the field is not overlooked, only to be re-discovered as the topics attract interest for new reasons, just as was the case with the Roman cement.

2.4.2 INTRODUCTION TO SOL-GEL PROCESS

The sol-gel process is a wet-chemical technique (a.k.a. chemical solution deposition) widely used recently in the fields of materials science and ceramic engineering. Such methods are used primarily for the fabrication of materials (typically a metal oxide) starting from a chemical solution, which acts as the precursor for an integrated network (or *gel*) of either discrete particles or network polymers. Typical precursors are metal alkoxides and metal chlorides, which undergo various forms of hydrolysis and polycondensation reactions. The formation of a metal oxide involves connecting the metal centers with oxo (M-O-M) or hydroxo (M-OH-M) bridges, therefore generating metal-oxo or metal-hydroxo polymers in solution. Thus, the sol evolves towards the formation of a gel-like diphasic system containing both a liquid phase and solid phase whose morphologies range from discrete particles to continuous polymer networks. In the case of the colloid, the volume fraction of particles (or particle density) may be so low that a significant amount of fluid may need to be removed initially for the gel-like properties to be recognized. This can be accomplished in any number of ways. The most simple method is to allow time for sedimentation to occur, and then pour off the remaining liquid. Centrifugation can also be used to accelerate the process of phase separation. Removal of the remaining liquid (solvent) phase

requires a drying process, which is typically accompanied by a significant amount of shrinkage and densification. The rate at which the solvent can be removed is ultimately determined by the distribution of porosity in the gel. The ultimate microstructure of the final component will clearly be strongly influenced by changes imposed upon the structural template during this phase of processing. Afterwards, a thermal treatment, or firing process, is often necessary in order to favor further polycondensation and enhance mechanical properties and structural stability via final sintering, densification and grain growth. One of the distinct advantages of using this methodology as opposed to the more traditional processing techniques is that densification is often achieved at a much lower temperature. The precursor sol can be either deposited on a substrate to form a film (e.g., by dip-coating or spin-coating), cast into a suitable container with the desired shape (e.g., to obtain monolithic ceramics, glasses, fibers, membranes, aerogels), or used to synthesize powders (e.g., microspheres and nanospheres). The sol-gel approach is a cheap and low-temperature technique that allows for the fine control of the product's chemical composition. Even small quantities of dopants, such as organic dyes and rare earth metals, can be introduced in the sol and end up in uniformly dispersed in the final product. It can be used in ceramics processing and manufacturing as an investment casting material, or as a means of producing very thin films of metal oxides for various purposes. Sol-gel derived materials have diverse applications in optics, electronics, energy, space, biosensors, medicine (e.g., controlled drug release), reactive material and separation (e.g., chromatography) technology. The interest in sol-gel processing can be traced back in the mid-1880s with the observation that the hydrolysis of tetraethyl orthosilicate (TEOS) under acidic conditions led to the formation of SiO_2 in the form of fibers and monoliths. Sol-gel research grew to be so important that in the 1990s more than 35,000 papers were published worldwide on the processing of fine ceramics, the irregular particle sizes and shapes in a typical powder often lead to non-uniform packing morphologies that result in packing density variations in the powder compact. Uncontrolled agglomeration of powders due to attractive van der Waals forces can also give rise to in microstructural inhomogeneities. Differential stresses that develop as a result of non-uniform drying shrinkage are directly related to the rate at which the solvent can be removed, and thus highly dependent upon the distribution of porosity. Such stresses have been associated with a plastic-to-brittle transition in consolidated bodies, and can yield to crack propagation in the unfired body if not

relieved. In addition, any fluctuations in packing density in the compact as it is prepared for the kiln are often amplified during the sintering process, yielding inhomogeneous densification. Some pores and other structural defects associated with density variations have been shown to play a detrimental role in the sintering process by growing and thus limiting end-point densities. Differential stresses arising from inhomogeneous densification have also been shown to result in the propagation of internal cracks, thus becoming the strength-controlling flaws. It would therefore appear desirable to process a material in such a way that it is physically uniform with regard to the distribution of components and porosity, rather than using particle size distributions, which will maximize the green density. The containment of a uniformly dispersed assembly of strongly interacting particles in suspension requires total control over particle-particle interactions. Monodisperse colloids provide this potential.

Mono disperse powders of colloidal silica, for example, may therefore be stabilized sufficiently to ensure a high degree of order in the colloidal crystal or polycrystalline colloidal solid which results from aggregation. The degree of order appears to be limited by the time and space allowed for longer-range correlations to be established. Such defective polycrystalline colloidal structures would appear to be the basic elements of submicrometre colloidal materials science, and, therefore, provide the first step in developing a more rigorous understanding of the mechanisms involved in microstructural evolution in inorganic systems such as polycrystalline ceramics.

2.4.3 DISCRETE PARTICLES VS NETWORK POLYMER

Thus, the sol-gel process is a wet-chemical technique for the fabrication of materials (typically a metal oxide) starting from a chemical solution that reacts to produce nanosized colloidal particles (or sol). Typical precursors are metal alkoxides and metal chlorides, which undergo hydrolysis and polycondensation reactions to form a colloid. The result is a system composed of solid particles (size ranging from 1 nm to 1 μm) dispersed in a solvent.

The term *colloid* is used primarily to describe a broad range of solid-liquid (and/or liquid-liquid) mixtures, all of which contain distinct solid (and/or liquid) particles which are dispersed to various degrees in a liquid medium. The term is

specific to the size of the individual particles, which are larger than atomic dimensions but small enough to exhibit Brownian motion. If the particles are large enough, then their dynamic behavior in any given period of time in suspension would be governed by forces of gravity and sedimentation. But if they are small enough to be colloids, then their irregular motion in suspension can be attributed to the collective bombardment of a myriad of thermally agitated molecules in the liquid suspending medium, as described originally by Albert Einstein in his Doctoral Thesis. Einstein concluded that this erratic behavior could adequately be described using the theory of Brownian motion, with sedimentation being a possible long term result. This critical size range (or particle diameter) typically ranges from tens of angstroms (10^{-10} m) to a few micrometres (10^{-6} m). Under certain chemical conditions (typically in base-catalyzed sols), the particles may grow to sufficient size to become colloids, which are affected both by sedimentation and forces of gravity. Stabilized suspensions of such sub-micrometer spherical particles may result eventually in their self-assembly—yielding highly ordered microstructures reminiscent of the prototype colloidal crystal: precious opal. Under certain chemical conditions (typically in acid-catalyzed sols), the inter particle forces have sufficient strength to cause considerable aggregation and/or flocculation prior to their growth. The formation of a more open continuous network of low density polymers exhibits certain advantages with regard to physical properties in the formation of high performance glass and glass/ceramic components in 2 and 3 dimensions. In ether case (discrete particles or continuous polymer network) the sol evolves then towards the formation of an inorganic network containing a liquid phase (gel). Formation of a metal oxide involves connecting the metal centers with oxo (M-O-M) or hydroxo (M-OH-M) bridges, therefore generating metal-oxo or metal-hydroxo polymers in solution. In both cases (discrete particles or continuous polymer network), the drying process serves to remove the liquid phase from the gel, yielding a micro-porous amorphous glass or micro-crystalline ceramic. Subsequent thermal treatment (firing) may be performed in order to favor further polycondensation and enhance mechanical properties. With the viscosity of a sol adjusted into a proper range, both optical quality glass fiber and refractory ceramic fiber can be drawn which are used for fiber optic sensors and thermal insulation, respectively. In addition, uniform ceramic powders of a wide range of chemical composition can be formed by precipitation.

2.4.4 POLYMERIZATION OF METAL ALKOXIDES

Metal alkoxides are members of the family of organometallic compounds, which are organic compounds which have one or metal atoms in the molecule. Metal alkoxides (R-O-M) are like alcohols (R-OH) with a metal atom, M, replacing the hydrogen H in the hydroxyl group. They constitute the class of chemical precursors most widely used in sol-gel synthesis. The most common mineral in the earth's crust is silicon dioxide (or silica), SiO_2. There are at least seven different crystalline forms of silica, including quartz. The basic building block of all of these crystalline forms of silica is the SiO_4 tetrahedron. Since each tetrahedron shares 2 of its edges with other SiO_4 tetrahedra, the overall ratio of oxygen to silicon is 2:1 instead of 4:1 (thus SiO_2). The intricate and highly specific geometry of this network of tetrahedra takes years to form under incredible terrestrial pressures at great depth. That is why SiO_2 is such a good glass former. Crystallization in a reasonable amount of time under the most ideal laboratory conditions is highly unlikely. Thus, amorphous silica is the major component of nearly all window glass. The most thoroughly studied metal alkoxide is silicon tetraethoxide, or tetraethyl orthosilicate (TEOS). The chemical formula for TEOS is given by: $Si(OC_2H_5)_4$, or $Si(OR)_4$ where the alkyl group R = C_2H_5. Metal alkoxide are ideal chemical precursors for sol-gel synthesis because they react readily with water. The reaction is called hydrolysis, because a hydroxyl ion becomes attached to the metal atom as follows:

$$Si(OR)_4 + H_2O \longrightarrow HO\text{-}Si(OR)_3 + R\text{-}OH$$

Depending on the amount of water and catalyst present, hydrolysis may proceed to completion, so that all of the OR groups are replaced by OH groups, as follows:

$$Si(OR)_4 + 4\,H_2O \longrightarrow Si(OH)_4 + 4\,R\text{-}OH$$

Any intermediate species $[(OR)_2\text{–}Si\text{-}(OH)_2]$ or $[(OR)_3\text{–}Si\text{-}(OH)]$ would be considered the result of partial hydrolysis. In addition, two partially hydrolyzed molecules can link together in a condensation reaction to form a siloxane [Si–O–Si] bond:

$$(OR)_3\text{–}Si\text{-}OH + HO\text{–}Si\text{-}(OR)_3 \longrightarrow [(OR)_3Si\text{–}O\text{–}Si(OR)_3] + H\text{-}O$$

$$\text{or } (OR)_3\text{–}Si\text{-}OR + HO\text{–}Si\text{-}(OR)_3 \longrightarrow [(OR)_3Si\text{–}O\text{–}Si(OR)_3] + R\text{-}OH$$

Thus, polymerization is associated with the formation of a 1, 2, or 3-dimensional network of siloxane [Si–O–Si] bonds accompanied by the production of H-O-H and R-O-H species. By definition, condensation liberates a small molecule, such as water or alcohol. This type of reaction can continue to build larger and larger

silicon-containing molecules by the process of polymerization. Thus, a polymer is a huge molecule (or macromolecule) formed from hundreds or thousands of units called monomers. The number of bonds that a monomer can form is called is functionality. Polymerization of silicon alkoxide, for instance, can lead to complex branching of the polymer, because a fully hydrolyzed monomer $Si(OH)_4$ is tetrafunctional (can branch or bond in 4 different directions). Alternatively, under certain conditions (e.g., low water concentration) fewer than 4 of the OR or OH groups (ligands) will be capable of condensation, so relatively little branching will occur. The mechanisms of hydrolysis and condensation, and the factors that bias the structure toward linear or branched structures are the most critical issues of sol-gel science and technology.

2.5 SOL-GEL METHOD

The entire sol-gel reaction mechanism can be described precisely in six steps:

1.Hydrolys

2.Condensation

3.Gelatin

4.Ageing

5.Drying

6.Densification

2.5.1 HYDROLYSIS

Metal salts in aqueous solution, pH and temperature control the hydrolysis

$$M(H_2O)_b^{z+} \leftrightarrow [M(H_2O)^{b-1}OH] + H^+$$

The first step of the hydrolysis of a silicon alkoxide can occur by acid catalyzed or base catalyzed processes, as shown in figure 2.5

ACID CATALYSED

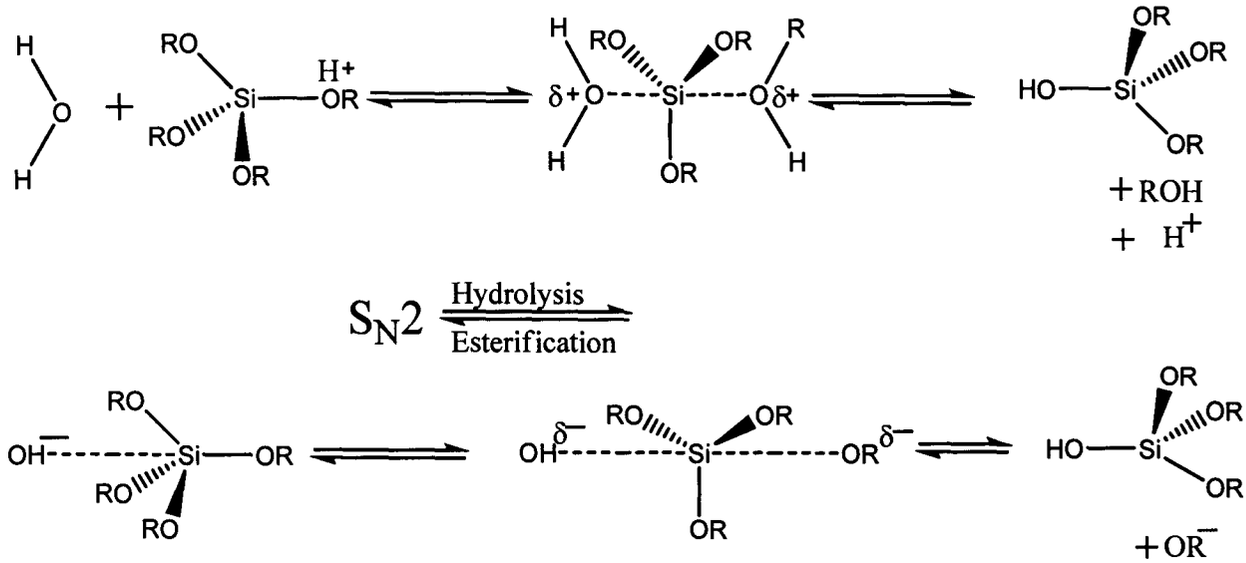

BASE CATALYSED

Fig 2.5 shows the role of acid and base in hydrolyses mechanisms

The effect of the catalysis may be judged by comparing the rate of reaction different pH values, bearing in mind that the isoelectric point of silica (where the equilibrium species has zero net charge) is at pH 2.2. The time to form gel (t_{gel}) gives an indication of the relative rates, as shown in figure 2.2: as expected, the gel time is longest at the isoelectric point, and rapidly decreases in acid or base conditions relative to theisoelectric point pH. (The slight rise at high pH is due to the dissolution of silica in highly alkaline conditions)

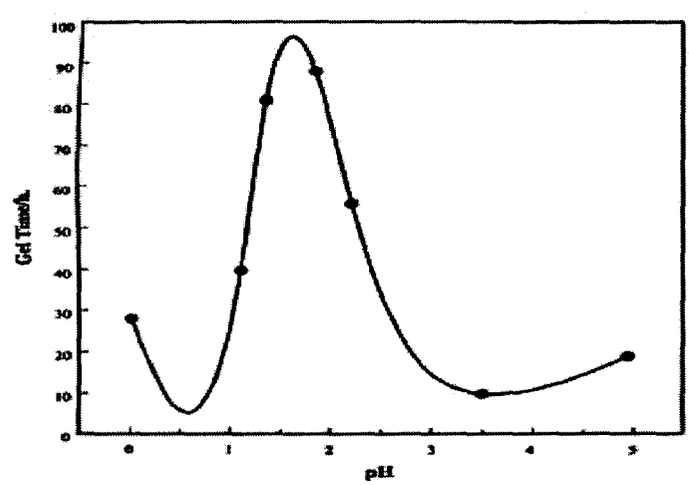

Fig 2.6 Gel time as a function of pH for HCL catalyzed TEOS (H2O: TEOS ratio, R=4)

2.5.1.1 PRECURSOR SUBSTITUENT EFFECTS

The rate trend in acid and base catalyzed process for successive hydrolysis of the four-alkoxy groups around silicon can be understood in terms of electronic effects. Alkoxy groups are electron donating than hydroxy groups. Thus for the positively charged transition state of the acid catalyzed reaction, as more alkoxy groups are replaced by hydroxy groups the transition state become less stabilized and the reaction rate decreases. Conversely, for the negatively charged transition state of the base catalyzed reaction, more OH groups means more stabilization of Transition State and faster reaction. When the rates of hydrolysis of different silicon alkoxides are compared, it is found that the steric bulk of the alkoxy group excretes a large influence. Larger alkoxy group led to more steric hindrance and over crowding of the Transition State, and thus led to slower reactions. Thus tetramethoxy silane (TMOS) hydrolysis faster than tetraethoxy silane (TEOS).

Steric effects: branching and increasing of the chain length lowers the hydrolysis rate

$$Si(OMe)_4 > Si(OEt)_4 > Si(O^n Pr)_4 > Si(O^iPr)4 > Si(O^nBu)\ 4 > Si(OHex)_4$$

Inductive effects: electronic stabilization/destabilization of the transition state.

Electron density at Si decreases:

R-Si > RO-Si > HO-Si > Si-O-Si

2.5.1.2 HYDROPHOBIC EFFECTS AND CO-SOLVANTS

In addition to the above-mentioned electronic and steric effects of the substituents, the hydrophobic or hydrophilic character of the precursor must also be taken into account. Because of the hydrophobic nature of ethoxy groups, TEOS and Water are immiscisble in all proportions and it is necessary to add co-solvent to achieve miscibility to facilitate hydrolysis.

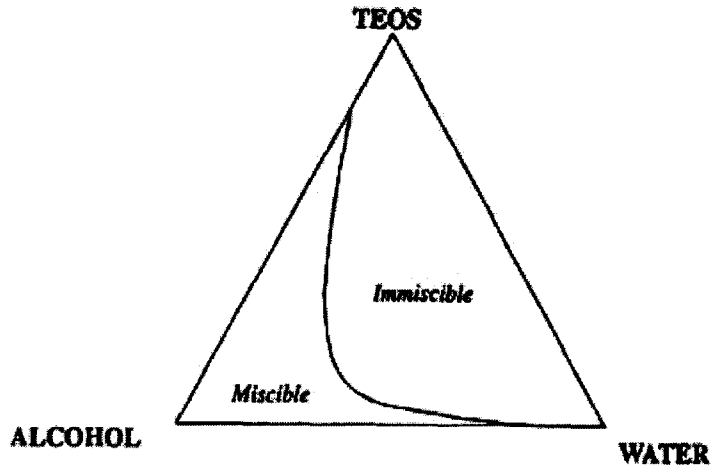

Fig 2.7 The phase diagram for the TEOS/Ethanol/Water

2.5.1.3 EFFECT OF WATER: ALKOXIDE RATIO (R)

The ratio of water: alkoxide determines the amount of co-solvent required, but this ratio also influences the reactions rate. The stoichiometric ratio of water: alkoxide for complete hydrolysis is 2.7:

$$Si(OEt)_4 + 4H_2O \rightarrow Si(OH)_4 + 4EtOH$$

However, less water than this can be used since the condensation reaction leads to production of water.

$$Si(OEt)_3OH + HOSi(OEt)_3 \rightarrow (EtO)_3SiOSi(OEt)_3 + H_2O$$

If the amount of water becomes very small, however, the hydrolysis rate slows down due to reduced reaction concentration. Similarly, if very large amounts of water are used the other reactant (alkoxide) is effectively diluted and gel time increases. The effect of gel time of varying ethanol: TEOS and Water: TEOS molar ratio are shown in figure 2.8.

Small amount of water = slow hydrolysis due to the reduced reactant conc.

Large amount of water = slow hydrolysis due to the reactant dilution

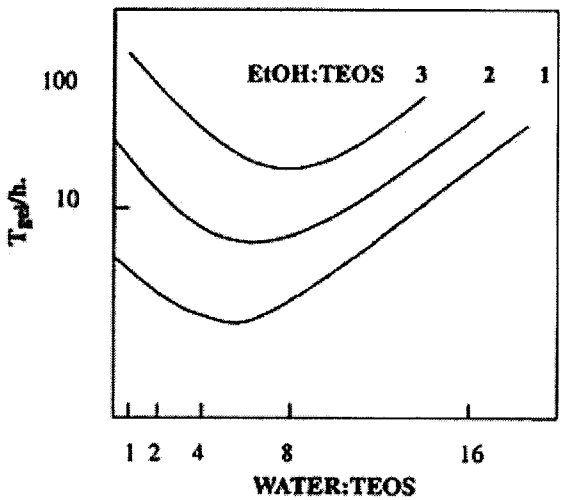

Fig 2.8 Gel time as a function of ethanol: TEOS and Water: TEOS ratio

2.5.2 CONDENSATION

Condensation reaction can be either water condensation (as shown in above) or alcohol condensation:

$$Si(OEt)_3OH + HOSi(OEt)_3 \rightarrow (EtO)_3SiOSi(OEt)_3 + H_2O$$

The reverse reactions are hydrolsis and alcoholsis, respectively. As with initial hydrolysis, condensation reactions may be acid base catalyzed, and in either case the reaction proceed via a rapid formation of charged intermediate by reaction with a proton or hydroxide ion, followed by slow attack of second neutral silicon species on those intermediate.

ACID CATALYSED

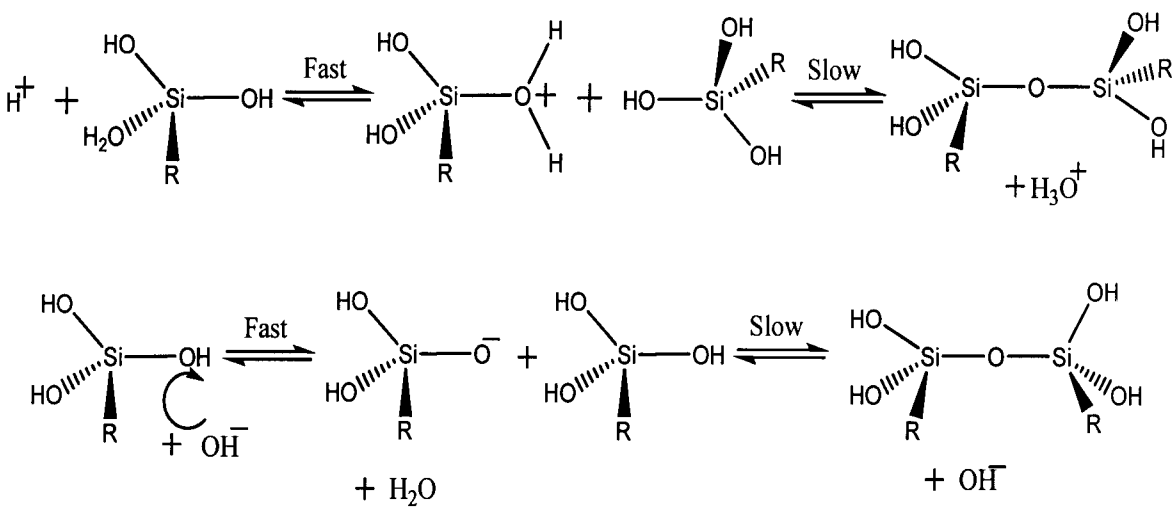

BASE CATALYSED

Fig 2.9 shows the role of condensation Mechanism

2.5.2.1 PRECURSOR SUBSTITUENT EFFECTS

Just as with hydrolysis, the relative rate of different species depends on streic effect and the change on the transition state. Thus for acid hydrolysis with a positively charged transition state stabilized by electron donating groups, $(RO)_3SiOH$ condenses faster than $(RO)_2Si(OH)_2$, Which condenses faster than $(RO)Si(OH)_3$ etc. this means that for acid catalyzed reactions, the first step of the hydrolysis and cross-condensation reactions. In contrast, in base catalyzed conditions the negatively charged transition state becomes more stable as more hydroxy groups replace the electron donating alkoxy groups. Thus successive hydrolysis steps occur increasingly rapidly, and the fully hydrolyzed species undergoes the fastest condensation reactions. As a consequence, in base catalyzed reactions highly cross-linked large sol particles are initially obtained which eventually link to form gels with large pores between the interconnected particles.

2.5.3 GELATIN

1. In the gelation step, alkoxide gel precursors in aqueous solution are hydrolyzed, and polymerize through alcohol or water producing condensations. The gel morphology is influenced by temperature, the concentrations of each species (attention focuses on *r*, the water/alkoxide molar ratio, typically between 1 and 50), and especially acidity:
2. Acid catalysis generally produces weakly-cross linked gels which easily compact under drying conditions, yielding low-porosity microporous (smaller than 2 nm) xerogel structures.
3. Conditions of neutral to basic pH result in relatively mesoporous xerogels after drying, as rigid clusters a few nanometers across pack to form mesopores. The clusters themselves may be microporous.
4. Under some conditions, base-catalyzed and two-step acid-base catalyzed gels (initial polymerization under acidic conditions and further gelation under basic conditions exhibit *hierarchical* structure and complex network topology. The

initial stages of gelation, when the average cluster size is very small, are best modeled

2.5.4 AGEING

2.5.4.1 CROSS-LINKING AND SYNERESIS

NMR studies of gelled samples show a continuing gradual increase in the number of Q^3 and Q^4 Si species (i.e. Si attached via 4 oxygen links to three and four other Si atoms), due to cross-linking via trans-pore condensation reactions of pore-surface hydroxy groups. This can continue for months for samples at room temperature, the rate depending on pH, temperature and gel composition. The net effect of these processes is a stiffening and shrinkage of the sample. Shrinkage occurs because new bonds are formed where there were formerly only weak interactions between surface hydroxy and alkoxy groups. This shrinkage leads to expulsion of liquid from the pores of the gel ,so that gel samples in sealed containers gradually change in appearance from homogeneous gels to transparent shrunken solid monoliths immersed in liquids. This process is known as Syneresis.

2.5.4.2 COARSENING AND RIPENING

Another process associated with ageing is often referred to as coarsening or ripening. In this process, material dissolves from the surface of large particles and deposits on the initially narrow necks, which join particles to each other.

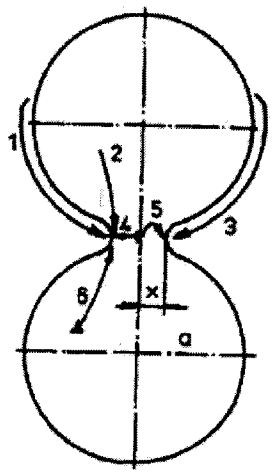

Fig 2.10 Radii of curvature of Particles and "Necks"

The surface of an individual particle has a positive radius of curvature, whereas that of the narrow neck between particles has a smaller negative radius of curvature. There is a pressure gradient across a curved interface between the two media and this leads to a difference in solubility of the material in the two regions. Thus smaller particles will have higher solubility, whereas the regions of negative surface curvature will have low solubility and will tend to accumulate material. This leads to change in the pore size and shapes.

2.5.4.3 SIGNIFICANCE OF AGEING

Ageing effects are often cited as a significant disadvantage in the use of sol-gel materials in technological applications, particularly where the sol-gel method is proposed as a low-temperature mild-condition method for entrapment of organic or biological species. It is therefore important to consider the following points arising from the above discussion:

1. Ageing usually improves the properties of the material.
2. The ageing process can be controlled the by varying the pH. Temperature, Pressure, ageing liquid medium and intial precursor mixture composition, and may thus be optimized.
3. Where regular production is envisaged, ageing need not lead to production delay once an initial aged stock has been generated, provided production requirements can be anticipated.

2.5.5 DRYING

2.5.5.1 THE CONSTANT RATE PERIOD

Initially a gel will shrink by an amount equal to the volume of water or other liquid, which has evaporated. This phase can occur in gels which are still flexible and complaint, and able to adjust to the reduced volume. If the gel becomes rigid due to cross-linking by the time excess water has evaporated, the constant rate period may cease soon. In this case pore size distribution will be strongly influenced by the cross-linking.

2.5.5.2 THE CRITICAL POINT

As gel dries and shrinks, its more compact structure and associated additional cross-linking lead to increased stiffness. At the critical point, the gel become sufficiently

stiff to resist further shrinkage as liquid continues to evaporate. At this point the liquid begins to recede into the porous structure of the gel. Due to its surface tension and the small size of the gel pores, very large pressure is generated across the curved interfaces of the liquid menisci in the pores. Unless the gel has been carefully aged, it will crack due to this capillary stress.

2.5.5.3 CONSEQUENCES OF DRYING

Several interesting observations may be explained in terms of the above stages:

i) As a flat monolith dries with its lower face in contact with the containing
vessel, evaporation is greater from the upper surface. The lower region of the sample therefore has filled pores while an increasingly large region of the upper surface has empty pores. The region of empty pores is able to distribute the residual capillary stress, and thus expands slightly relative to the lower region. Hence these samples tend to develop lower concave surface, even on flat-bottomed containing vessels.

ii) Soluble materials from the bulk of the material may be transported along
the thin film of liquid on pore walls and deposited as a white efflorescence
at or near the surface of the sample. This may be avoided by washing out the material before drying.

iii) As surface layers dry before the bulk of the sample, a slight surface cloudiness may sometimes be observed in partially dried samples depending on pore sizes with a purely atomistic approach.

2.5.5.4 AVOIDING CRACKING

1. All the above problems of stress and cracking may be avoided by the use of supercritical drying. In this process, water is first exchanged for alcohol, which is then removed under super-critical conditions where the distinction between liquid and vapour no longer exists. Hence, no capillary stresses are set up during the drying. This requires high temperatures and pressures, and is expensive and potentially dangerous. The use of alcohol is necessary as the original research showed that silica gel would dissolve in water under the

conditions necessary to obtain supercritical water. One consequence of the use of supercritical alcohol is that the gels are hydrophobic, due to re-esterification reactions of surface hydroxyl groups in supercritical alcohol. These materials are known as aerogels and have only slightly smaller volumes than those of the original wet gels, although they collapse on re-immersion in liquids. Recently progress has been made on the use of supercritical carbon dioxide in this process, although complete preliminary solvent exchange is necessary as Carbon dioxide is immiscible in water. The great advantage of supercritical carbon dioxide is the relatively mild conditions required (31°C and 7.4 Mpa, c.f ethanol 243 °C and 6.4 Mpa).

2. Freeze drying (freezing the liquid in the gel and removal by vacuum sublimation) also avoids the capillary stress effects associated with the direct removal of liquids from gels. However, this cannot be used to produce crack-free dry monoliths, since the water crystallizes and stresses the surrounding matrix in the process, leading to extensive fracturing and pore damage.
3. Various Drying Control Chemical Additives (DCCAs) have been reported. All of these additives modify other properties of the gels to some extent, and may therefore be undesirable and moreover difficult to remove.
4. Ageing gels strengthens them, increasing resistance to cracking. Although this is time consuming, it is cheap, produces more stable and reproducible gel properties and involves no contaminating additives.
5. Since, it is the small pores, which contribute most to capillary stress, synthesis of gels with large pores (> 50 nm) would yield substantial benefits in reducing cracking. For example, mixing commercial colloidal silica with Potassium Silicate at high PH and gelling by addition of formamide gives a product in which silicate polymers are nucleated from solution by the silica colloid. Controlled pore sizes between 10 and 360 nm were obtained by controlling the ratio of the two starting materials and the samples with pore sizes greater than 60 nm could be dried rapidly without cracking, even in dimensions of many centimeters.

2.5.6 DENSIFICATION

2.5.6.1 STAGES OF DENSIFICATION

Although there are many applications of silica gel prepared and dried at or near room temperature (particularly applications which involve entrapping functional organic or biological molecules with in gel pores in mild conditions), heat treatment is necessary for the production of dense glasses and from gels.

1. At low temperature (Typically<200^0C)weight loss occurs as surface water or alcohol is desorbed, but little further shrinkage takes place, and in some cases a net expansion is observed. In this range, the skeletal structure of the silica gel behaves as a molecular solid rather than bulk silica.
2. At intermediate temperature in the range from 150-200^0C to typically 500-700^0C,

   Samples generally show both weight loss and shrinkage. Three processes occur in this range: loss of organics (leading to weight loss but little shrinkage), further consideration (producing both weight loss and shrinkage) and of organics proves that the matrix is still porous in this stage. The space previously occupied by the organics species now become pores with similar size and shape to the organics themselves.
3. At temperature above the upper limit for region (ii) behavior, a sharp increase in

   shrinkage rate is observed with little or no further weight loss. The transition temperature is close to the glass transition temperature for the material; above which viscous flow occur leading to rapid densification as thermal energy permits extended structural reorganization. The densification process is strongly favored thermodynamically because of the very large reduction in surface in surface area of the material and the associated large reduction in interfacial energy.

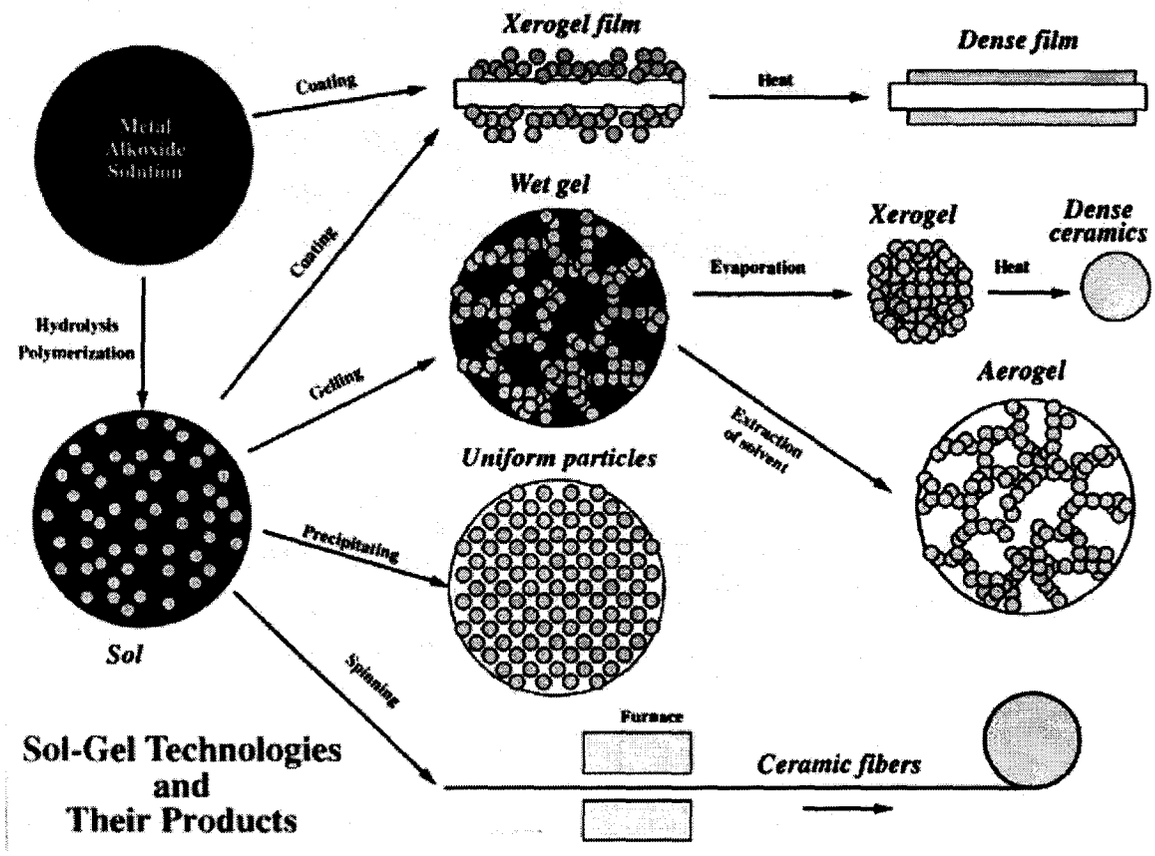

Fig 2.11 shows the systematic diagram in sol-gel route

2.6 ADVANTAGES OF SOL-GEL TECHNIQUE

1. Can produce thin bond-coating to provide excellent adhesion between the metallic substrate and the top coat.
2. Can produce thick coating to provide corrosion protection performance.
3. Can easily shape materials into complex geometries in a gel state.
4. Can produce high purity products because the organo-metallic precursor of the desired ceramic oxides can be mixed, dissolved in a specified solvent and hydrolyzed into a sol, and subsequently a gel, the composition can be highly controllable.
5. Can have low temperature sintering capability, usually 200-600°C.6.
6. Can provide a simple, economic and effective method to produce high quality coatings.
7. The low temperature of sol-gel process is generally below the crystallization temperature for oxide materials, and this allows the production of unusual amorphous materials.

8. The optical quality of materials is often good, leading to application for optical components.
9. By controlling the ageing and drying conditions, further pore size and mechanical strength control may be achieved.
10. Since organmetallic precursors involving different metals are frequently miscible, homogenous controlled doping is easy to achieve.

2.7 LIMITATIONS OF SOL-GEL TECHNIQUE

Despite its advantages, sol-gel technique never arrives at its full industrial potential due to some limitations, e.g. weak bonding, low wear-resistance, high permeability, and difficult controlling of porosity. In particular the limit of the maximum coating thickness is 0.5 μm when the crack-free property is an indispensable requirement. The trapped organics with the thick coating often result in failure during thermal process. The present sol-gel technique is very substrate-dependent, and the thermal expansion mismatch limits the wide application of sol-gel technique.

2.8 ADVANTAGES OF POLYMER COMPONENTS IN SOL-GEL IN SOL GEL CERAMIC

Some substrates, such as mild steel are prone to corrosion during aqueous CB-CSG processing, which typically proceeds in acidic environment of pH=2-4. A conventional method to address this matter is to phosphate the substrate, e.g. using zinc or iron phosphate. However, these thin (less than a few microns) and micro-porous phosphate films are unstable at the elevated process temperature of chemical bonding of 300°C that may lead to additional interfacial porosity and opening again access of corrosive species to steel surface. Such coating system will not provide long-term corrosion protection to the steel surface.

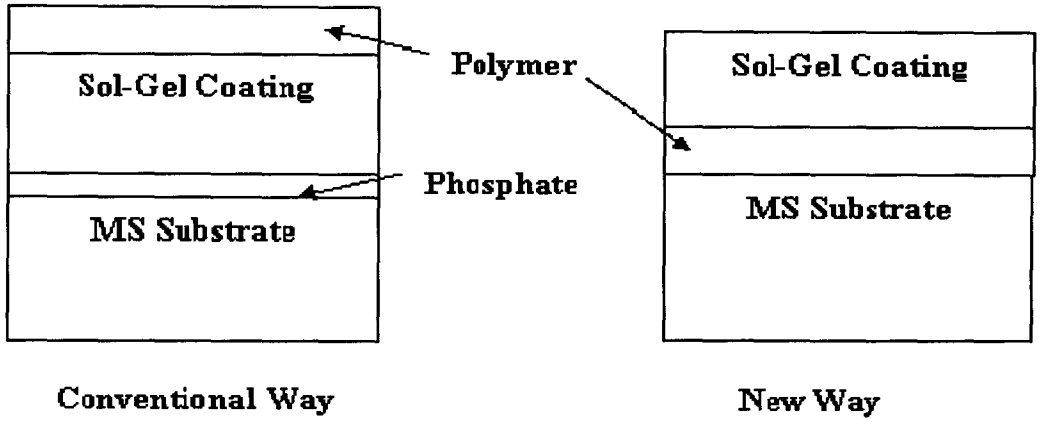

Fig 2.12 Comparison of conventional and new sol-gel coating on mild steel (MS)

In order to overcome some of the limitations of traditional CB-CSG coatings, we have developed a non-porous and thermally stable "bond-coat" alumina reinforced siloxane film (ASMC) on a mild steel surface (Fig. 2.12), which would protect the surface both during CB-CSG processing, as well as provide a non-permeable membrane for corrosion protection in storage and service[10]. Therefore, in this system the "topcoat" of CB-CSG protects the siloxane bond coat (and the metallic substrate) from the wear damage. The siloxane bond coat provides a fluid impermeable function and relaxes the thermal stresses. We sometimes term it "multi-layer functionally graded bond coating" (FGBC). At the initial stage, we hypothesized that the multilayer functionally gradient coating systems additionally benefited from relaxing interfacial thermal-strain during cooling from the process temperature through elastic and plastic deformation of the siloxane bond coat, which notably increased the bond strength of the entire coating system by releasing the energy of the CTE mismatch. Moreover, we will note that this bond strength increased the intrinsic adhesion of the coating significantly by its unique way of relaxing the thermal stress. However, if polymeric components were directly added into the ceramic sol, people usually think that it will risk reducing the connectivity of the sol-gel network and decreasing condensation reaction rates (i.e., a longer time) during the gelling which, in turn, will result in a less dense microstructure of gel network upon the removal of solvent. If the impregnation of polymer took place after the gel process, it is believed that it will prevent the reduced adhesion between the coating and substrate, and then decrease the permeability.

2.8 APPLICATIONS

The applications for sol gel-derived products are numerous. For example, scientists have used it to produce the world's lightest materials and also some of its toughest ceramics. One of the largest application areas is thin films, which can be produced on a piece of substrate by spin-coating or dip-coating. Other methods include spraying, electrophoresis, inkjet printing or roll coating. Optical coatings, protective and decorative coatings, and electro-optic components can be applied to glass, metal and other types of substrates with these methods. Cast into a mold, and with further drying and heat-treatment, dense ceramic or glass articles with novel properties can be formed that cannot be created by any other method. Macroscopic optical elements and active optical components as well as large area hot mirrors, cold mirrors, lenses and beam splitters all with optimal geometry can be made quickly and at low cost via the sol-gel route. With the viscosity of a sol adjusted into a proper range, both optical and refractory ceramic fibers can be drawn which are used for fiber optic sensors and thermal insulation, respectively. Ultra-fine and uniform ceramic powders can be formed by precipitation. These powders of single and multiple component compositions can be made in sub-micrometre particle size for dental and biomedical applications. Composite powders have been patented for use as agrochemicals and herbicides. Also powder abrasives, used in a variety of finishing operations, are made using a sol-gel type process. One of the more important applications of sol-gel processing is to carry out zeolite synthesis. Other elements (metals, metal oxides) can be easily incorporated into the final product and the silicalite sol formed by this method is very stable. Other products fabricated with this process include various ceramic membranes for microfiltration, ultrafiltration, nanofiltration, pervaporation and reverse osmosis. If the liquid in a wet gel is removed under a supercritical condition, a highly porous and extremely low density material called aerogel is obtained. Drying the gel by means of low temperature treatments (25-100 °C), it is possible to obtain porous solid matrices called xerogels. Finally of historical note, a sol-gel process was developed in the 1950s for the production of radioactive powders of UO_2 and ThO_2 for nuclear fuels, without generation of large quantities of dust.

CHAPTER-3

NONLINEARITY

3.1 INTRODUCTION

3.1.1 LINEAR OPTICS

When an electromagnetic wave propagates through a dielectric medium its behaviour is entirely described by the relation between the polarization density vector P(r ,t) and the electric field vector E(r,t). A transparent dielectric medium placed in an electric field becomes electrically polarized and the displacement of electron density away from the nucleus results in a charge separation called induced dipole with a dipole moment Pi. The displacement of charge from equilibrium position is proportional to the strength of the field

$$Pi = \alpha' E \qquad \text{..... (1)}$$

Where, α' is the linear polarizability of the molecule or atom and E is the applied electric field. The induced polarization will have the same frequency and phase as that of the oscillating field if the response is instantaneous. The polarization density P is given as

$$P = \varepsilon_o \chi E \qquad \text{..... (2)}$$

Where, ε_o is the permittivity of the free space and χ is the dielectric susceptibility of the medium and the quantity is a constant in the sense of being independent of E, and its magnitude is a function of frequency.

3.1.2 NONLINEAR OPTICS

Nonlinear optics describes the behaviour of light in nonlinear media, ie, media in which the dielectric polarization responds nonlinearly to the electric field E of the light. The nonlinearity is observed only at very high light intensities.

The nonlinear polarization is given by the equation,

$$P = \varepsilon_o \left[\chi^{(1)} E_0 \cos wt + \chi^{(2)} E^2 + \chi^{(3)} E^{3+} \text{.....} \right] \qquad \text{...(3)}$$

Where,$\chi^{(1)}$ is the first order susceptibility, ,$\chi^{(2)}$ and ,$\chi^{(3)}$ are the second and third order susceptibilities respectively. The optical characteristics of a medium such as dielectric permittivity, refractive index etc which depend on susceptibility also become functions of field strength E. The optical nonlinearity is the property of the

medium through which it pass through and not the property of the light itself. The nonlinear polarization contains new frequency components, which are not present in the exciting beam. Table 3.1 gives a comparison between linear and non-linear optics.

Table 3.1 Comparison of Linear Optics (LO) and Non-Linear Optics (NLO)

Linear optics	Non linear optics
$P=\varepsilon\chi_{ij}^{(1)} Ej$, Where: ε is permitivity of free space $\chi_{ij}^{(1)}$ is linear susceptibility.	Using power series, polarization can be expanded as $P= \varepsilon(\chi^{(1)} E+ \chi^{(2)} E.E+ \chi^{(3)} E.E.E....)$ Where $\chi^{(1)}$, $\chi^{(2)}$, $\chi^{(3)}$.... are n^{th} orders of non-linear susceptibility.
The magnitude of the electric field is small.	The magnitude of the electric field is large.
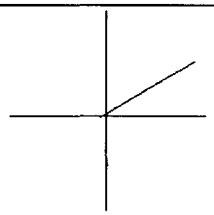 The graph of polarization (Vertical Axis) versus electric field (Horizontal Axis)	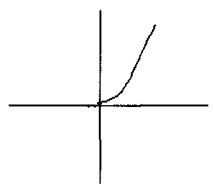 The graph of polarization (Vertical Axis) versus electric field (Horizontal Axis)

3.2 ORIGIN OF THE TERM NON-LINEAR OPTICS

In this section we will see from where the word linear and non-linear optics came. If the laser radiation is sufficiently intensive (so that optical characteristics are functions of light intensity), susceptibility χ stops being constant and becomes a function of field strength E in the light wave. Theory shows that in the first approximation of this function can be expressed as a sum.

i.e. $$\chi(E) = \chi_0 + \chi_1 E + \chi_2 E^2 + ... \qquad \text{.....(4)}$$

Where χ_0, χ_1, χ_2..... are parameters of a medium characterizing its polarizability. Note that all optical characterization of the mediums not only susceptibility but also dielectric permittivity and refractive index become functions of field strength in sufficiently intensive light fields. We recall that polarization is given by

$$P = \chi E \qquad \text{.....(5)}$$

Substituting above equation (4) in to (5) P, we obtain

$$P = \chi_0 E + \chi_1 E^2 + \chi_2 E^3 + ... \qquad .....(6)$$

Equation shows nonlinear with respect to field strength in the wave. Hence the term non-linear optics. If the field of strength in the light field is sufficiently low, only the first term can be retained and equation (6) becomes

$$P = \chi_0 E \qquad ..... (7)$$

This situation precisely corresponds to the pre-laser optics. Polarization of the medium is described by a linear formula given by equation (7).

Hence the term linear optics. The relation between wave field strength and polarization of the medium is therefore linear if the light wave strength is relatively low; the medium's polarizability is represented then by the parameter χ_0 called the linear susceptibility. If, however, the light field strength in the laser beam is sufficiently high, the relation in question becomes non linear; additional parameters (χ_1, χ_2.....) referred to as nonlinear susceptibility and then required to describe polarizability of the medium.

3.2.1 NON-LINEAR POLARIZATION OF THE MEDIUM ALLOWS MIXING OF FREQUENCY

Let the polarization of a non-linear medium be

$$P = \chi_0 E + \chi_1 E^2 \qquad .....(8)$$

We assume that two coherent light waves with unequal frequencies are incident on the medium; $E_1 \cos(2\pi\nu_1 t)$ and $E_2 \cos(2\pi\nu_2 t)$. If the sum of these waves

$E = E_1 \cos(2\pi\nu_1 t) + E_2 \cos(2\pi\nu_2 t)$ is substituted in equation, the final expression for the polarization of the medium will contain a term

$$P_{1,2} = 2\chi_1 E_1 E_2 \cos(2\pi\nu_1 t)\cos(2\pi\nu_2 t) \qquad .....(9)$$

Making use of relation $2\cos\alpha\cos\beta = \cos(\alpha+\beta) + \cos(\alpha-\beta)$, we transfer equation to the following

$$P_{1,2} = \chi_1 E_1 E_2 \cos(2\pi(\nu_1 + \nu_2)t) + \chi_1 E_1 E_2 \cos(2\pi(\nu_1 - \nu_2)t) \qquad ... (10)$$

The fact that the expression for non-linear polarization of the medium contains the term means that light can be re-emitted at the frequency $\nu_1 + \nu_2 and \nu_1 - \nu_2$. Hence, non-linear mediums make it possible to realize summation and subtraction of light

wave frequencies. Here we saw what non-linear and linear optics mean. In the coming section we try to compare the linear and non-linear optics.

3.2.2 PHYSICS OF NONLINEAR LIGHT TRANSMISSION

Depending on the characteristic response of the medium to the frequency of light, the transmission of light through a medium gets affected by the scattering or absorption of the light by the medium. When the intensity of the input light is such that the corresponding electric field is sufficient to evoke the otherwise small nonlinear terms in the dipole oscillation, it modifies the properties of the medium. The light will in turn get affected. The change in transmittance of a medium as a function of the input intensity or fluence is referred to as nonlinear absorption or nonlinear light transmission. At sufficiently high intensities, the probability of an absorber absorbing more than one photon before relaxing to the ground state can be enhanced.

3.3 SECOND AND THIRD ORDER NONLINEAR POLARIZATION

The second order nonlinear polarization occurs in crystals with noncentro symmetric crystal structure or in antistrophic materials. The nonlinear polarization then has a component, which depends quadratically on the electric field of an incident light wave. The third order nonlinearity occurs in case of Centro–symmetric crystals and other media, which exhibit inversion symmetry. The electric polarization can only have odd power electric field amplitudes. The electric displacement D of the medium is given by the equation

$$D = \varepsilon_0 E + P = \varepsilon_0 \left(1 + \chi^{(1)}\right) E + \varepsilon_0 \chi(3) E^3 = \varepsilon_0 (1 + \chi^{(1)} + \chi^{(3)} E^2) E \quad \ldots\ldots\ldots\ldots$$

(11) The linear dielectric constant,

$$\varepsilon_1 = \varepsilon_0 \left(1 + \chi^{(1)}\right) \quad \ldots\ldots\ldots\ldots$$

(12)

Nonlinear change in dielectric constant produced by the applied field,

$$\varepsilon_2 E^2 = \chi^{(3)} E^2 \quad \ldots\ldots\ldots\ldots$$

(13)

The nonlinear dependence of index of refraction on the applied signal strength is given by $n = no + n_2 I$

$$no = \left(\frac{\varepsilon_1}{\varepsilon_2}\right)^{1/2}$$ = Linear refractive index

n_2I = The intensity dependent nonlinear refractive index.

3.4 NONLINEAR ABSORPTION

3.4.1 TWO-PHOTON ABSORPTION

The process of the transition of a system from the ground state to a higher level by the simultaneous absorption of two photons from an incident radiation field is termed as two-photon absorption. Two-Photon Absorption (TPA) spectroscopy complements linear absorption spectroscopy in studying the excited state of a system. Two photons of frequency ω of the incident field are simultaneously absorbed by the system to make the transition to a state that is approximately resonant at 2ω. The intermediate level being virtual, the two photons should be simultaneously absorbed making the process sensitive to the instantaneous optical intensity of the incident radiation. On the other hand, the two-step absorption that involves a single photon pumped real intermediate state is referred to as excited state absorption. The two-photon absorption process is proportional to on the square of the input intensity. The propagation of the laser light (which is sufficiently intense to initiate the nonlinear light –matter interaction), through the system describing the optical loss is given by

$$\frac{dI}{dz} = -\alpha I - \beta I^2 \qquad \text{.....}$$

(14)

where α is the linear absorption coefficient (which can be very small) and β the two-photon absorption coefficient. β is a macroscopic parameter that characterizes the material and is related to the individual molecular TPA absorption cross section σ_2 through

$$\sigma_2 = \frac{\hbar\omega\beta}{N} \qquad \text{.....} \quad (15)$$

Where N is the number density of the molecules in the system and ω is the incident radiation frequency. It is the imaginary part of the third order nonlinear susceptibility of the system that determines the strength of the two-photon absorption. The relation between the TPA coefficient and the third order susceptibility of a centrosymmetric system for linearly polarized incident light is given as:

$$\beta = \frac{3\pi}{\varepsilon_0 n^2 c\lambda} \mathrm{Im}[\chi^{(3)}_{xxxx}(-\omega;\omega,\omega,-\omega)] \qquad \text{(in SI units)} \quad \ldots\ldots\ldots$$

(16)

Since the physical quantity that is measured is the transmitted energy in a typical light transmission measurement, the transmittance is conveniently defined as the ratio of the transmitted and incident energies. For a pulsed laser beam that is spatially and temporally Gaussian the transmittance T in the presence of TPA is given as:

$$T = \frac{(1-R)^2 \exp(-\alpha L)}{\sqrt{\pi} q_0} \int_{-\infty}^{\infty} \ln[1 + q_0 \exp(-\tau^2)] d\tau \quad \ldots\ldots\ldots$$

(18)

where R is the Fresnel reflection at the interface of the material with air, α the linear absorption coefficient and L the length of the medium. q_0 is given by

$$q_0 = \beta(1-R) I_0 L_{eff} \quad \ldots\ldots\ldots\ldots$$

(19)

where I_0 is the peak on-axis intensity incident on the material from air. The effective length in the medium is given as:

$$L_{eff} = \frac{1 - \exp(-\alpha L)}{\alpha} \quad \ldots\ldots\ldots\ldots \quad (20)$$

3.4.2 THREE-PHOTON ABSORPTION

The simultaneous absorption of three photons by a system from an incident radiation field is known as three-photon absorption (3PA). It is a fifth order nonlinear process, and the propagation equation for a medium having significant three-photon absorption is given as

$$\frac{dI}{dz} = -\alpha I - \gamma I^3 \quad \ldots\ldots\ldots\ldots \quad (21)$$

where α is the linear absorption , which can be typically small, and γ is the three-photon absorption coefficient. For a centrosymmetric system and linearly polarized light, γ is related to the imaginary part of the fifth order susceptibility through [Sutherland pg. 589]

$$\gamma = \frac{5\pi}{\varepsilon_0^{\,2} n^3 c^2 \lambda} \mathrm{Im}[\chi^{(5)}_{xxxxx}(-\omega;\omega,\omega,\omega,-\omega,-\omega)] \text{ (in SI units)} \quad \text{..... (22)}$$

The transmittance of a system with three-photon absorption, when the incident laser that is spatially and temporally Gaussian, is given as:

$$T = \frac{(1-R)^2 \exp(-\alpha L)}{\sqrt{\pi} p_0} \int_{-\infty}^{\infty} \ln[\sqrt{1 + p_0^{\,2} \exp(-2\tau^2)} + p_0 \exp(-\tau^2)] d\tau \quad \text{..... (23)}$$

where $p_0 = \sqrt{2\gamma(1-R)^2 I_0^{\,2} L'_{eff}}$ ..... (24)

with $L'_{eff} = \dfrac{1-\exp(-2\alpha L)}{2\alpha}$ ..... (25)

3.5 NONLINEAR MEASUREMENTS- Z SCAN TECHNIQUE

3.5.1 OPEN APERTURE Z-SCAN SETUP

We used the open aperture zscan experiment [Sheik Bahae *et al.*] to measure the nonlinear transmission in the samples. The experimental set up is given in figure 2.1.

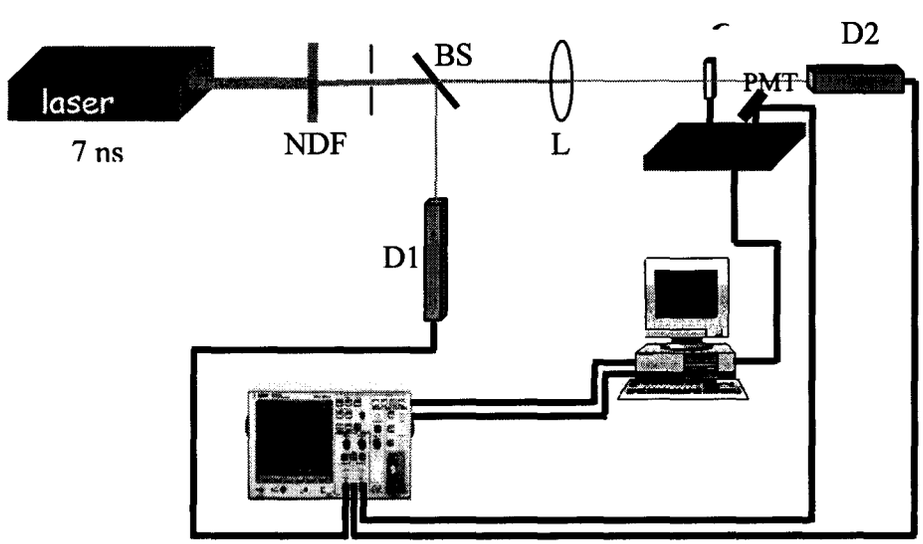

Figure 3.1: Typical zscan experimental set up. NDF: Neutral density filters, BS: Beam Spliter, L: Lens, D1 & D2: Detector 1 & 2

In the z-scan, the laser beam is focused using a lens, and the sample is translated along the beam axis (z-axis) through the focal region, over a length several times that of the confocal distance. At each position z the sample sees a different laser fluence, and the position dependent (i.e., fluence dependent) transmission is measured using a pyroelectric energy probe placed after the sample. The focal beam spot size is measured to be 20 ± 2 μm in our experiment. By running the laser flash lamps at full

power, the pulse to pulse energy stability is improved to better than ±5%; these small fluctuations are nevertheless accounted for by using a reference energy probe in the experiment. Energy reaching the sample is appropriately reduced using neutral density filters. The samples are subjected to a smoothly varying input laser intensity by scanning them through the focal region by using a stepper motor driven translation stage. Data acquisition is done using a storage oscilloscope that is interfaced to a computer via serial port communication. The stepper motor is also controlled by the computer using the parallel port.

3.6 APPLICATION OF NONLINEARITY: OPTICAL LIMITING

3.6.1 INTRODUCTION

Controlling the intensity of light in a predetermined manner is the important requirement in the field of optical communications and optical computing. There are various methods to switch, limit, amplify or modulate the amplitude of an optical signal and they are broadly classified into two types as dynamic and passive methods.The device with active feedback comes under dynamic control. Dynamic devices have number of disadvantages like increased complexity and slower speeds. The increased complexity is due to multiple components. But, in contrast the passive control is accomplished by using nonlinear optical material. There are two different types of passive devices used to control amplitude of optical signal they are optical switches and optical limiters.

3.6.2 PASSIVE OPTICAL LIMIT

There are a variety of nonlinear optical phenomena that can be used to construct optical limiters. These include two photon absorption, free carrier absorption, self-focusing, photo refraction and optically induced scattering.

3.6.2.1 TWO PHOTON ABSORPTION

It involves the simultaneous absorption of two photons from an incident electromagnetic field to excite an electron from its initial state to a final state. The electron can be assumed to be passing through an intermediate virtual state. Two-photon absorption is an instantaneous nonlinear process. As the two-photon absorption coefficient ß is small in usual materials, high energies are required to really observe two-photon absorption in such materials.

3.6.2.2 REVERSE SATURABLE ABSORPTION

Reverse saturable absorption occurs in systems where excited state absorbs stronger than the ground state. To understand the process let $\sigma 1$ be the cross-section of absorption from ground state and $\sigma 2$ be the cross section of absorption from first excited state to second excited state. When the material absorbs light, the first excited $\sigma 2$ state becomes more populated and contributes to total absorption cross-section. Now, if $\sigma 2$ is smaller than $\sigma 1$ the material becomes more transparent at high intensities. Such a material is called a saturable absorber. But, if $\sigma 1$ is larger than $\sigma 2$ then the total absorption increases and the material becomes a reverse saturable absorber.

3.6.2.3 FREE CARRIER ABSORPTION

The optically generated charge carriers can be excited to higher energy state either by single or two-photon absorption and this process is often phonon assisted. This phonon assisted absorption phenomenon is referred to as free carrier absorption. It is a cumulative nonlinearity since it depends upon the build up of carrier population in the band as the incident optical pulse energy is absorbed. This process plays a role on semiconductor limiter where significant charge carriers are produced.

3.6.2.4 NONLINEAR REFRACTION

Optical limiters based on self-focusing and defocusing effect form another class of promising devices. Both self-focusing and defocusing limiters operate by refracting the incident light. A converging lens is used to focus the incident laser beam on the nonlinear medium and the output beam from the nonlinear medium passes through an aperture before falling on the detector. When a nonlinear refraction occurs within the medium it results in generation of spatially non-uniform refractive index, which allows the sample to act as either negative or positive lens, which depends on the refractive nonlinearity caused by the incident beam. Self-focusing effect will lead to damage of the nonlinear medium.

3.6.2.5 INDUCED SCATTERING

Scattering mechanism is caused by light interaction with small scattering centers, this scattering can be highly directional and uniform depending on the size of the scattering centers. The scattering results in a reduced transmission of the medium. The scattering centers induced by optical signal is reversible in case of liquid medium because the excited liquid can return to equilibrium if chemical or structural decomposition has not occurred. Even if such decomposition occurs then it still get

reversed because the illuminated portion can be refreshed either by diffusive process or by circulation. However the scattering centers generated in solid medium are not usually reversed since the decomposition process will result in degradation in the linear operation of the sample.

There are two types of scattering: "Rayleigh scattering" where the scattering centers are much smaller than the wavelength of light or where the particles are nonabsorbent, and "Mei scattering" where the particle size is comparable or larger than wavelength of light. Limiting based on Mie scattering is less effective when compared to Rayleigh scattering because as the size of the scattering particle increases then most of the scattered radiation is forward scattered.

3.6.3 APPLICATION OF OPTICAL LIMITERS

Optical limiters are utilized in a case where a decreasing transmission is needed with increasing excitation. These devices can be used for various applications like pulse shaping, passive mode locking, smoothing of amplitude modulated pulse, pulse compression, to reduce background in pulsed, and infrared excited photo thermal spectroscopy and protection in optical systems etc.

CHAPTER-4

SAMPLE CHARACTERIZATION

The prepared nanomaterials are characterized by means of Atomic force Microscope, Scanning Electron Microscope, UV-Visible absorption spectra, Fourier Infrared Spectroscopy, and X-Ray diffraction. These characterization techniques are discussed in detail in this chapter.

4.1 ATOMIC FORCE MICROSCOPY

The atomic force microscope (AFM) or scanning force microscope (SFM) is a very high-resolution type of scanning probe microscopy, with demonstrated resolution of fractions of a nanometer, more than 1000 times better than the optical diffraction limit. The precursor to the AFM, the scanning tunneling microscope, was developed by Gerd Binnig and Heinrich Rohrer in the early 1980s, a development that earned them the Nobel Prize for Physics in 1986.

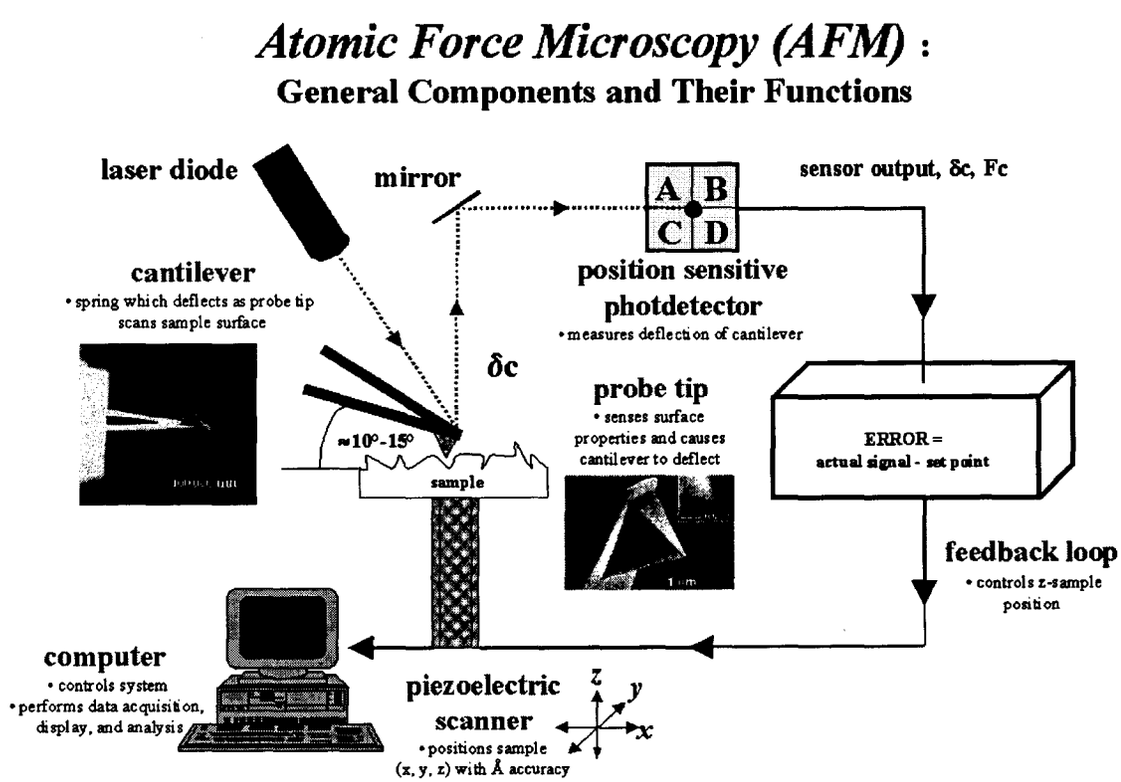

Fig. 4.1 Schematic of a traditional AFM setup

Binnig, Quate and Gerber invented the first AFM in 1986. The AFM is one of the foremost tools for imaging, measuring and manipulating matter at the nanoscale. The information is gathered by "feeling" the surface with a mechanical probe.

Piezoelectric elements that facilitate tiny but accurate and precise movements on (electronic) command enable the very precise scanning.

4.1.1 BASIC PRINCIPLE

The AFM consists of a microscale cantilever with a sharp tip (probe) at its end that is used to scan the specimen surface. The cantilever is typically silicon or silicon nitride with a tip radius of curvature on the order of nanometers. When the tip is brought into proximity of a sample surface, forces between the tip and the sample lead to a deflection of the cantilever according to Hooke's law. Depending on the situation, forces that are measured in AFM include mechanical contact force, Van der Waals forces, capillary forces, chemical bonding, electrostatic forces, magnetic forces (see Magnetic force microscope (MFM)), Casimir forces, solvation forces etc. As well as force, additional quantities may simultaneously be measured through the use of specialized types of probe (see Scanning thermal microscopy, photothermal microspectroscopy, etc.). Typically, the deflection is measured using a laser spot reflected from the top surface of the cantilever into an array of photodiodes. Other methods that are used include optical interferometry, capacitive sensing or piezoresistive AFM cantilevers. These cantilevers are fabricated with piezoresistive elements that act as a strain gauge. Using a Wheatstone bridge, strain in the AFM cantilever due to deflection can be measured, but this method is not as sensitive as laser deflection or interferometry.

If the tip was scanned at a constant height, a risk would exist that the tip collides with the surface, causing damage. Hence, in most cases a feedback mechanism is employed to adjust the tip-to-sample distance to maintain a constant force between the tip and the sample. Traditionally, the sample is mounted on a piezoelectric tube, that can move the sample in the z direction for maintaining a constant force, and the x and y directions for scanning the sample. Alternatively a 'tripod' configuration of three piezo crystals may be employed, with each responsible for scanning in the x,y and z directions. This eliminates some of the distortion effects seen with a tube scanner. In newer designs, the tip is mounted on a vertical piezo scanner while the sample is being scanned in X and Y using another piezo block. The resulting map of the area $s = f(x,y)$ represents the topography of the sample.

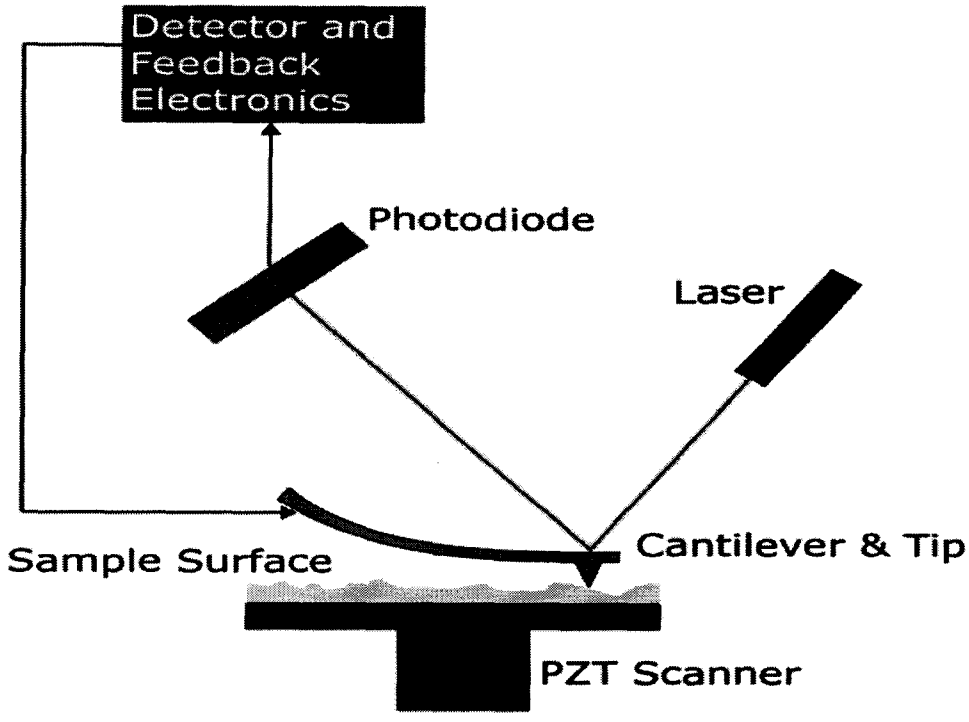

Fig 4.2: Schematic of the AFM cantilever and detector

The AFM can be operated in a number of modes, depending on the application. In general, possible imaging modes are divided into static (also called Contact) modes and a variety of dynamic (or non-contact) modes where the cantilever is vibrated.

4.1.2 IMAGING MODES

The primary modes of operation are static (contact) mode and dynamic mode. In the static mode operation, the static tip deflection is used as a feedback signal. Because the measurement of a static signal is prone to noise and drift, low stiffness cantilevers are used to boost the deflection signal. However, close to the surface of the sample, attractive forces can be quite strong, causing the tip to 'snap-in' to the surface. Thus static mode AFM is almost always done in contact where the overall force is repulsive. Consequently, this technique is typically called 'contact mode'. In contact mode, the force between the tip and the surface is kept constant during scanning by maintaining a constant deflection. In the dynamic mode, the cantilever is externally oscillated at or close to its fundamental resonance frequency or a harmonic. The oscillation amplitude, phase and resonance frequency are modified by tip-sample interaction forces; these changes in oscillation with respect to the external reference oscillation provide information about the sample's characteristics. Schemes for dynamic mode operation include frequency modulation and the more common amplitude modulation. In frequency modulation, changes in the oscillation frequency

provide information about tip-sample interactions. Frequency can be measured with very high sensitivity and thus the frequency modulation mode allows for the use of very stiff cantilevers. Stiff cantilevers provide stability very close to the surface and, as a result, this technique was the first AFM technique to provide true atomic resolution in ultra-high vacuum conditions (Giessibl).

In amplitude modulation, changes in the oscillation amplitude or phase provide the feedback signal for imaging. In amplitude modulation, changes in the phase of oscillation can be used to discriminate between different types of materials on the surface. Amplitude modulation can be operated either in the non-contact or in the intermittent contact regime. In ambient conditions, most samples develop a liquid meniscus layer. Because of this, keeping the probe tip close enough to the sample for short-range forces to become detectable while preventing the tip from sticking to the surface presents a major hurdle for the non-contact dynamic mode in ambient conditions. Dynamic contact mode (also called intermittent contact or tapping mode) was developed to bypass this problem (Zhong et al.). In dynamic contact mode, the cantilever is oscillated such that the separation distance between the cantilever tip and the sample surface is modulated. Amplitude modulation has also been used in the non-contact regime to image with atomic resolution by using very stiff cantilevers and small amplitudes in an ultra-high vacuum environment.

4.1.2.1 TRAPPING MODE

In *tapping mode* the cantilever is driven to oscillate up and down at near its resonance frequency by a small piezoelectric element mounted in the AFM tip holder. The amplitude of this oscillation is greater than 10 nm, typically 100 to 200 nm. Due to the interaction of forces acting on the cantilever when the tip comes close to the surface, Van der Waals force or dipole-dipole interaction, electrostatic forces, etc cause the amplitude of this oscillation to decrease as the tip gets closer to the sample. An electronic servo uses the piezoelectric actuator to control the height of the cantilever above the sample. The servo adjusts the height to maintain a set cantilever oscillation amplitude as the cantilever is scanned over the sample. A *Tapping AFM* image is therefore produced by imaging the force of the oscillating contacts of the tip with the sample surface. This is an improvement on conventional contact AFM, in which the cantilever just drags across the surface at constant force and can result in surface damage. Tapping mode is gentle enough even for the visualization of supported lipid

bilayers or adsorbed single polymer molecules (for instance, 0.4 nm thick chains of synthetic polyelectrolytes) under liquid medium. At the application of proper scanning parameters, the conformation of single molecules remains unchanged for hours (Roiter and Minko, 2005).

4.2.1.2 NON-CONTACT MODE

Here the tip of the cantilever does not contact the sample surface. The cantilever is instead oscillated at a frequency slightly above its resonance frequency where the amplitude of oscillation is typically a few nanometers (<10nm). The van der Waals forces, which are strongest from 1nm to 10nm above the surface, or any other long range force which extends above the surface acts to decrease the resonance frequency of the cantilever. This decrease in resonance frequency combined with the feedback loop system maintains a constant oscillation amplitude or frequency by adjusting the average tip-to-sample distance. Measuring the tip-to-sample distance at each (x,y) data point allows the scanning software to construct a topographic image of the sample surface.

Non-contact mode AFM does not suffer from tip or sample degradation effects that are sometimes observed after taking numerous scans with contact AFM. This makes non-contact AFM preferable to contact AFM for measuring soft samples. In the case of rigid samples, contact and non-contact images may look the same. However, if a few monolayers of adsorbed fluid are lying on the surface of a rigid sample, the images may look quite different. An AFM operating in contact mode will penetrate the liquid layer to image the underlying surface, whereas in non-contact mode an AFM will oscillates above the adsorbed fluid layer to image both the liquid and surface.

4.1.3 AFM -BEAM DEFLECTION DETECTION

Laser light from a solid state diode is reflected off the back of the cantilever and collected by a position sensitive detector (PSD) consisting of two closely spaced photodiodes whose output signal is collected by a differential amplifier. Angular displacement of cantilever results in one photodiode collecting more light than the other photodiode, producing an output signal (the difference between the photodiode signals normalized by their sum) which is proportional to the deflection of the cantilever. It detects cantilever deflections <1Å (thermal noise limited). A long beam path (several cm) amplifies changes in beam angle.

4.1.4 FORCE SPECTROSCOPY

Another major application of AFM (besides imaging) is force spectroscopy, the measurement of force-distance curves. For this method, the AFM tip is extended towards and retracted from the surface as the static deflection of the cantilever is monitored as a function of piezoelectric displacement. These measurements have been used to measure nanoscale contacts, atomic bonding, Van der Waals forces, and Casimir forces, dissolution forces in liquids and single molecule stretching and rupture forces (Hinterdorfer & Dufrêne). Forces of the order of a few pico-Newton can now be routinely measured with a vertical distance resolution of better than 0.1 nanometer.

Problems with the technique include no direct measurement of the tip-sample separation and the common need for low stiffness cantilevers which tend to 'snap' to the surface. The snap-in can be reduced by measuring in liquids or by using stiffer cantilevers, but in the latter case a more sensitive deflection sensor is needed. By applying a small dither to the tip, the stiffness (force gradient) of the bond can be measured as well (Hoffmann et al.).

4.1.5 IDENTIFICATION OF INDIVIDUAL SURFACE ATOMS

The AFM can be used to image and manipulate atoms and structures on a variety of surfaces. The atom at the apex of the tip "senses" individual atoms on the underlying surface when it forms incipient chemical bonds with each atom. Because these chemical interactions subtly alter the tip's vibration frequency, they can be detected and mapped. Physicist Oscar Custance (Osaka University, Graduate School of Engineering, Osaka, Japan) and his team used this principle to distinguish between atoms of silicon, tin and lead on an alloy. The trick is to first measure these forces precisely for each type of atom expected in the sample. The team found that the tip interacted most strongly with silicon atoms, and interacted 23% and 41% less strongly with tin and lead atoms, respectively. Thus, each different type of atom can be identified in the matrix as the tip is moved across the surface. Such a technique has been used now in biology and extended recently to cell biology. Forces corresponding to (i) the unbinding of receptor ligand couples (ii) unfolding of proteins (iii) cell adhesion at single cell scale have been gathered.

4.1.6 PIEZOELECTRIC SCANNERS

AFM scanners are made from piezoelectric material, which expands and contracts proportionally to an applied voltage. Whether they elongate or contract depends upon the polarity of the voltage applied. The scanner is constructed by combining independently operated piezo electrodes for X, Y, & Z into a single tube, forming a scanner which can manipulate samples and probes with extreme precision in 3 dimensions. Scanners are characterized by their sensitivity which is the ratio of piezo movement to piezo voltage, i.e. by how much the piezo material extends or contracts per applied volt. Because of differences in material or size, the sensitivity varies from scanner to scanner.

Typical scanner piezo tube and X-Y-Z configurations. AC Signals applied to conductive areas of the tube create piezo movement along the three major axes

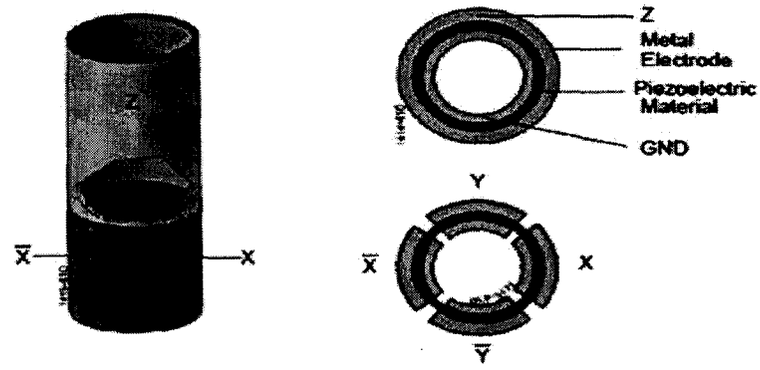

AC voltages applied to the different electrodes of the piezoelectric scanner produce a scanning raster motion in X and Y. There are two segments of the piezoelectric crystal for X (X & X̄) and Y (Y & Ȳ).

Fig 4.3: Piezoelectric scanners

Sensitivity varies non-linearly with respect to scan size. Piezo scanners exhibit more sensitivity at the end than at the beginning of a scan. This causes the forward and reverse scans to behave differently and display hysteresis between the two scan directions. This can be corrected by applying a non-linear voltage to the piezo electrodes to cause linear scanner movement and calibrating the scanner accordingly. The sensitivity of piezoelectric materials decreases exponentially with time. This causes most of the change in sensitivity to occur in the initial stages of the scanner's life. Piezoelectric scanners are run for approximately 48 hours before they are shipped from the factory so that they are past the point where we can expect large changes in sensitivity. As the scanner ages, the sensitivity will change less with time and the scanner would seldom require recalibration.

4.1.7 ADVANTAGES AND DISADVANTAGES

The AFM has several advantages over the scanning electron microscope (SEM). Unlike the electron microscope which provides a two-dimensional projection or a two-dimensional image of a sample, the AFM provides a true three-dimensional surface profile. Additionally, samples viewed by AFM do not require any special treatments (such as metal/carbon coatings) that would irreversibly change or damage the sample. While an electron microscope needs an expensive vacuum environment for proper operation, most AFM modes can work perfectly well in ambient air or even a liquid environment. This makes it possible to study biological macromolecules and even living organisms. In principle, AFM can provide higher resolution than SEM. It has been shown to give true atomic resolution in ultra-high vacuum (UHV) and, more recently, in liquid environments. High resolution AFM is comparable in resolution to Scanning Tunneling Microscopy and Transmission Electron Microscopy. A disadvantage of AFM compared with the scanning electron microscope (SEM) is the image size. The SEM can image an area on the order of millimetres by millimetres with a depth of field on the order of millimetres. The AFM can only image a maximum height on the order of micrometres and a maximum scanning area of around 150 by 150 micrometres. Another inconvenience is that an incorrect choice of tip for the required resolution can lead to image artifacts. Traditionally the AFM could not scan images as fast as an SEM, requiring several minutes for a typical scan, while a SEM is capable of scanning at near real-time (although at relatively low quality) after the chamber is evacuated. The relatively slow rate of scanning during AFM imaging often leads to thermal drift in the image (Lapshin, 2004, 2007), making the AFM microscope less suited for measuring accurate distances between artifacts on the image. However, several fast-acting designs were suggested to increase microscope scanning productivity (Lapshin and Obyedkov, 1993) including what is being termed video AFM (reasonable quality images are being obtained with video AFM at video rate - faster than the average SEM). To eliminate image distortions induced by thermodrift, several methods were also proposed (Lapshin, 2004, 2007).AFM images can also be affected by hysteresis of the piezoelectric material (Lapshin, 1995) and cross-talk between the (x,y,z) axes that may require software enhancement and filtering. Such filtering could "flatten" out real topographical features. However, newer AFM use real-time correction software (for example, feature-oriented

scanning, Lapshin, 2004, 2007) or closed-loop scanners which practically eliminate these problems. Some AFM also use separated orthogonal scanners (as opposed to a single tube) which also serve to eliminate cross-talk problems. Due to the nature of AFM probes, they cannot normally measure steep walls or overhangs. Specially made cantilevers can be modulated sideways as well as up and down (as with dynamic contact and non-contact modes) to measure sidewalls, at the cost of more expensive cantilevers and additional artifacts.

4.2 SCANNING ELECTRON MICROSCOPE (SEM)

The scanning electron microscope (SEM) is a type of electron microscope that images the sample surface by scanning it with a high-energy beam of electrons in a raster scan pattern. The electrons interact with the atoms that make up the sample producing signals that contain information about the sample's surface topography, composition and other properties such as electrical conductivity. The types of signals produced by an SEM include secondary electrons, back scattered electrons (BSE), characteristic x-rays, light (cathodoluminescence), specimen current and transmitted electrons. These types of signal all require specialized detectors for their detection that are not usually all present on a single machine. The signals result from interactions of the electron beam with atoms at or near the surface of the sample. In the most common or standard detection mode, secondary electron imaging or SEI, the SEM can produce very high-resolution images of a sample surface, revealing details about 1 to 5 nm in size. Due to the way these images are created, SEM micrographs have a very large depth of field yielding a characteristic three-dimensional appearance useful for understanding the surface structure of a sample.

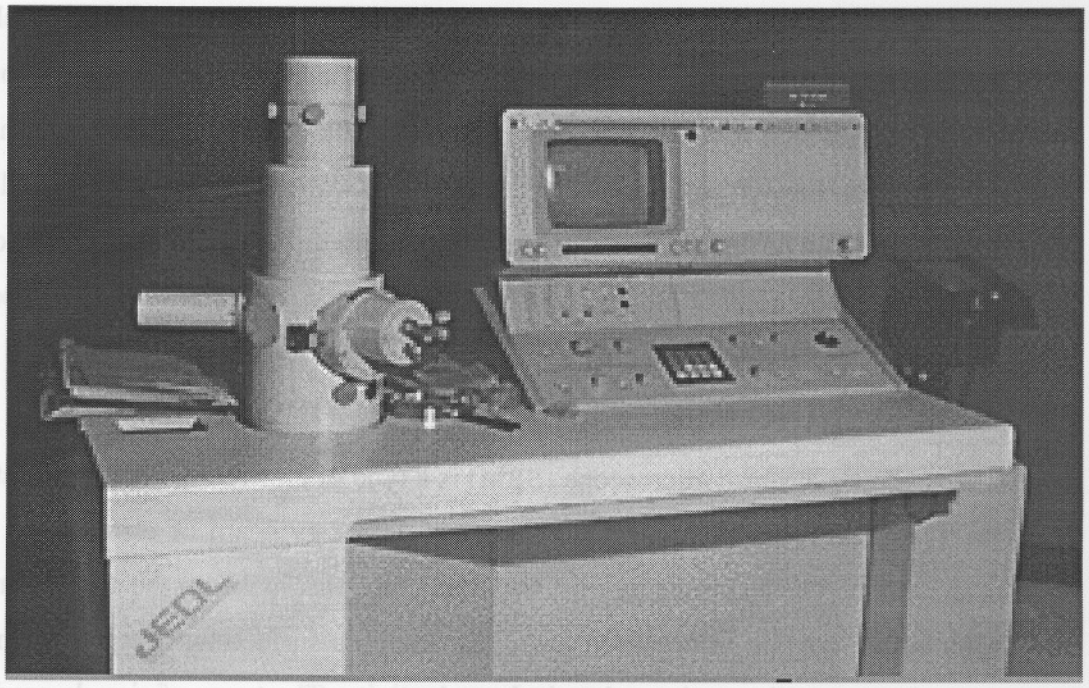

Fig 4.4: Photograph of an SEM

This is exemplified by the micrograph of pollen shown to the right. A wide range of magnifications is possible, from about x 25 (about equivalent to that of a powerful hand-lens) to about x 250,000, about 250 times the magnification limit of the best light microscopes. Back-scattered electrons (BSE) are beam electrons that are reflected from the sample by elastic scattering. BSE are often used in analytical SEM along with the spectra made from the characteristic x-rays. Because the intensity of the BSE signal is strongly related to the atomic number (Z) of the specimen, BSE images can provide information about the distribution of different elements in the sample. For the same reason BSE imaging can image colloidal gold immuno-labels of 5 or 10 nm diameter, that would otherwise be difficult or impossible to detect in secondary electron images in biological specimens. Characteristic X-rays are emitted when the electron beam removes an inner shell electron from the sample, causing a higher energy electron to fill the shell and release energy. These characteristic x-rays are used to identify the composition and measure the abundance of elements in the sample.

4.2.1 SCANNING PROCESS AND IMAGE FORMATION

In a typical SEM, an electron beam is thermionically emitted from an electron gun fitted with a tungsten filament cathode. Tungsten is normally used in thermionic electron guns because it has the highest melting point and lowest vapour pressure of all metals, thereby allowing it to be heated for electron emission, and because of its

low cost. Other types of electron emitters include lanthanum hexaboride (LaB_6) cathodes, which can be used in a standard tungsten filament SEM if the vacuum system is upgraded and field emission guns (FEG), which may be of the cold-cathode type using tungsten single crystal emitters or the thermally-assisted Schottky type, using emitters of zirconium oxide.The electron beam, which typically has an energy ranging from a few hundred eV to 40 keV, is focused by one or two condenser lenses to a spot about 0.4 nm to 5 nm in diameter. The beam passes through pairs of scanning coils or pairs of deflector plates in the electron column, typically in the final lens, which deflect the beam in the *x* and *y* axes so that it scans in a raster fashion over a rectangular area of the sample surface.When the primary electron beam interacts with the sample, the electrons lose energy by repeated random scattering and absorption within a teardrop-shaped volume of the specimen known as the interaction volume, which extends from less than 100 nm to around 5 μm into the surface. The size of the interaction volume depends on the electron's landing energy, the atomic number of the specimen and the specimen's density. The energy exchange between the electron beam and the sample results in the reflection of high-energy electrons by elastic scattering, emission of secondary electrons by inelastic scattering and the emission of electromagnetic radiation, each of which can be detected by specialized detectors. The beam current absorbed by the specimen can also be detected and used to create images of the distribution of specimen current. Electronic amplifiers of various types are used to amplify the signals which are displayed as variations in brightness on a cathode ray tube. The raster scanning of the CRT display is synchronized with that of the beam on the specimen in the microscope, and the resulting image is therefore a distribution map of the intensity of the signal being emitted from the scanned area of the specimen. The image may be captured by photography from a high resolution cathode ray tube, but in modern machines is digitally captured and displayed on a computer monitor and saved to a computer's hard disc.

4.2.2 MAGNIFICATION

Magnification in a SEM can be controlled over a range of up to 6 orders of magnitude from about x25 to x 250,000 and exceptionally to 2 million times in the Hitachi S-5500 in-lens Field Emission SEM, imaging a specimen area about 60nm wide with resolution up to 0.4 nm. Unlike optical and transmission electron microscopes, image

magnification in the SEM is not a function of the power of the objective lens. SEMs may have condenser and objective lenses, but their function is to focus the beam to a spot, and not to image the specimen. Provided the electron gun can generate a beam with sufficiently small diameter, an SEM could in principle work entirely without condenser or objective lenses, although it might not be very versatile or achieve very high resolution. In an SEM, as in scanning probe microscopy, magnification results from the ratio of the dimensions of the raster on the specimen and the raster on the display device. Assuming that the display screen has a fixed size, higher magnification results from reducing the size of the raster on the specimen, and vice versa. Magnification is therefore controlled by the current supplied to the x,y scanning coils, and not by objective lens power.

4.2.3 SAMPLE PREPARATION:

An insect coated in gold, having been prepared for viewing with a scanning electron microscope. All samples must also be of an appropriate size to fit in the specimen chamber and are generally mounted rigidly on a specimen holder called a specimen stub. Several models of SEM can examine any part of a 6-inch (15 cm) semiconductor wafer, and some can tilt an object of that size to 45 degrees.

For conventional imaging in the SEM, specimens must be electrically conductive, at least at the surface, and electrically grounded to prevent the accumulation of electrostatic charge at the surface. Metal objects require little special preparation for SEM except for cleaning and mounting on a specimen stub. Nonconductive specimens tend to charge when scanned by the electron beam, and especially in secondary electron imaging mode, this causes scanning faults and other image artifacts. They are therefore usually coated with an ultrathin coating of electrically-conducting material, commonly gold, deposited on the sample either by low vacuum sputter coating or by high vacuum evaporation. Conductive materials in current use for specimen coating include gold, gold/palladium alloy, platinum, osmium, iridium, tungsten, chromium and graphite. Coating prevents the accumulation of static electric charge on the specimen during electron irradiation.

Two important reasons for coating, even when there is more than enough specimen conductivity to prevent charging, are to maximise signal and improve spatial resolution, especially with samples of low atomic number (Z). Broadly, signal increases with atomic number, especially for backscattered electron imaging. The

improvement in resolution arises because in low-Z materials such as carbon, the electron beam can penetrate several micrometres below the surface, generating signals from an interaction volume much larger than the beam diameter and reducing spatial resolution. Coating with a high-Z material such as gold maximizes secondary electron yield from within a surface layer a few nm thick, and suppresses secondary electrons generated at greater depths, so that the signal is predominantly derived from locations closer to the beam and closer to the specimen surface than would be the case in an uncoated, low-Z material. These effects are particularly, but not exclusively, relevant to biological samples.

An alternative to coating for some biological samples is to increase the bulk conductivity of the material by impregnation with osmium using variants of the OTO process. Nonconducting specimens may be imaged uncoated using specialized SEM instrumentation such as the "Environmental SEM" (ESEM) or field emission gun (FEG) SEMs operated at low voltage. Environmental SEM instruments place the specimen in a relatively high pressure chamber where the working distance is short and the electron optical column is differentially pumped to keep vacuum adequately low at the electron gun. The high pressure region around the sample in the ESEM neutralizes charge and provides an amplification of the secondary electron signal. Low voltage (LV) SEM of non-conducting specimens can be operationally difficult to accomplish in a conventional SEM and is typically a research application for specimens that are sensitive to the process of applying conductive coatings. LV-SEM is typically conducted in an FEG-SEM because the FEG is capable of producing high primary electron brightness even at low accelerating potentials. Operating conditions must be adjusted such that the local space charge is at or near neutral with adequate low voltage secondary electrons being available to neutralize any positively charged surface sites. This requires that the primary electron beam's potential and current be tuned to the characteristics of the sample specimen. Embedding in a resin with further polishing to a mirror-like finish can be used for both biological and materials specimens when imaging in backscattered electrons or when doing quantitative X-ray microanalysis.

4.2.4 BIOLOGICAL SAMPLES

For SEM, a specimen is normally required to be completely dry, since the specimen chamber is at high vacuum. Hard, dry materials such as wood, bone, feathers, dried

insects or shells can be examined with little further treatment, but living cells and tissues and whole, soft-bodied organisms usually require chemical fixation to preserve and stabilize their structure. Fixation is usually performed by incubation in a solution of a buffered chemical fixative, such as glutaraldehyde, sometimes in combination with formaldehyde and other fixatives, and optionally followed by postfixation with osmium tetroxide. The fixed tissue is then dehydrated. Because air-drying causes collapse and shrinkage, this is commonly achieved by critical point drying, which involves replacement of water in the cells with organic solvents such as ethanol or acetone, and replacement of these solvents in turn with a transitional fluid such as liquid carbon dioxide at high pressure. The carbon dioxide is finally removed while in a supercritical state, so that no gas-liquid interface is present within the sample during drying. The dry specimen is usually mounted on a specimen stub using an adhesive such as epoxy resin or electrically-conductive double-sided adhesive tape, and sputter coated with gold or gold/palladium alloy before examination in the microscope. Low-temperature SEM magnification series for a snow crystal. The crystals are captured, stored, and sputter coated with platinum at cryo-temperatures for imaging. Click the image to view a higher resolution image. If the SEM is equipped with a cold stage for cryo-microscopy, cryofixation may be used and low-temperature scanning electron microscopy performed on the cryogenically fixed specimens. Cryo-fixed specimens may be cryo-fractured under vacuum in a special apparatus to reveal internal structure, sputter coated and transferred onto the SEM cryo-stage while still frozen. Low-temperature scanning electron microscopy is also applicable to the imaging of temperature-sensitive materials such as ice (see e.g. illustration at right) and fats. Freeze-fracturing, freeze-etch or freeze&break is a preparation method particularly useful for examining lipid membranes and their incorporated proteins in "face on" view. The preparation method reveals the proteins embedded in the lipid bilayer.

Gold has a high atomic number and sputter coating with gold produces high topographic contrast and resolution. However, the coating has a thickness of a few micrometres, and can obscure the underlying fine detail of the specimen at very high magnification. Low-vacuum SEMs with differential pumping apertures allow samples to be imaged without such coating and without the loss of natural contrast caused by the coating, but are unable to achieve the resolution attainable by conventional SEMs with coated specimens.

4.2.5 MATERIALS

Back scattered electron imaging, quantitative x-ray analysis, and x-ray mapping of geological specimens and metals requires that the surfaces be ground and polished to an ultra smooth surface. Geological specimens that undergo WDS or EDS analysis are often carbon coated. Metals are not generally coated prior to imaging in the SEM because they are conductive and provide their own pathway to ground.

Fractography is the study of fractured surfaces that can be done on a light microscope or commonly, on an SEM. The fractured surface is cut to a suitable size, cleaned of any organic residues, and mounted on a specimen holder for viewing in the SEM. Integrated circuits may be cut with a FIB or other ion beam milling instrument for viewing in the SEM. The SEM in the first case may be incorporated into the FIB. Metals, geological specimens, and integrated circuits all may also be chemically polished for viewing in the SEM. Special high resolution coating techniques are required for high magnification imaging of inorganic thin films.

4.2.5.1 SPUTTER COATER:

A sputter coater coats the sample with gold atoms. The purpose is to make non-metallic samples electrically conductive. The sputter coater uses argon gas and a small electric field. The sample is placed in a small chamber which is at vacuum. Argon gas is then introduced and an electric field is used to cause an electron to be removed from the argon atoms to make the atoms ions with a positive charge. The Ar ions are then attracted to a negatively charged piece of gold foil. The Ar ions act like sand in a sandblaster, knocking gold atoms from the surface of the foil. These gold atoms now settle onto the surface of the sample, producing a gold coating.

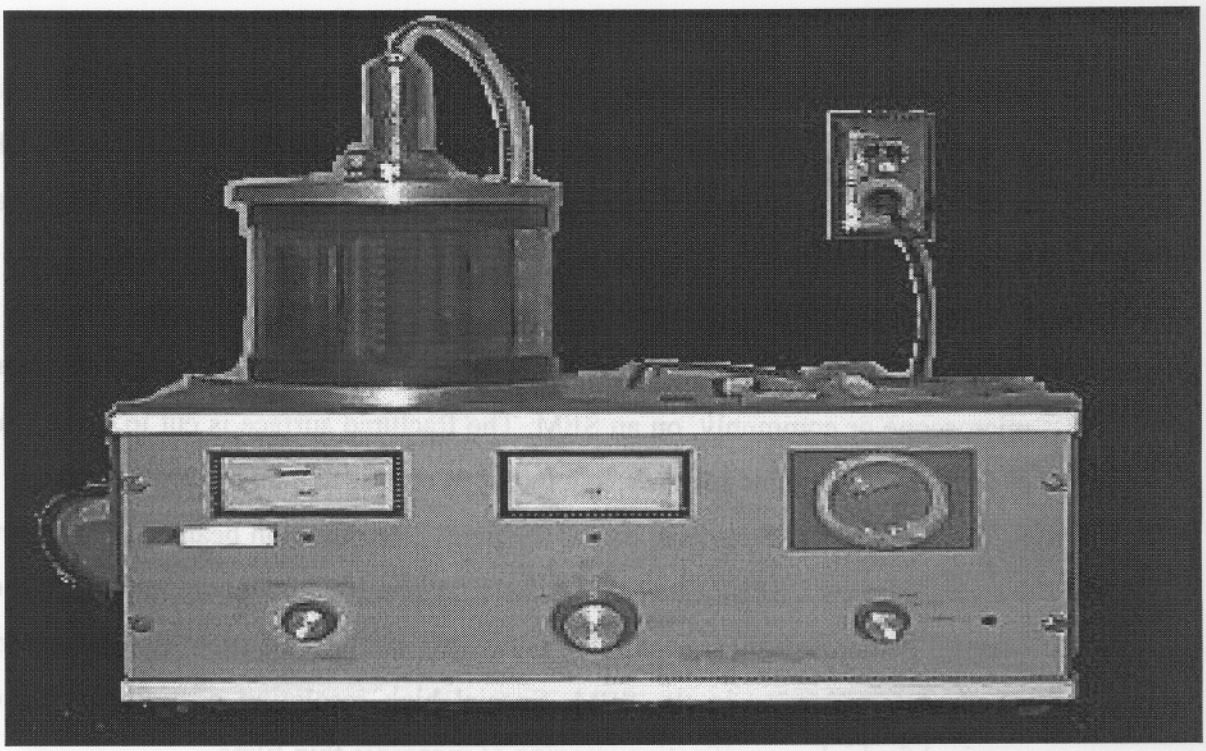

Fig 4.5: A sputter coater used for SEM sample preparation

4.3 FOURIER INFRARED SPECTROSCOPY

FTIR is most useful in identifying chemicals whether they are either organic or inorganic. It can be utilized to quantitate some components of unknown mixture. The FTIR gives information on C-O bond stretching modes of various chemicals. It is a powerful tool for identifying type of chemical bonds from the wavelength of the light absorbed which is the characteristic of the bonds. FTIR can be used for quantitative analyses, as the strength of absorption is proportional to the concentration

4.3.1 PRINCIPLE

Molecular bonds vibrate at various frequencies depending upon the elements and type of bonds. There are several specific frequencies at which bond can vibrate. These frequencies correspond to the ground state and several excited states. Exciting with suitable wavelength equal to difference in the energy between two states (ground and first excited state) the frequency of molecular vibration can be increased. The energy corresponding to these transitions between molecular vibration states is generally 1-10 kilocalories/mole, which corresponds to the infrared portion of the electromagnetic spectrum.

4.3.2 SAMPLE PREPARATION

In case of liquid samples one drop of sample is placed in between two plates of sodium chloride and it forms a thin film between the plates(salt is transparent to infrared light)which can be studied .In case of Solid samples they are milled with potassium bromide as it is transparent to IR to form a very fine powder. This powder is then compressed and made into a thin pellet, which can be analyzed. Solutions can be analyzed by using a liquid cell made of NaCl.

The FTIR graph is plotted between the percentage of transmission and wave number along Y and X-axis respectively. Each and every peak in the graph gives information on the bond structure of the molecules present in the samples and about bond stretching. The sample is scanned from 4000 to 400 cm^{-1}.

4.4 Z- SCAN MEASURMENT

Many experimental techniques have been developed to measure the magnitude and dynamics of third order nonlinearties. Two such commonly used methods are Degenerate Four –Wave Mixing and Z- Scan method. The Z-Scan is the simplest method to measure the intensity dependent nonlinear susceptibility of the materials. It is a single beam technique to measure the nonlinear refractive index and nonlinear absorption coefficients for wide variety of materials. The Z- Scan utilizes the self-focussing effect of the propagating beam to measures the nonlinear refractive index. The nonlinear transmittance method is utilized to measure the β value from the transmittance. In Z- Scan the sample is translated along the axis of the focused Gaussian beam in and out of the focal region of an incident laser beam thereby varying the intensity of light falling on the sample and the far field intensity is measured as a function of sample position. Analysis of the intensity versus sample position the Z- Scan curve gives the real and imaginary part of third order nonlinear susceptibility. By varying the aperture placed in front of the detector one can make the Z- Scan transmittance more or less sensitive to real or imaginary part of the nonlinear response of the material. There are two types of Z-Scan techniques namely closed aperture and the open aperture Z – Scan.

4.4.1 EXPERIMENTAL SETUP

In a typical experimental setup initially the input high intense laser beam is passed through a 50:50 beam splitter. Here part of the beam, which is transmitted through the beam splitter reaches a detector that measures the intensity of this direct beam and the other part of the beam, which is reflected from the beam splitter reaches a lens which

focuses the incident transverse Gaussian beam towards the sample (nonlinear medium) mounted on a sample holder. The thickness of the sample for the study should be less than the Rayleigh range. The sample holder is mounted over a stepper motor arrangement, which is helpful to move the sample in and out of the focal region of the beam along the axial direction of the focused beam. The sample experiences the maximum intensity at the point of focus, which progressively decreases in either direction of motion from the focus. A suitable detector is placed in the far field to measure the transmitted intensity as a function of sample position, which is an open aperture setup. In case of closed aperture Z-Scan an aperture of suitable "S" value is placed closely in front of the detector and the experiment is repeated as before.

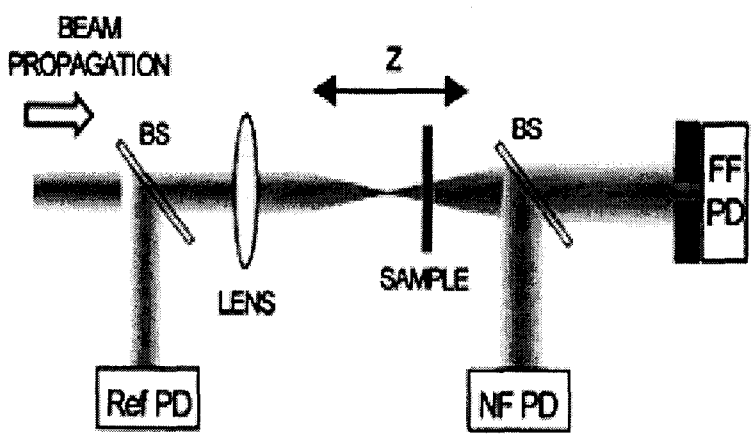

Fig: 4.6 Schematic of a Z-scan setup

4.4.2 CLOSED APERTURE Z-SCAN

This method gives quantitative information on the nonlinear refraction of the samples. In this setup there is a possibility for either of the effects like negative lensing and positive lensing, which happens is a case of material with negative nonlinear refractive index and positive nonlinear refractive index respectively.

4.4.3 WORKING

Assume a material with a negative nonlinear refractive index and thickness smaller than diffraction length of the focused beam, which can be regarded as a thin lens of variable focal length. Starting the scan the sample is moved from a distance far away from the focus close to the lens (negative Z direction) the beam irradiance on the sample is low and negligible nonlinear refraction occurs resulting in relatively

constant transmittance. Now, the sample is moved closer to the point of focus the beam irradiance on the material also starts increasing leading to self lensing in the sample. As the width of the beam decreases towards focus the entire energy of the beam is concentrated into a small area in the sample. A negative self-lensing will collimate the beam causing narrowing of beam at the aperture resulting increase in measured transmittance. Now, when the sample is moved towards positive Z direction Self de focusing will come into play where the beam reaching the aperture gets diverged more resulting in decreased transmittance. This suggests that there is null as the sample crosses the focal plane. This is analogous to placing a thin lens at or near the focus.

A prefocal transmittance maximum (Peak) followed by a post focal transmittance minimum (Valley) is the Z-Scan signature of negative refractive index nonlinearity.

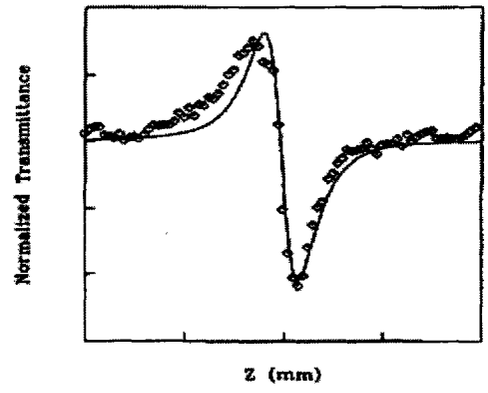

Fig :4.7 A Typical closed aperture Z scan curve

Positive nonlinear refraction gives rise to the opposite valley-peak configuration. The sensitivity to nonlinear refraction is due to the presence of the aperture and removal of aperture will completely eliminate the effect. For a transparent nonlinear medium the Z-Scan curve will be symmetrical about Z=0. However if some absorptive nonlinearties are present the symmetry will be lost. Example, multiphoton absorption suppresses the peak and enhances the valley while saturable absorption enhances the peak and suppresses the valley.

4.4.4 OPEN APERTURE Z-SCAN

The nonlinear absorption in a nonlinear medium may arise due to multiple photon absorption, saturation of single photon absorption or free carrier absorption.In case of open aperture Z-Scan technique the aperture placed close to the detector is removed and the sample transmission for different Z values is measured as before. The transmittance will be minimum in case of two-photon absorption and maximum for saturable absorption.

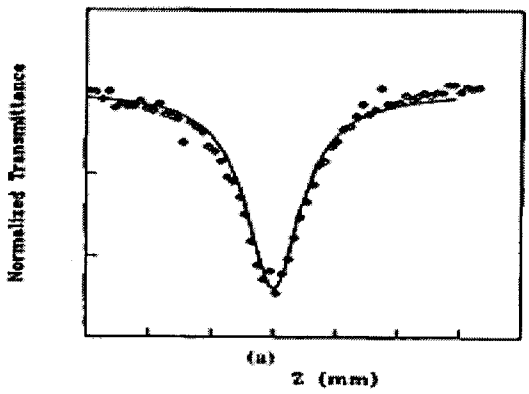

Fig 4.7: A Typical open aperture Z scan curve

Although Z-Scan method has several advantage, disadvantages of this technique includes a need for high quality Gaussian beam for absolute measurement, Sample distortions or sample tilting during translation cause beam to walk off the far field aperture.

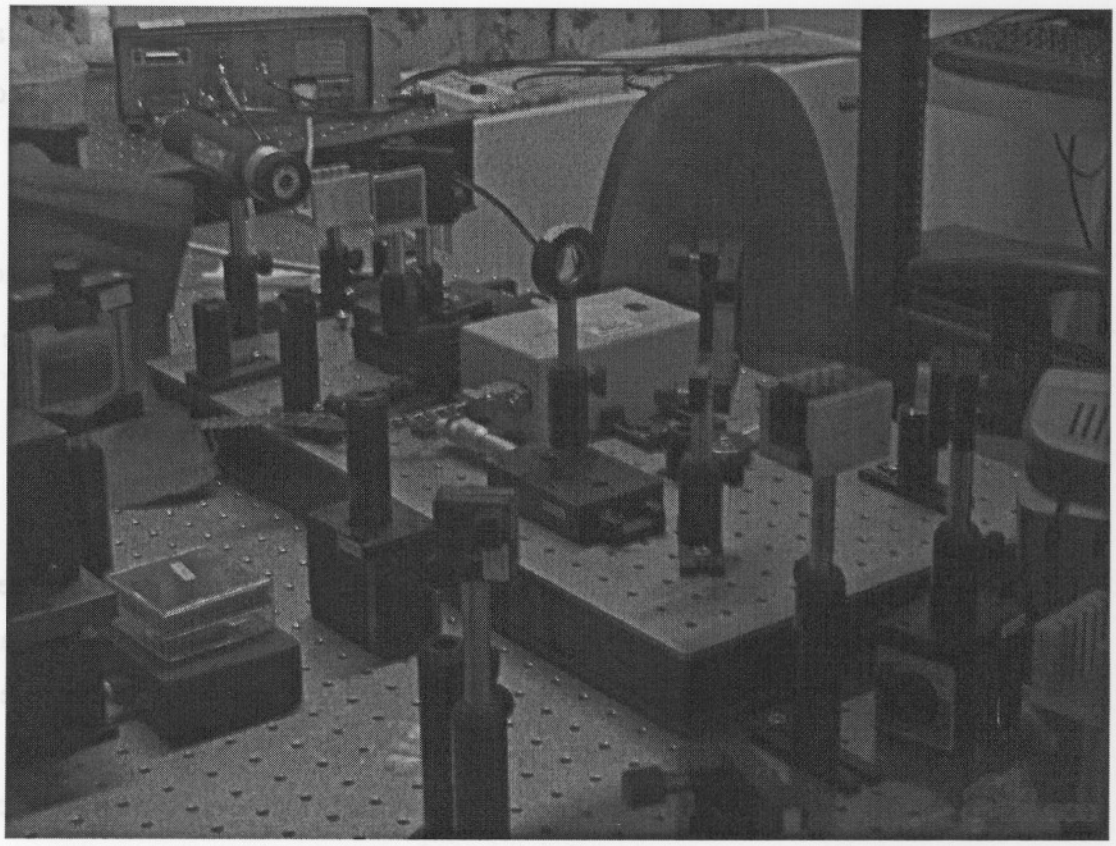

Fig. 4.8: Photograph of Z-Scan experimental setup

4.4.5: CURVE FITTING EQUATION

The Two photon absorption transmission equation

$$T = \left((1-R)^2 \exp(-\alpha_0 L)/\sqrt{\pi} q_0\right) \int_{-\infty}^{+\infty} \ln\left[\sqrt{1+q_0 \exp(-t^2)}\right] dt$$

where T is the net transmission of the samples. L and R are the sample length and surface reflectivity respectively, and α_0 is the linear absorption coefficient. q_0 in eqn.1 is given by $\beta(1\text{-}R)I_0L_{eff}$, where I_0 is the on-axis peak intensity, L_{eff} is given by $[1\text{-}\exp(-\alpha_0 L)]/\alpha_0$, and β is the effective nonlinear absorption coefficient.

The Three-photon absorption equation is given by

$$T = \frac{(1-R)^2 \exp(-\alpha L)}{\sqrt{\pi} p_0} \int_{-\infty}^{+\infty} \ln\left[\sqrt{1+p_0^{\,2} \exp(-2t^2)} + p_0 \exp(-t^2)\right] dt$$

where $p_0 = [2\gamma(1-R)^2 I_0^2 L_{eff}]^{1/2}$. Here R is the Fresnel reflection coefficient at the sample-air interface, α is the absorption coefficient, L is the sample length, and I_0 is the incident intensity. L_{eff} is given by $[1-\exp(-2\alpha L)]/2\alpha$.

4.4.6 FLUENCE CALCULATION

For a Gaussian beam, each z position corresponds to an input fluence of $4\sqrt{\ln 2}E_{in} / \pi^{3/2}\omega(z)^2$, where E_{in} is the input laser pulse energy and ω (z) is the beam radius. $\omega(z)$ is the beam radius given by $\omega(0)/[1+ (z/z_0)^2]$, where $\omega(0)$ is the beam radius at the focus, and $z_0 = \pi\omega_0^2/\lambda$ is the Rayleigh range.

4.5 X-RAY DIFFRACTION

Diffraction can occur when electromagnetic radiation interacts with the periodic structure whose repeat distance is same as the wavelength of the radiation. X-rays are electromagnetic radiation of wavelengths in the order of angstrom. They are short wavelength rays of high frequency and high energy. The x-ray diffraction gives information regarding structures of crystalline solids, which can be used to determine molecular structures, relative atomic positions and interatomic spacing. The intensity of diffracted beam depends on the atomic number and arrangement of atoms which is helpful in determining position of atoms.

4.5.1 PRINCIPLE

X-Ray primarily interacts with electrons in an atom, when they collide with these electrons some of the photons from the incident ray will be deflected away from the original path of travel. These scattered rays carry information about the electron distribution in the material. If the scattered photons do not have any change in wavelength (lose of energy and only momentum transfer) then it is called elastic scattering. If the scattered ray changes in wavelength then it is called inelastic scattering. These diffracted waves from different atomic structure will interfere with each other and produce interference pattern resulting in modulation of the resultant intensity distribution. If the atoms are arranged in a periodic fashion then diffracted waves will consist of sharp interference peak (Max). The peaks in X-Ray diffraction are directly related to atomic distances.

Bragg's law of diffraction gives the condition for diffraction to take place.

$$2d\sin\theta = n\lambda.$$

Where, λ is the wavelength of X –ray, θ scattering angle, and n is an integer.

4.5.2 POWDER AND SMALL ANGLE X-RAY DIFFRACTION

The powder sample consists of fine grains of single crystalline here the crystalline domains are randomly oriented. When the 2-D diffraction pattern is recorded for these samples it shows concentric rings of scattering peaks corresponding to the various d spacing in the crystal lattice. The structure and phase of the material are identified from the position and intensity of the peak. Small angle X-Ray diffraction is concerned with scattering angle less than 1 degree it gives information about the structures with large d- spacing. This technique is utilized to study structures like high molecular weight polymer, biological macromolecules and self assembled super structures.

4.5.3 GRAPH

The XRD graph is plotted between the scattering intensity Vs scattering angle. The peak position, intensities, width and shape all provide information about the structure of the material. The grain size can be calculated from the Scherrer formulae.

$$D = \frac{0.9\lambda}{B\cos\theta_B}$$

Where, λ is the wavelength of filament used in XRD. B is the width of the peak at half of its intensity and θ_B is the angle of the same peak and D is the particle diameter. The Cu Kα radiation (wavelength = 1.54) is utilized for X-Ray diffraction study.

4.6 UV- VISIBLE SPECTROMETER

A UV-Visible spectrometer generally uses two light sources, a deuterium lamp for ultraviolet light and a halogen lamp for visible light. The mirrorM1 is raised to permit radiation from the lamps to strike source mirror M2.The radiation from the source lamp is reflected from source mirror M2 through an optical filter to passes through a slit and hits a diffraction grating (monochromator) which can be rotated allowing a specific (single) wavelength to be selected. Appropriate optical filter on a filter wheel assembly located on the beam path to pre filter the radiation before it enters the monochromator. The radiation is dispersed at the monochromator to produce a spectrum. The rotational position of the grating effectively selects a segment of the spectrum, reflecting this segment through exit the slit 2 to mirror M3.This slits provide a spectral selectable band pass of 0.5,1,2or 4nm. From the mirror M3 the radiation is reflected onto a beam splitter, which allows 50% of the radiation to pass onto the plane mirrorM4, and reflects on a filter wheel assembly located on the beam

path to pre filter the radiation before it enters the monochromator. The radiation is dispersed at the monochromator to produce a spectrum. The rotational position of the grating effectively selects a segment of the spectrum, reflecting this segment through exit the slit 2 to mirror M3.This slits provide a spectral selectable band pass of 0.5,1,2or 4nm. From the mirror M3 the radiation is reflected onto a beam splitter, which allows 50% of the radiation to pass onto the plane mirrorM4, and reflects 50% of the radiation onto the plane mirror M5. Mirror M4 focuses the radiation beam to the sample cell. The beam then passes through a convex lens onto the photodiode detector. Mirror M5 focuses the radiation beam in to reference cell. . The beam then passes through a convex lens onto the photodiode detector.

The advantage of double-beam operation is the better stability and allows reference to be measured and corrected in real time and fast scanning is done. The grating monochromator used here is a holographic concave grating with 1053 lines /mm in the center. Photodiodes are used as detectors. The optical path length in the sample compartment is 121mm. This spectrometer can be operated in a ambient operating temperature of 15 C to 35 C and humidity range of 20% to 80% without condensation. The power requirements to operate this spectrometer are about 100V to 240 V AC, frequency of 50/60Hz

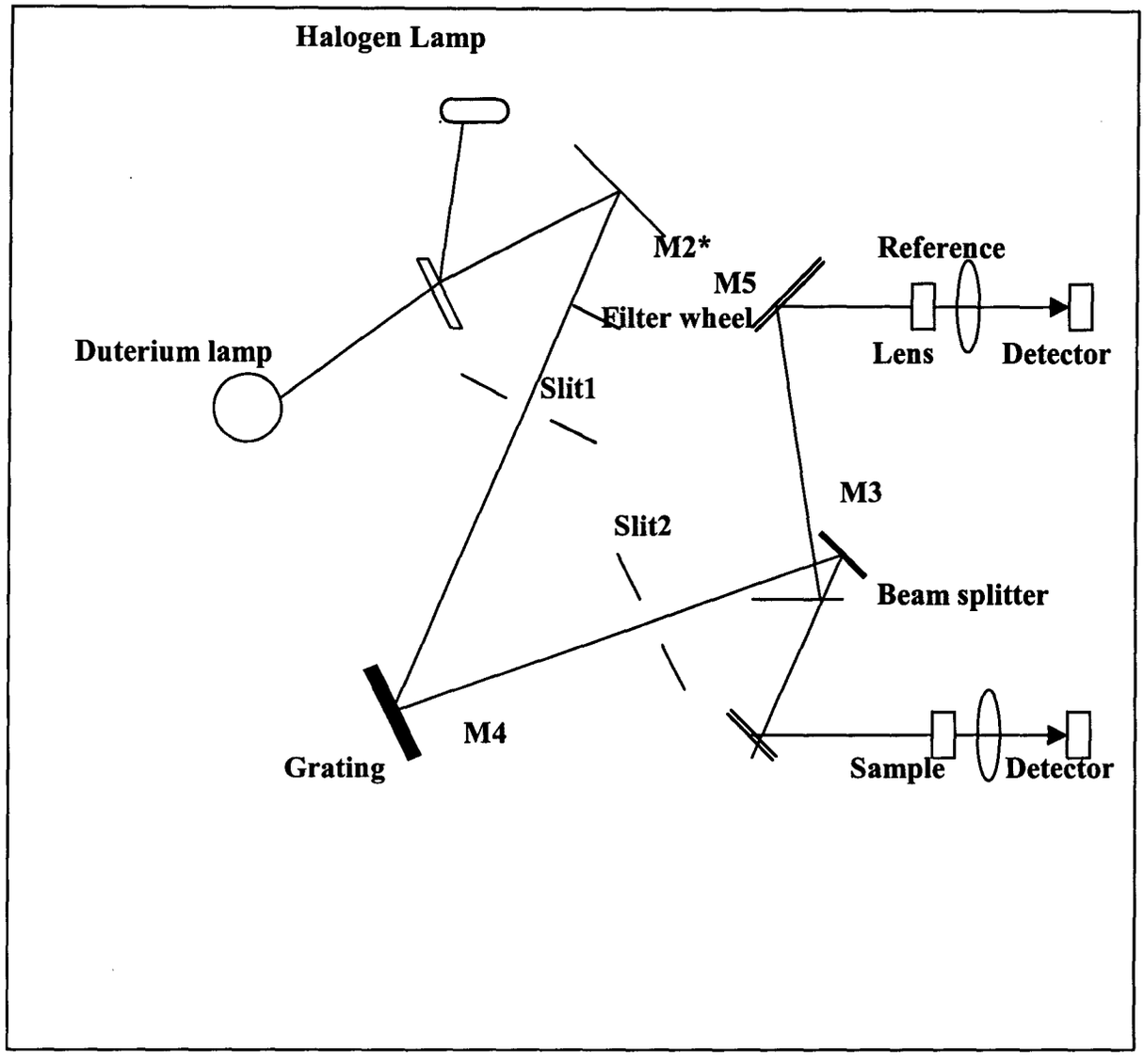

Fig 4.8 : Block diagram of U.V visible spectrometer

CHAPTER-5

EXPERIMENTAL PROCEDURE

INTRODUCTION

5.1 STRONTIUM

Strontium is a chemical element with the symbol **Sr** and the atomic number 38. An alkaline earth metal, strontium is a soft silver-white or yellowish metallic element that is highly reactive chemically. The metal turns yellow when exposed to air. It occurs naturally in the minerals celestine and strontianite. The ^{90}Sr isotope is present in radioactive fallout and has a half-life of 28.90 years. Both strontium and strontianite are named after Strontian, a village in Scotland near which the mineral was first discovered.

5.2 CHARACTERISTICS

Due to its extreme reactivity with oxygen and water, this element occurs naturally only in compounds with other elements, as in the minerals strontianite and celestite.Strontium is a grey/silvery metal that is softer than calcium and even more reactive in water, with which strontium reacts on contact to produce strontium hydroxide and hydrogen gas. It burns in air to produce both strontium oxide and strontium nitride, but since it does not react with nitrogen below 380°C it will only form the oxide spontaneously at room temperature. It should be kept under kerosene to prevent oxidation; freshly exposed strontium metal rapidly turns a yellowish color with the formation of the oxide. Finely powdered strontium metal will ignite spontaneously in air at room temperature. Volatile strontium salts impart a crimson color to flames, and these salts are used in pyrotechnics and in the production of flares. Natural strontium is a mixture of four radiostable isotopes.

As a pure metal strontium is used in strontium 90%-aluminium 10% alloys of an eutectic composition for the modification of aluminium-silicon casting alloys.The primary use for

strontium compounds is in glass for colour television cathode ray tubes to prevent X-ray emission.

Other uses:

- ^{89}Sr is the active ingredient in Metastron, a radiopharmaceutical used for bone pain secondary to metastatic bone cancer. The strontium acts like calcium and is preferentially incorporated into bone at sites of increased osteogenesis. This localization focuses the radiation exposure on the cancerous lesion.
- ^{90}Sr has been used as a power source for radioisotope thermoelectric generators (RTGs). ^{90}Sr produces about 0.93 watts of heat per gram (it is lower for the grade of ^{90}Sr used in RTGs, which is strontium fluoride).However, ^{90}Sr has a lifetime approximately 3 times shorter and has a lower density than ^{238}Pu, another RTG fuel. The main advantage of ^{90}Sr is that it is cheaper than ^{238}Pu and is found in nuclear waste.
- ^{90}Sr is also used in cancer therapy. Its beta emission and long half-life is ideal for superficial radiotherapy.
- Strontium is one of the constituents of AJ62 alloy, a durable magnesium alloy used in car and motorcycle engines by BMW.

- Since Strontium is so similar to calcium, it is incorporated in the bone. All four isotopes are incorporated, in roughly similar proportions as they are found in nature (please see below). However the actual distribution of the isotopes tends to vary greatly from one geographical location to another. Thus analyzing the bone of an individual can help determine the region it came from. This approach helps to identify the ancient migration patterns as well as the origin of commingled human remains in battlefield burial sites. Strontium thus helps forensic scientists too.

- Strontium is used in studies of neurotransmitter release in neurons. Like calcium, strontium facilitates synaptic vesicle fusion with the synaptic membrane. But unlike calcium, strontium causes asynchronous vesicle fusion. Therefore,

replacing calcium in the culture medium with strontium allows scientists to measure the effects of a single vesicle fusion event, e.g., the size of the postsynaptic response elicited by the neurotransmitter content of a single vesicle.

$^{87}Sr/^{86}Sr$ ratios are commonly used to determine the likely provenance areas of sediment in natural systems, especially in marine and fluvial environments. Dasch (1969) showed that surface sediments of Atlantic displayed $^{87}Sr/^{86}Sr$ ratios that could be regarded as bulk averages of the $^{87}Sr/^{86}Sr$ ratios of geological terranes from adjacent landmasses. A good example of a fluvial-marine system to which Sr isotope provenance studies have been successfully employed is the River Nile-Mediterranean system (Krom et al., 1999; Krom et al., 2002; Talbot et al. 2000). Due to the differing ages of the rocks that constitute the majority of the Blue and White Nile catchment areas of the changing provenance of sediment reaching the River Nile delta and East Mediterranean Sea can be discerned through Sr isotopic studies. Such changes are climatically controlled in the Late Quaternary.More recently, $^{87}Sr/^{86}Sr$ ratios have also been used to determine the source of ancient archaeological materials such as timbers and corn in Chaco Canyon, New Mexico (English et al., 2001; Benson et al., 2003). $^{87}Sr/^{86}Sr$ ratios in teeth may also be used to track animal migrations (Barnett-Johnson, 2007; Porder et al., 2003) or in criminal forensics.Strontium atoms are used in an experimental atomic clock with record-setting accuracy

5.3 SAMPLE PREPARATION OF STRONTIUM FERRITE

Strontium hexaferrite nanoparticles $SrFe_{12}O_{19}$ were synthesised via a sol–gel route using citric acid to complex the ions followed by an auto-combustion reaction. This method shows promise for the synthesis of complex ferrite powders with small particle size. Optical properties of strontium ferrite powders with Fe/Sr ratios varying from different annealing temperatures range of 250 to 1000 °C were studied. The resultant powders were investigated by UV visible, XRD, SEM, , FTIR,DSc and surface area measurement.. Initially Strontium Nitrate, Ferric Nitrate,Citric Acid are mixed in the distilled waterto make the homogeneous solution.After that we make the sol neutral by adding the Ammonium hydroxide. The solution is stirred till than the Gel formed. After

that the gel is kept into the furnace for drying the gel.for several hours. After drying it the gel is annealed for 3-4 hours. The powder is now sinterd for various temperature range i.e. 250 to 1000 for 10^0C/min. for 5 hours. After that the furnace is cooled down . we got the Strontium hexaferrite nanopowder.

Quantities of materias used:

1.$Sr(NO_3)_3$ - 1.9gm

2.$Fe(NO_3)_3 .9H_2O$ - 33gm

3.$C(OH)(COOH).(CH_2COOH).H_20$ - 19gm

4.NH_4OH) - up to pH 7.0

INTRODUCTION (PART- B)

5.4 SILVER

Silver is a chemical element with the chemical symbol **Ag** and atomic number 47. A soft, white, lustrous transition metal, it has the highest electrical conductivity of any element and the highest thermal conductivity of any metal. The metal occurs naturally in its pure, free form (native silver), as an alloy with gold (electrum) and other metals, and in minerals such as argentite and chlorargyrite. Most silver is produced as a by-product of copper, gold, lead, and zinc refining.

Silver has been known since ancient times and has long been valued as a precious metal, used to make ornaments, jewelry, high-value tableware, utensils (hence the term *silverware*), and currency coins. Today, silver metal is used in electrical contacts and conductors, in mirrors and in catalysis of chemical reactions. Its compounds are used in photographic film and dilute solutions of silver nitrate and other silver compounds are used as disinfectants. Although the antimicrobial uses of silver have largely been supplanted by the use of antibiotics, further research into its clinical potential is in progress.

5.5 CHARACTERISTICS

Silver is a very ductile and malleable (slightly harder than gold) monovalent coinage metal with a brilliant white metallic luster that can take a high degree of polish. It has the highest electrical conductivity of all metals, even higher than copper, but its greater cost and tarnishability have prevented it from being widely used in place of copper for electrical purposes, though 13540 tons were used in the electromagnets used for enriching uranium during World War II (mainly because of the wartime shortage of copper). Another notable exception is in high-end audio cables.

Among metals, pure silver has the highest thermal conductivity(the non-metal diamond and superfluid helium II are higher), the whitest color, and the highest optical reflectivity(although aluminium slightly outdoes it in parts of the visible spectrum, and it is a poor reflector of ultraviolet light). Silver also has the lowest contact resistance of any metal. Silver halides are photosensitive and are remarkable for their ability to record a latent image that can later be developed chemically. Silver is stable in pure air and water, but tarnishes when it is exposed to air or water containing ozone or hydrogen sulfide to form a black layer of silver sulfide which can be cleaned off with dilute hydrochloric acid. The most common oxidation state of silver is +1 (for example, silver nitrate: $AgNO_3$; in addition, +2 compounds (for example, silver(II) fluoride: AgF_2) and +3 compounds (for example, potassium tetrafluoroargentate: $K[AgF_4]$) are known.

5.6 APPLICATIONS

5.6.1 PRECIOUS METAL

A Chinese Tang Dynasty (618–907 CE) gilt-silver cup with flower designA major use of silver is as a precious metal, and it has long been used for making high-value objects reflecting the wealth and status of the owner.Jewellery and silverware are traditionally made from sterling silver (standard silver), an alloy of 92.5% silver with 7.5% copper. In the United States, only an alloy consisting of at least 92.5% fine silver can be marketed as "silver". Sterling silver is harder than pure silver, and has a lower melting point (893 °C) than either pure silver or pure copper. Britannia silver is an alternative hallmark-quality standard containing 95.8% silver, often used to make silver tableware and wrought plate. With the addition of germanium, the patented modified alloy Argentium Sterling Silver is formed, with improved properties including resistance to firescale.Sterling silver jewelry is often plated with a thin coat of .999 fine silver to give the item a shiny finish. This process is called "flashing". Silver jewelry can also be plated with rhodium (for a bright, shiny look) or gold.

Silver is a constituent of almost all colored carat gold alloys and carat gold solders, giving the alloys paler colour and greater hardness. White 9 carat gold contains 62.5% silver and 37.5% gold, while 22 carat gold contains up to 8.4% silver or 8.4% copper.Silver is used in medals, denoting second place. Some high-end musical instruments are made from sterling silver, such as the flute.

5.6.2 DENTISTRY

Silver can be alloyed with mercury, tin and other metals at room temperature to make amalgams that are widely used for dental fillings. To make dental amalgam, a mixture of powdered silver and other metals is mixed with mercury to make a stiff paste that can be adapted to the shape of a cavity. The dental amalgam achieves initial hardness within minutes but sets hard in a few hours.

5.6.3 PHOTOGRAPHY AND ELECTRONICS

Photography used 30.98% of the silver consumed in 1998 in the form of silver nitrate and silver halides, and in 2001, 23.47% for photography, while 20.03% was used in jewelry, 38.51% for industrial uses, and only 3.5% for coins and medals. The use of silver in photography has rapidly declined, due to the lower demand for consumer colour film from the advent of digital technology, since in 2007 of the 894.5 million ounces of silver in supply, just 128.3 million ounces (14.3%) were consumed by the photographic sector, and the total amount of silver consumed in 2007 by the photographic sector compared to 1998 is just 50%.

Some electrical and electronic products use silver for its superior conductivity, even when tarnished. For example, printed circuits are made using silver paints, and computer keyboards use silver electrical contacts. Some high-end audio hardware (DACs, preamplifiers, etc.) are fully silver-wired, which is believed to cause the least loss of quality in the signal. Silver cadmium oxide is used in high voltage contacts because it can withstand arcing.

During World War II the short supply of copper brought about the government's use of silver from the Treasury vaults for conductors at Oak Ridge National Laboratory. (After the war ended the silver was returned to the vaults.)

5.6.4 SOLDER AND BRAZING

Silver is used to make solder and brazing alloys, electrical contacts, and high-capacity silver-zinc and silver-cadmium batteries. Silver in a thin layer on top of a bearing material can provide a significant increase in galling resistance and reduce wear under heavy load, particularly against steel.

5.6.5 MIRRORS AND OPTICS

Mirrors which need superior reflectivity for visible light are made with silver as the reflecting material in a process called silvering, though common mirrors are backed with aluminium. Using a process called sputtering, silver (and sometimes gold) can be applied to glass at various thicknesses, allowing different amounts of light to penetrate. Silver is usually reserved for coatings of specialized optics, and the silvering most often seen in architectural glass and tinted windows on vehicles is produced by sputtered aluminium, which is cheaper and less susceptible to tarnishing and corrosion.

5.6.6 NUCLEAR REACTORS

Because silver readily absorbs free neutrons, it is commonly used to make control rods that regulate the fission chain reaction in pressurized water nuclear reactors, generally in the form of an alloy containing 80% silver, 15% indium, and 5% cadmium.

5.6.7 CATALYST

Silver's catalytic properties make it ideal for use as a catalyst in oxidation reactions, for example, the production of formaldehyde from methanol and air by means of silver screens or crystallites containing a minimum 99.95 weight-percent silver. Silver (upon some suitable support) is probably the only catalyst available today to convert ethylene to ethylene oxide (later hydrolyzed to ethylene glycol, used for making polyesters)—a very important industrial reaction.Oxygen dissolves in silver relatively easily compared to other gases present in air. Attempts have been made to construct silver membranes of only a few monolayers thickness. Such a membrane could be used to filter pure oxygen from air and water.

5.6.8 MEDICINE

Silver ions and silver compounds show a toxic effect on some bacteria, viruses, algae and fungi, typical for heavy metals like lead or mercury, but without the high toxicity to humans that are normally associated with these other metals. Its germicidal effects kill many microbial organisms *in vitro*, but testing and standardization of silver products is difficult.Hippocrates, the father of modern medicine, wrote that silver had beneficial healing and anti-disease properties, and the Phoenicians used to store water, wine, and vinegar in silver bottles to prevent spoiling. In the early 1900s people would put silver dollars in milk bottles to prolong the milk's freshness. Its germicidal effects increase its value in utensils and as jewellery. The exact process of silver's germicidal effect is still not well understood, although theories exist. One of these is the oligodynamic effect, which explains the effect on microorganisms but would not explain antiviral effects.The widespread use of silver went out of fashion with the development of modern antibiotics.

However, recently there has been renewed interest in silver as a broad-spectrum antimicrobial. In particular, silver is being used with alginate, a naturally occurring biopolymer derived from seaweed, in a range of products designed to prevent infections as part of wound management procedures, particularly applicable to burn victims. In 2007, AGC Flat Glass Europe introduced the first antibacterial glass to fight hospital-caught infection: it is covered with a thin layer of silver. In addition, Samsung has introduced washing machines with a final rinse containing silver ions to provide several days of antibacterial protection in the clothes. Kohler has introduced a line of toilet seats that have silver ions embedded to kill germs. A company called Thomson Research Associates has begun treating products with Ultra Fresh, an anti-microbial technology involving "proprietary nano-technology to produce the ultra-fine silver particles essential to ease of application and long-term protection. The U.S. Food and Drug Administration (FDA) has recently approved an endotracheal breathing tube with a fine coat of silver for use in mechanical ventilation, after studies found it reduced the risk of ventilator-associated pneumonia.It has long been known that antibacterial action of silver is enhanced by the presence of an electric field. Applying a few volts of electricity across silver electrodes drastically enhances the rate that bacteria in solution are killed. It was found recently that the antibacterial action of silver electrodes is greatly improved if the electrodes are covered with silver nanorods.

5.6.9 MEDICATION

Today, various kinds of silver compounds, or devices to make solutions or colloids containing silver, are sold as remedies for a wide variety of diseases. Although most colloidal silver preparations are harmless, some people using these home-made solutions excessively have developed argyria over a period of months or years. High doses of colloidal silver can result in coma, pleural edema, and hemolysis. Silver is widely used in topical gels and impregnated into bandages because of its wide-spectrum antimicrobial activity. The anti-microbial properties of silver stem from the chemical properties of its ionized form, Ag^+. This ion forms strong molecular bonds with other substances used by bacteria to respire, such as molecules containing sulfur, nitrogen, and oxygen.Once the Ag^+ ion complexes with these molecules, they are rendered unusable by the bacteria, depriving it of necessary compounds and eventually leading to the bacteria's death.

5.6.10 FOOD

In India and Pakistan, foods, especially sweets, can be found decorated with a thin layer of silver known as vark. Silver as a food additive is given the E number E174 and is classed as a food coloring. It is used solely for external decoration, such as on chocolate confectionery, in the covering of dragées and the decoration of sugar-coated flour confectionery. In Australia, it is banned as a food additive.

5.6.11 CLOTHING

Goddess Minerva on a Roman silver plate, 1st century BC. Silver inhibits the growth of bacteria and fungi. It keeps odour to a minimum and reduces the risk of bacterial and fungal infection. In clothing, the combination of silver and moisture movement (wicking) may help to reduce the harmful effects of prolonged use in active and humid conditions. Silver is used in clothing in two main forms:

- A form in which silver ions are integrated into the polymer from which yarns are made (a form of nanotechnology)
- A form in which the silver is coated onto the yarns.

In both cases the silver prevents the growth of a broad spectrum of bacteria and fungi. Recorded use of silver to prevent infection dates to ancient Greece and Rome, it was rediscovered in the Middle Ages, where it was used for several purposes, such as to disinfect water and food during storage, and also for the treatment of burns and wounds as wound dressing. In the 19th century, sailors on long ocean voyages would put silver coins in barrels of water and wine to keep the liquid pure. Pioneers in America used the same idea as they made their journey from coast to coast. Silver solutions were approved in the 1920s by the US Food and Drug Administration for use as antibacterial agents. Today, wound dressings containing silver are well established for clinical wound care and have recently been introduced in consumer products such as sticking plasters.

5.6.12 Ag NPs

Metal nanoparticles are being intensively investigated because of their unique optical, electric, and catalytic properties which make them a potential material for utilization in the field of medicine, optoelectronics, composites and in many other frontier areas of science and technology. Much work has been done to improve the electrical and mechanical properties of epoxy-based electrically conductive adhesives in the past decade. Some results also showed that a good interface between silver particles and the epoxy resin can promote the conductivity, which play an important role for the performance of dielectric composites. In this way, amine coated Ag nanocomposite can be used by increasing the Ag/epoxy composite conductivity employing a low Ag amount. In general, silver and gold nanoparticles can be synthesized by several methods, for example: chemical reduction in aqueous solutions, chemical and and ultrasonic irradiation. photo reduction.

However, most of these procedures only render stable silver dispersions at a relatively low concentration of the metal; hence, they are not suitable for large-scale manufacturing. To prepare a stable colloidal solution of metal nanoparticles it is necessary to cap the metal with an appropriate chemical agent like a polymer or a surfactant with specific functional groups that can interact with the metal surface. In the surfactant-assisted synthesis, various physicochemical properties, including the relative concentration of the surfactant, its molecular weight and the pH of the solution, among others, have a great influence on the morphology of the particles as well as on the final optical, electrical, catalytic and/or magnetic properties. The objective of this work is to study the synthesis of Ag nanoparticles with amine functional groups for applications in electronics. The nanoparticles were in ethanol, obtained by chemical reduction of $AgNO_3$ using triethylenetetramine as surfactant, according to a simple method developed by Frattini and coworkers. They prepared a diluted Ag nanoparticle solution by chemical reduction in alcoholic medium using aminosilanes as surfactants in different concentrations without the precipitation of particles. In this work, an analysis of the temperature influence on the precipitation of silver nanoparticles was carried out. Also, the nanoparticles were functionalized using triethylenetetramine in order to improve the adhesion between the epoxy resin and the filler.

5.6.13 SAMPLE PREPARATION FOR Ag NANOPARTICLE

The chemicals used during this research were of high purity. The triethylenetetramine (DEH 24) was supplied by Dow Chemical, whereas the ethanol and silver nitrate ($AgNO_3$) were obtained from Cicarelli and Fluka, respectively. were added to 200 ml of ethanol 300 mg of $AgNO_3$ in a glass container at 70°C, under constant stirring. The triethilenetetramine, previously dissolved in ethanol was dispersed into the AgNO3 alcoholic solution 1:10; $AgNO_3$: Amine ratio. The UV absorption spectra of these samples were obtained in spectrophotometer using ethanol as reference. The systems were precipitated by alcohol evaporation at 70°C for 2 h. The latter showed the precipitation of particles before the evaporation of the alcohol. As result, a solution of amine with precipitated silver
nanoparticles was achieved.

Quantities of materias used:

1.$AgNO_3$ - 300mg

2.C_2H_5OH - 200mg

3.Triethilenetetramine - 5ml

CHAPTER 6

RESULTS AND DISCUSSION

6.1 AFM STUDIES ON AMINE COATED AG NANOPARTICLES

We carried out controlled experiments to investigate the formation of Amine coated Ag NPs in the mixture a drop nanoparticle solution prepared in the ethanol is was deposited on mica substrate and allowed to evaporate. For AFM studied, we used a muscovite mica substrate, which was freshly cleaved by means of Scotch tape. AFM studied were carried out using Pico plus (Molecular Imaging, Agilent) AFM in ac (tapping) mode with an n-doped silicon tip

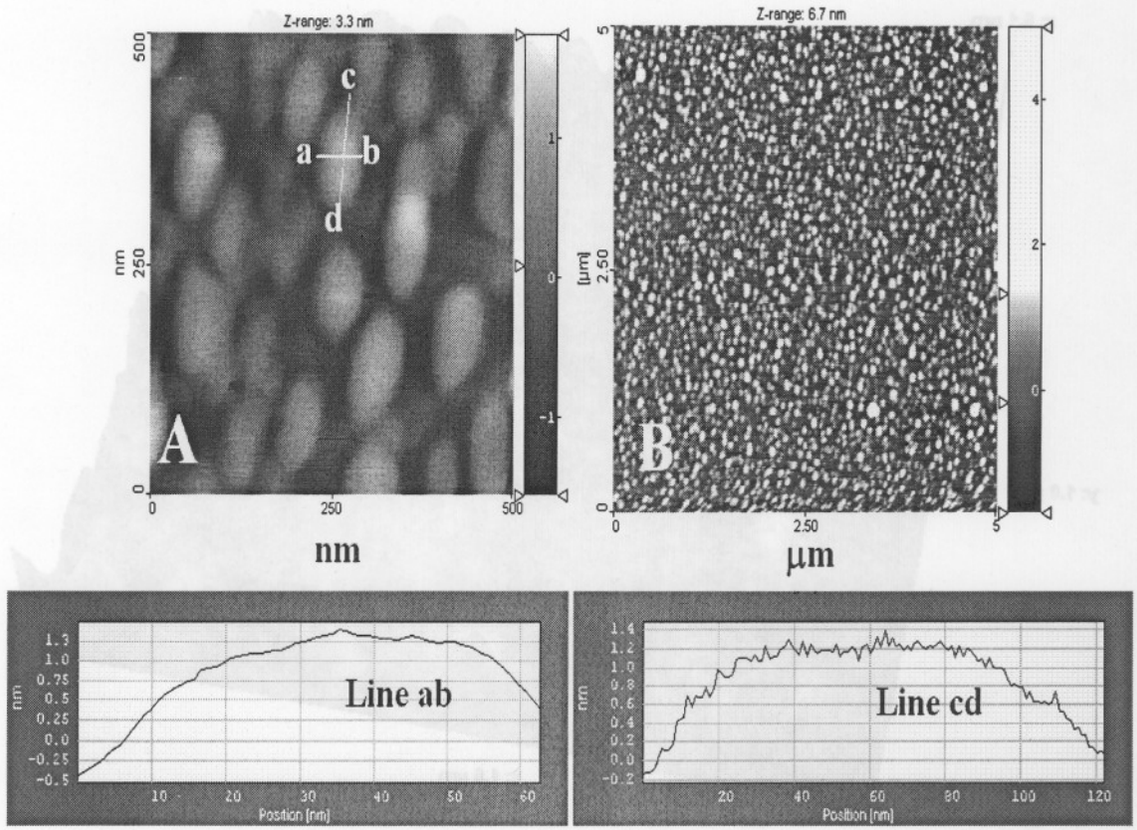

Fig. 6.1: (A) 500nm×500nm & (B) 5µ × 5µ shows the uniformly ellipsoid NPs

The images obtained were raw images, which were plane corrected using the scanning probe image processor (SPIP) software (Image Metrology, Denmark). Fig. 6.1 (A) shows the tapping mode AFM topographic image of nanoparticles dispersed on mica.

It shows a dense distribution of elliptical shaped nanoparticle on mica substrate. The line drawn on the image 6.1(A); ab & cd shows the dimension of individual elliptical shaped nanoparticle. Dimensions observed are 60nm and 120nm. In addition, a few bigger cluster are also observed in the topographic image. We carried out AFM phase imaging, as it is known to yield much sharper features than the topographic images. Fig 6.1 B shows the 5μ × 5μ AFM phase image of the NPs on mica. The fig 6.1 A shows the zoomed images where the well-resolved individual NPs can be clearly seen. The phase image confirms that most of the NPs are uniform size. Also Fig. 6.2 shows 1μ × 1μ AFM images of the ellipsoid amine coated Ag NPs where approximately uniform sized particle can be seen.

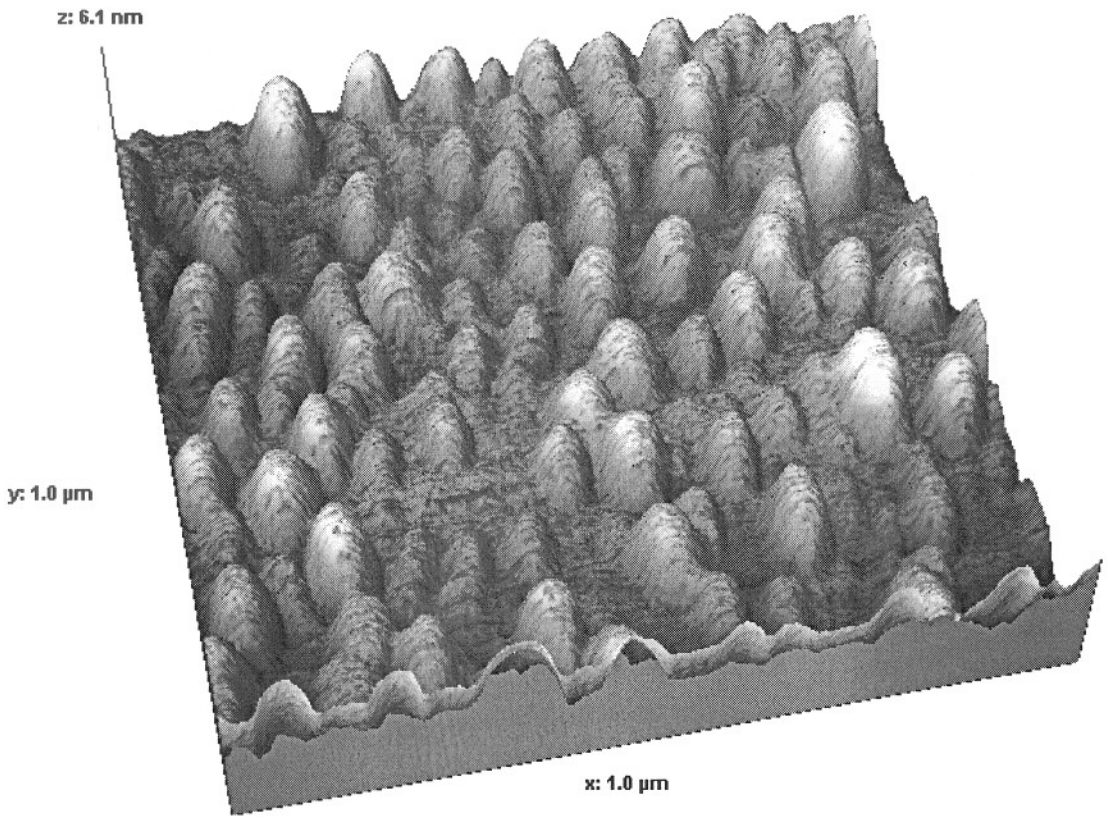

Fig. 6.2 : 1μ × 1μ AFM image of the Ag nanoparticels

6.2 SEM STUDIES FOR $SrFe_{12}O_{19}$

The Stontium ferrite sample annealed at 250^0C is an aggregate of nanoparticles that forms micron sized particles. In Fig 6.3, the FESEM image shows the low magnification image of Sr ferrite sample. The sample is formed at a relatively high temperature and hence there is sintering of the nanoparticles that is taking place in this case. Fig 6.4 shows the higher magnification image of a single particle, which confirms that these micron sized particles are indeed formed from nanoparticles of strontium ferrite.

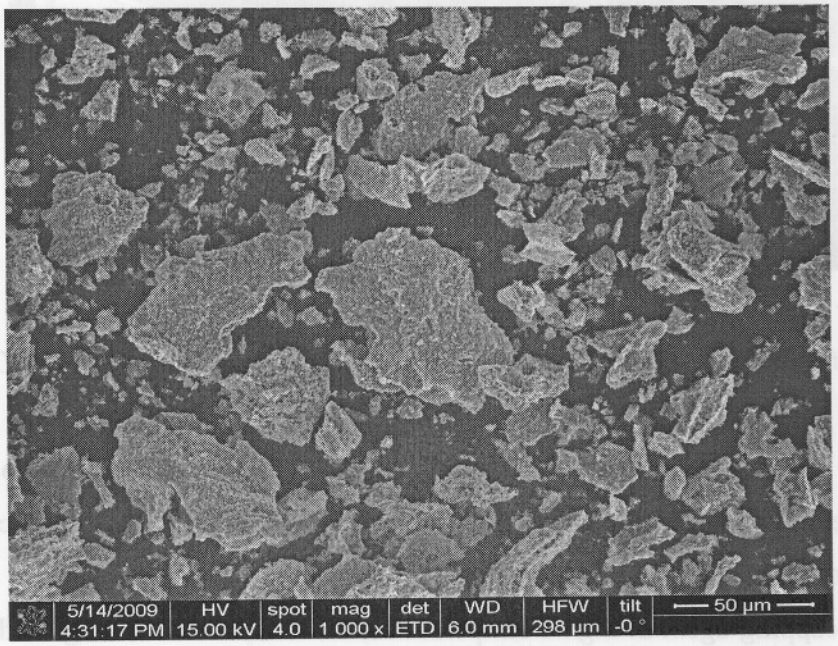

Fig 6.3: FESEM image of Sr ferrite Nps sintered at 250^0C

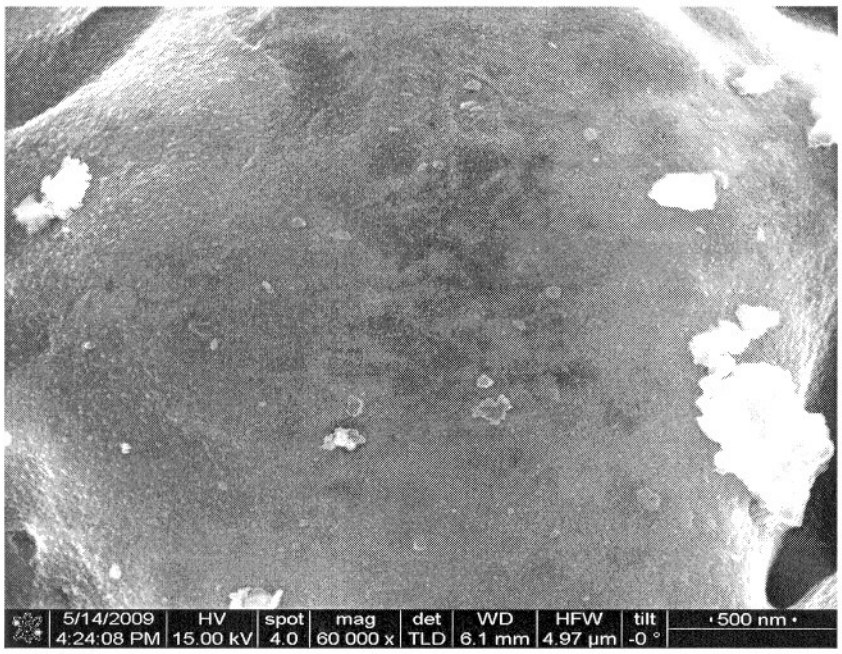

Fig. 6.4: Magnified FESEM image of Sr ferrite Nps sintered at 250^0C

The Sr ferrite sample annealed at 350^0C also is an aggregate of nanoparticles. In Fig 6.5, the lower magnification FESEM image shows micron sized particles and at higher magnification, the Fig 6.6 confirms that the particles are in fused state and due to the lack of capping agent at higher temperatures, the sample sinters to give these micro particles. The as-synthesized samples are analyzed with a field-emission scanning electron microscope (FE-SEM, FEI Nova-Nano SEM-600, Netherlands.

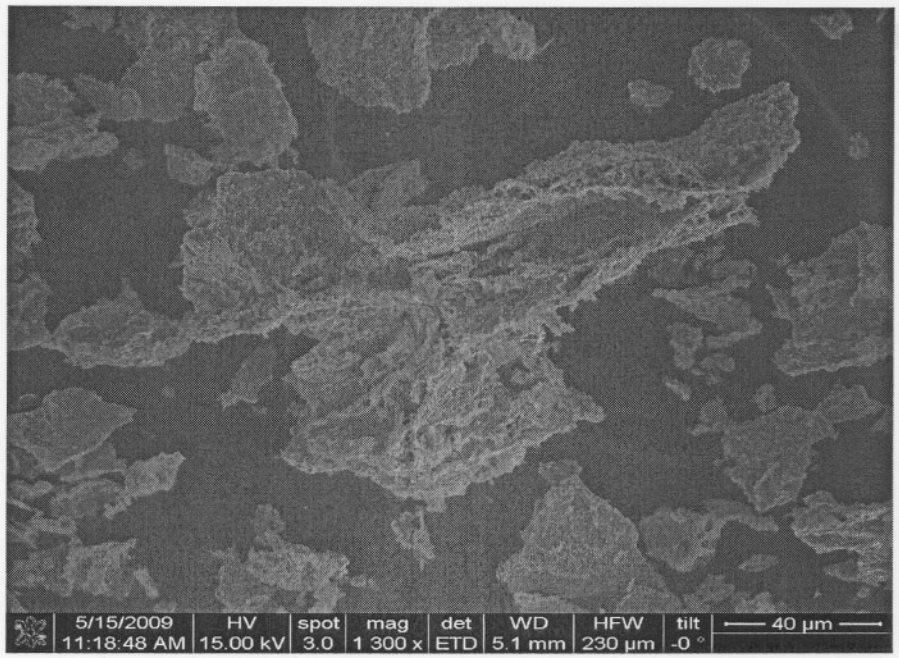

Fig. 6.5: FESEM image of Sr ferrite Nps sintered at 350^0C

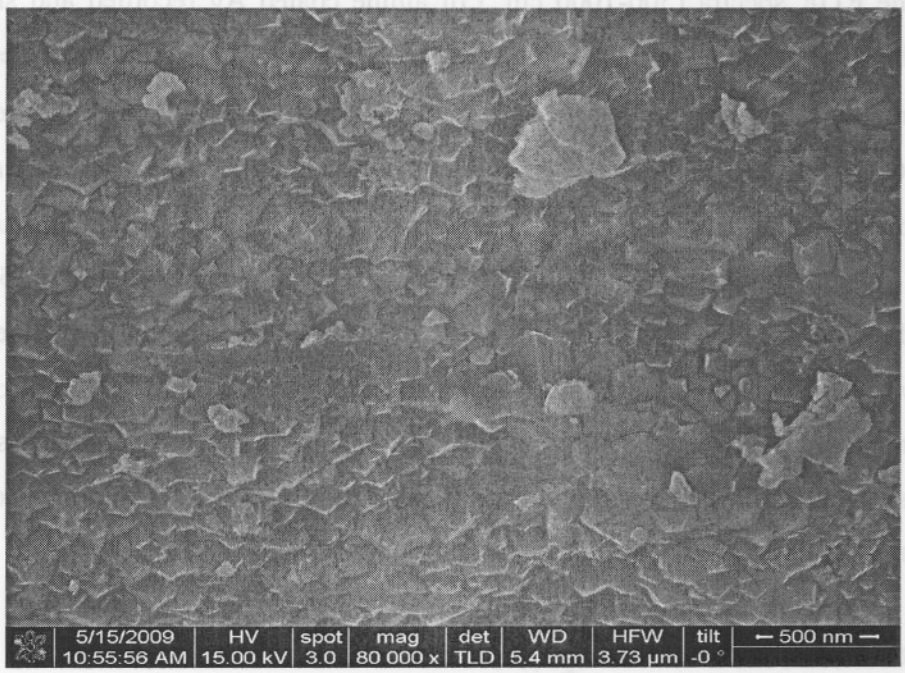

Fig. 6.6: Magnified FESEM image of Sr ferrite Nps sintered at 350^0C

6.3 FTIR ANALYSIS FOR Ag

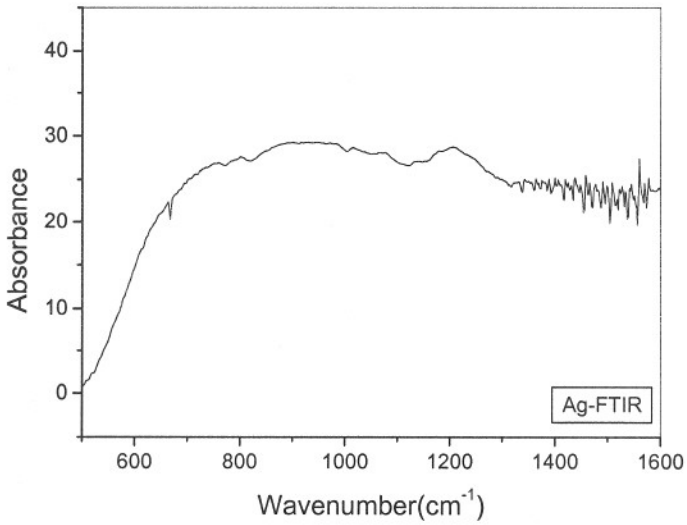

Fig.6.7: FTIR spectra of triethylenetetramine and Ag NPs

The FTIR spectra (500-1000 cm^{-1}) of amine coated Ag recorded and shows as figure. The band observed in the sample are characteristics of the vibration modes ν_a and ν_b of the methylene groups groups ($-CH_2-$). Also, the band 1120 and 1480 cm^{-1} are typical of the ν-C-OC, δs-CH_2 and δa-CH_3 vbrations. These vibration modes are invariant with respect to at the nanoparticles surface. Then, it is suggested that the alkyl chains adopt the stretched conformation irrespectievely.The spectra also show peaks at 1321, 1580 cm^{-1} attributed to ν-C-N, δ-NH_2 and respectively. The position and the intensity of these band change with respect to the pure amine. The variation of the $-NH_2$ and –NH infrared bands formation the links between the NPs, and the attachment of TEA to Ag can be easily seen into the spectra. The medium strong absorption frequency of the N-Ag appeared at 665 cm^{-1} along with the other absorption frequencies of amine.

6.4 FTIR ANALYSIS FOR $SrFe_{13}O_{19}$

The FTIR spectra obtained are presented below. The measurements were done using a Shimadzu FTIR spectrometer.

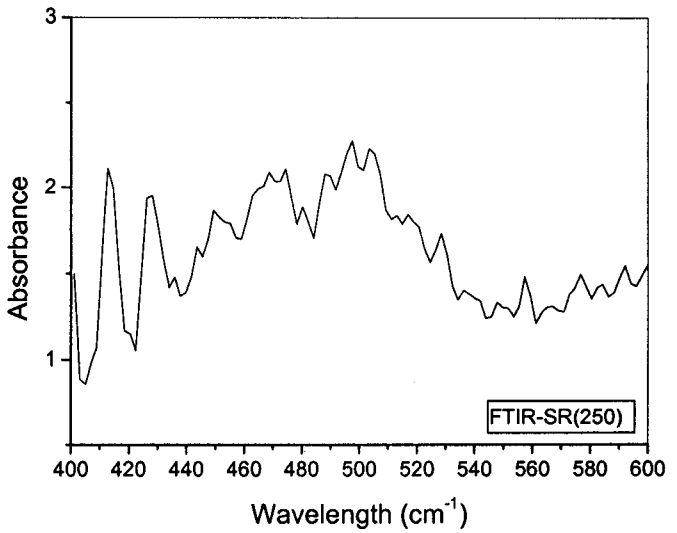

Fig. 6.8: FTIR spectra of $SrFe_{12}O_{19}$ (250^0c)

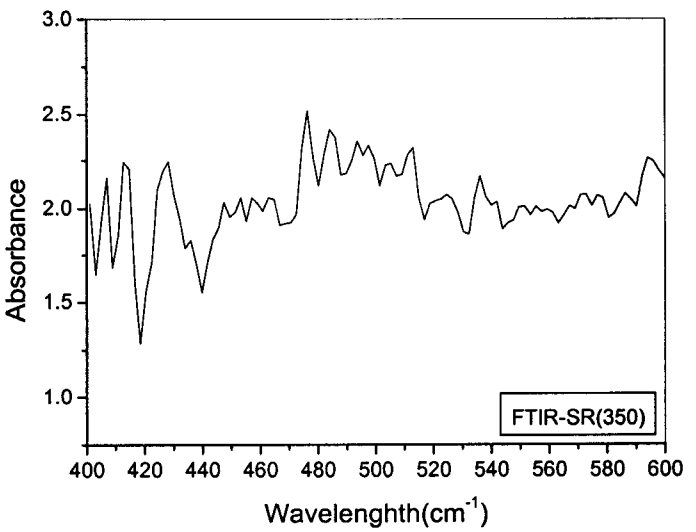

Fig.6.9: FTIR spectra of $SrFe_{12}O_{19}$ (350^0c)

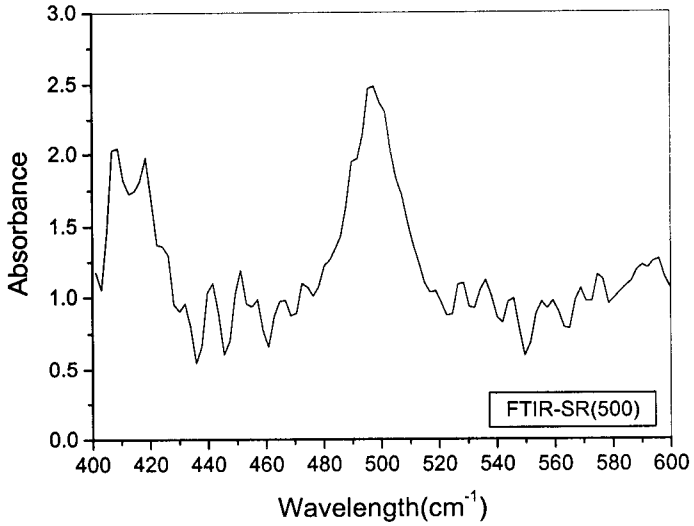

Fig.6.10: FTIR spectra of $SrFe_{13}O_{19}$ (500^0c)

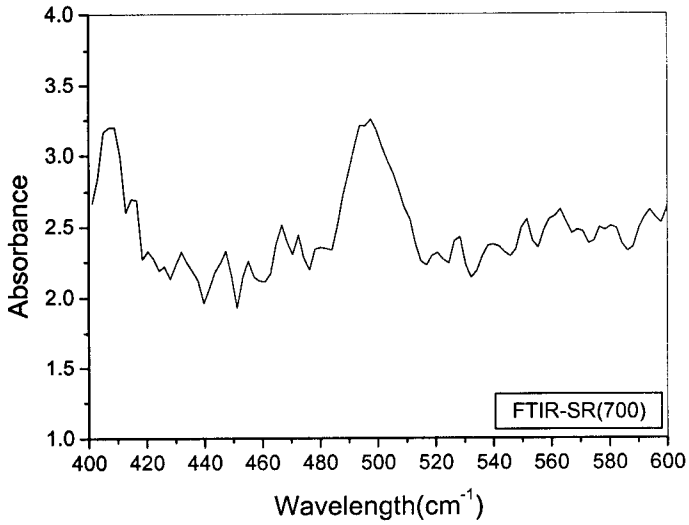

Fig.6.11: FTIR spectra of $SrFe_{13}O_{19}$ (700^0c)

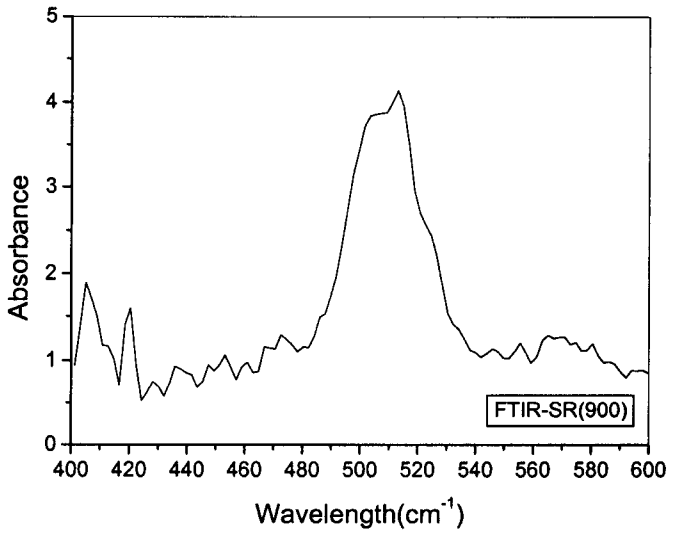

Fig.6.12: FTIR spectra of $SrFe_{13}O_{19}$ (900^0c)

The FTIR spectra of $SrFe_{13}O_{19}$ were recorded at different annealing temperatures. These spectra support the formation of desired Sr ferrite Nps as well as its stability at various temperatures. The characteristic absorption frequency of $SrFe_{13}O_{19}$ was recorded as medium intense band at 422 and 440 cm^{-1}. On heating the compound, the stability of this composite material retain up to 350^0C temperature (fig. 6.8 and 6.9), but on higher temperature, it looses the interaction between the associated atoms and the characteristic absorption frequency of ferrite gets disappeared as shown in figure 6.10, 6.11,and 6.12 respectively corresponding to the temperature values of 500, 700 and 900 ^0C.

6.5 UV-Vis Absorption measurements of Ag nanoparticles

The UV –Vis spectra for the particles were recorded using a Perkin Elmer lambda 35 spectrophotometer. Samples were taken in 1cm quartz cuvette and baseline and reference spectrum subtraction techniques were employed while taking the spectrum. The Ag nanoparticles prepared at 70^0C was labeled Ag1 and the one annealed to 90^0C was labeled Ag2. These were dissolved in ethanol for taking the absorption spectra.

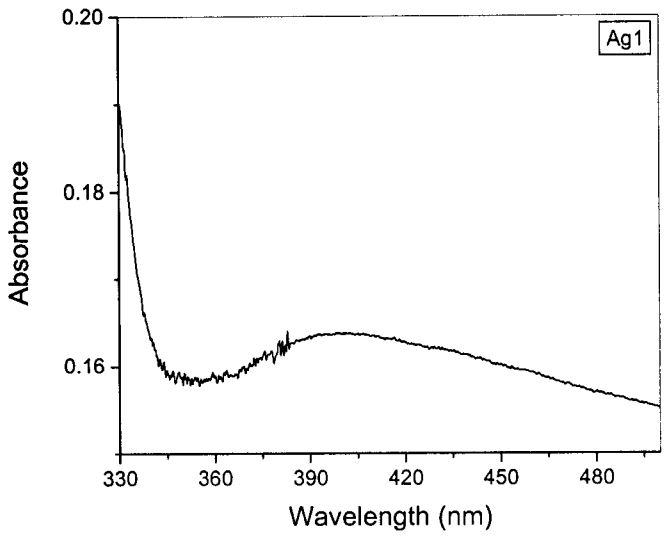

Fig.6.13: UV-VIS spectra for the amine coated Ag nanoparticles prepared.

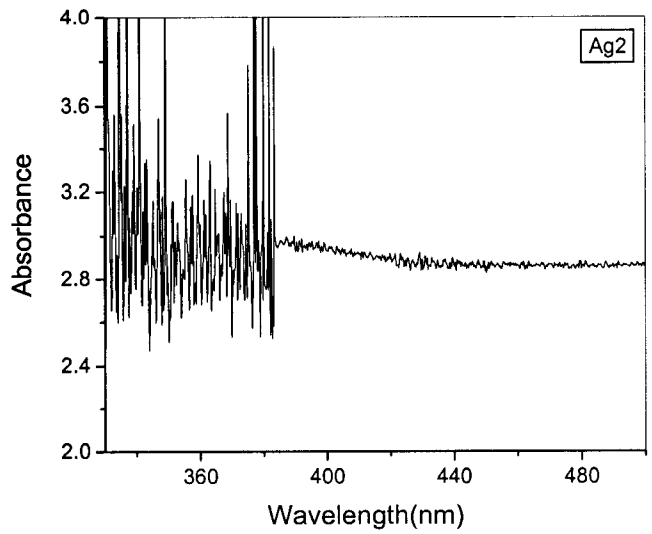

Fig.6.14: UV-VIS spectra for the amine coated Ag nanoparticles annealed at 90^0C.

The UV-Vis spectra of the un annealed Ag nanoparticles show a characteristic absorption at around 400nm, which corresponds to the surface plasmon absorption of the silver nanoparticles. This peak is attenuated in the case of the annealed sample, which can be correlated to precipitation happening at higher temperature.

6.6 UV-Vis Absorption measurements of Strontium nanoparticles

The UV-VIS spectra of the prepared nanoparticles are shown below (Fig. 6.15-6.20). The samples were dissolved in ethanol were taken in 1cm quartz cuvette and baseline and reference spectrum subtraction techniques were employed while taking the spectrum.

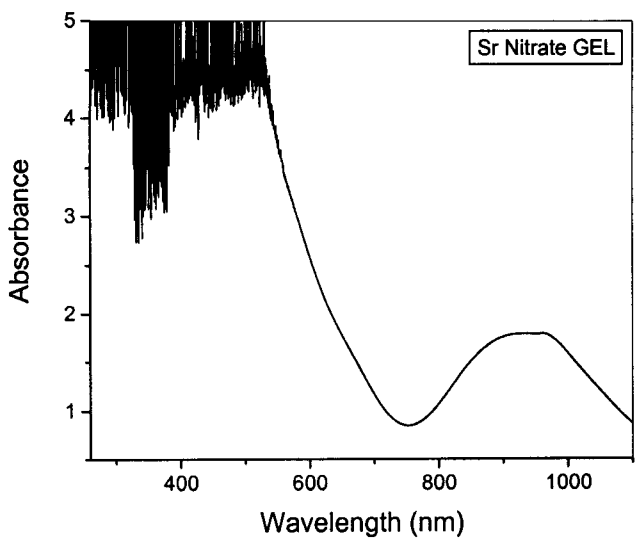

Fig 6.15 : Absorption spectra of the as prepared Strontium nanoparticles

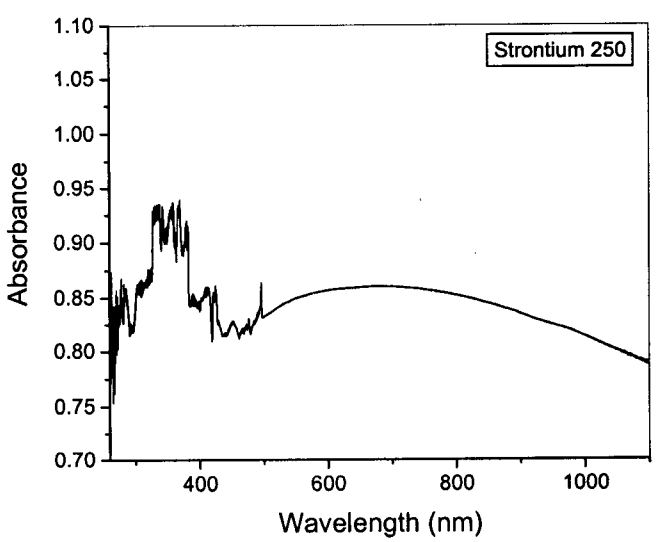

Fig 6.16 : Absorption spectra of the prepared Strontium nanoparticles annealed at 250^{0}C

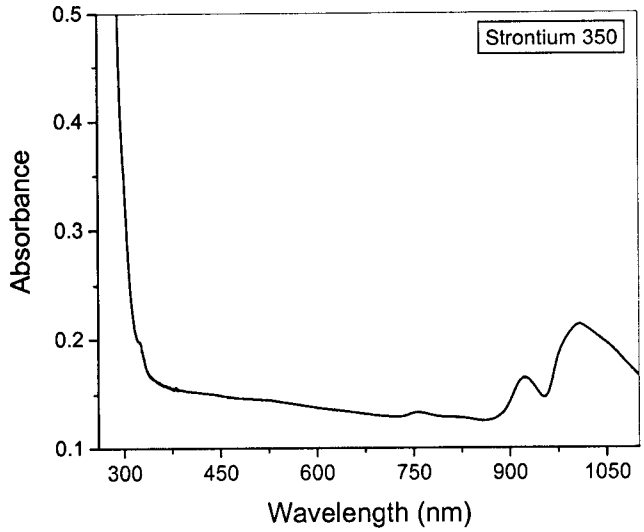

Fig 6.17 : Absorption spectra of the prepared Strontium nanoparticles annealed at 350^0C

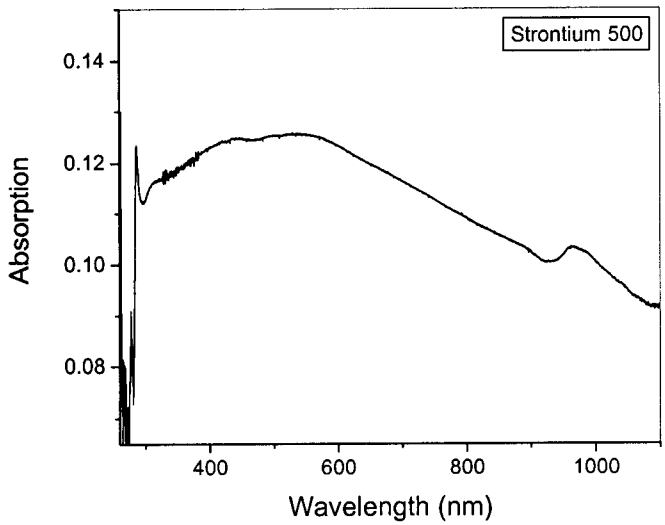

Fig 6.18 : Absorption spectra of the prepared Strontium nanoparticles annealed at 500^0C

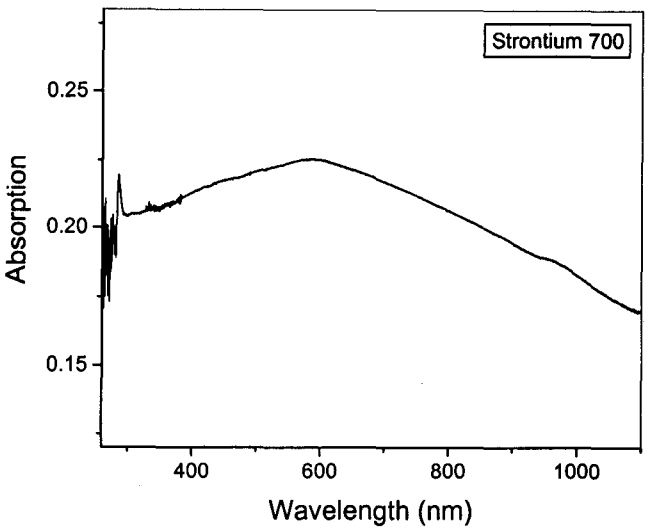

Fig 6.19 : Absorption spectra of the prepared Strontium nanoparticles annealed at 700^{0}C

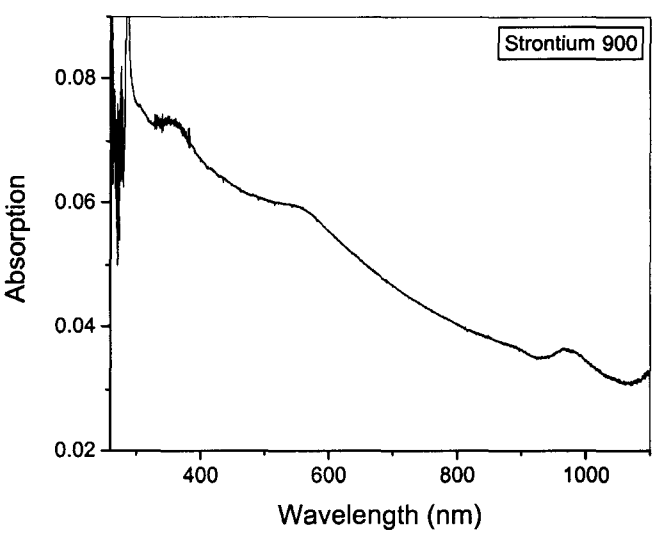

Fig 6.20 : Absorption spectra of the prepared Strontium nanoparticles annealed at 900^{0}C

6.7 Nonlinear Optical Properties:

Miniaturization of devices to micro and nano dimensions is an area of ongoing interest in the electronic and photonic industries. Occasionally this miniaturization can be the cornerstone for fabricating systems with enhanced efficiency and functionality of

metal ions and metal oxides in nano structures can lead to effects like enhancement of fluorescence and delayed/controlled excitonic recombination. In the present study we have found that the absorptive optical nonlinearities in amine coated Ag nanoparticle dispersions as well as in the strontium ferrite nanoparticles are of the fifth order (causing three-photon absorption), when excited using laser pulses of a few nanoseconds temporal duration.

Nanosecond laser pulses from a Q-Switched, frequency-doubled Nd:YAG laser (Minilite, Continum Inc.) were used for the z-scan experiment. In the z-scan experiment the laser beam is focused using a lens, and the sample is translated along the beam axis (z-axis) through the focal region over a distance several times that of the diffraction length. At each position z, the sample sees a different laser intensity, and the position dependent (ie, intensity-dependent) transmission is measured using an energy probe placed after the sample. Laser pulses were fired at a repetition rate of 1 Hz, and the data acquisition was automated. The low repetition rate is chosen to avoid accumulative thermal effects in the samples.

We performed open-aperture z-scan measrements on the samples with the intention of calculating their two-photon absorption coefficients. Interestingly, the nonlinear transmission is found to fit to a three-photon type absorption, rather than to a two-photon process. The experimental data fits well to the corresponding nonlinear transmission equation, given by

$$T = \frac{(1-R)^2 \exp(-\alpha L)}{\sqrt{\pi}\, p_0} \int_{-\infty}^{+\infty} \ln\left[\sqrt{1 + p_0^{\,2} \exp(-2t^2)} + p_0 \exp(-t^2)\right] dt$$

where 'R' is the surface reflectivity and p_0 is given by $2\gamma(1\text{-}R)^2 I_0^2 L$, where γ is the three photon absorption co-efficient and I is the on-axis peak intensity. α is the linear absorption coefficient. The z-scan and the input laser fluence vs. normalized transmittance curves for sample are shown in Figures 6.21-6.27.

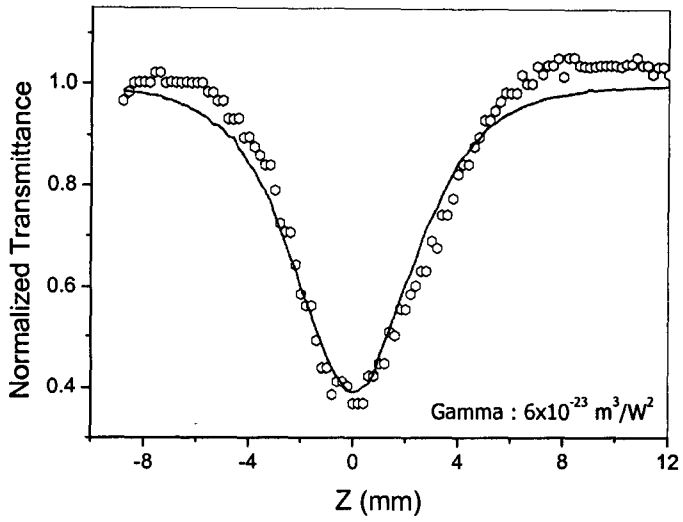

Fig 6.21 : Amine coated Ag nanoparticles excited with 100μJ laser pulses

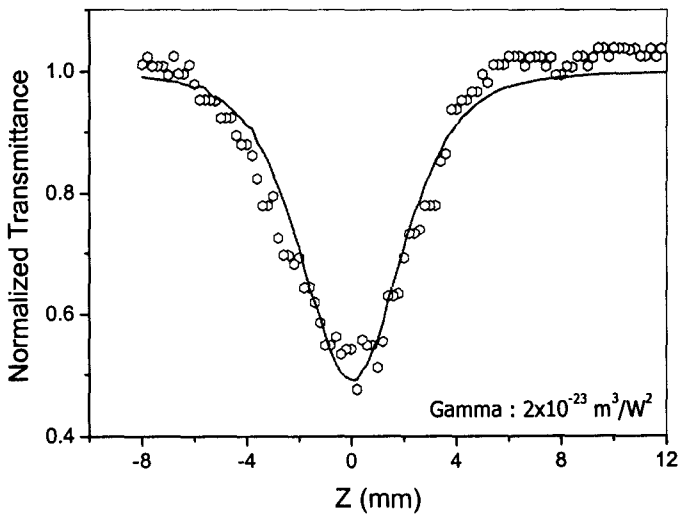

Fig 6.22 : Amine coated Ag nanoparticles excited with 120μJ laser pulses

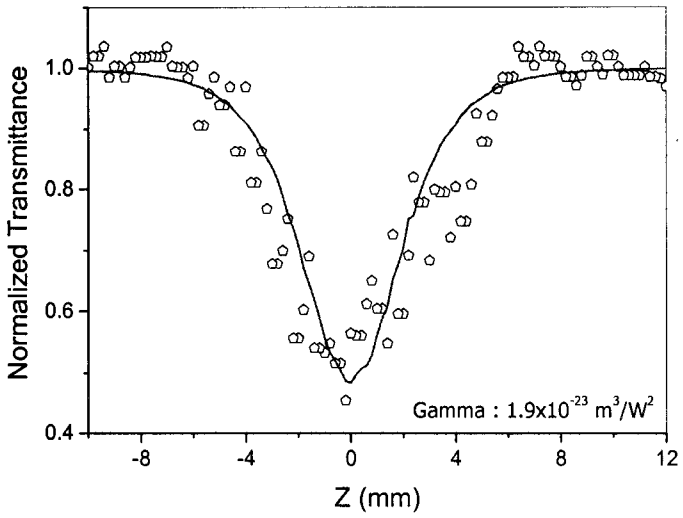

Fig 6.23 : Strontium Ferrite particles annealed at 250 ^{0}C excited with 130μJ laser pulses

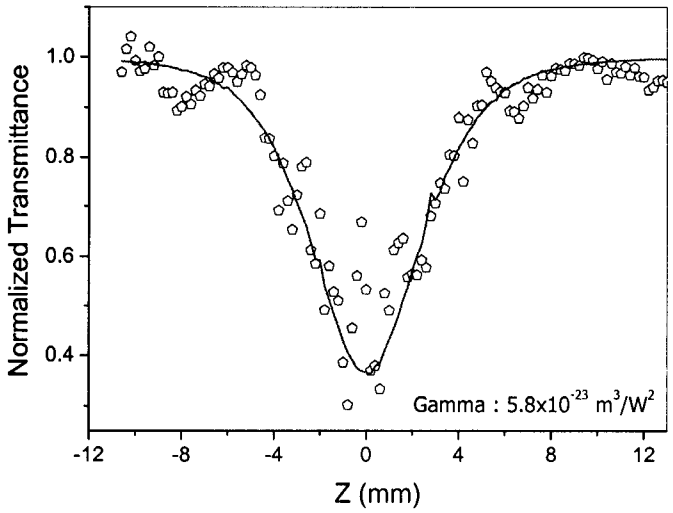

Fig 6.24 : Strontium Ferrite particles annealed at 350 ^{0}C excited with 130μJ laser pulses

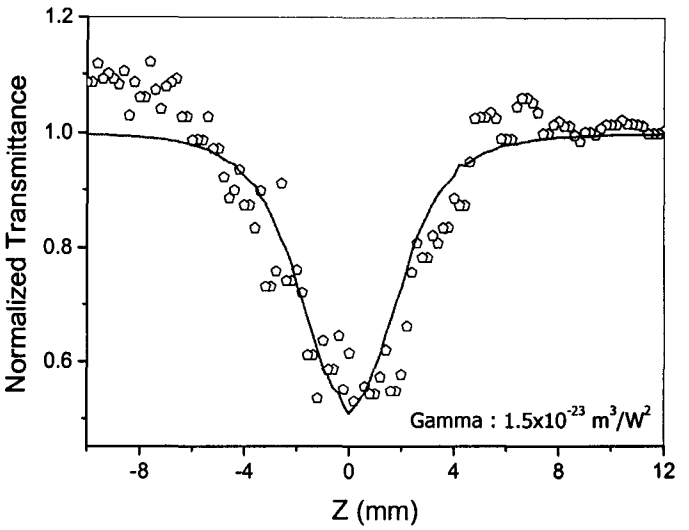

Fig 6.25 : Strontium Ferrite particles annealed at 500 ^{0}C excited with 130μJ laser pulses

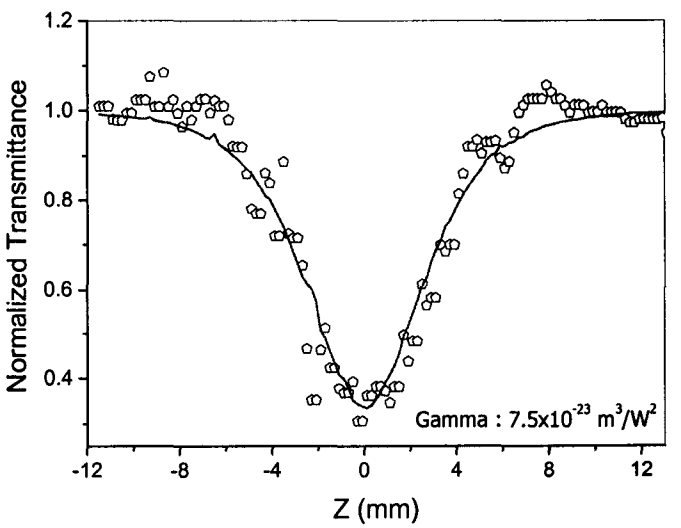

Fig 6.26 : Strontium Ferrite particles annealed at 700 ^{0}C excited with 130μJ laser pulses

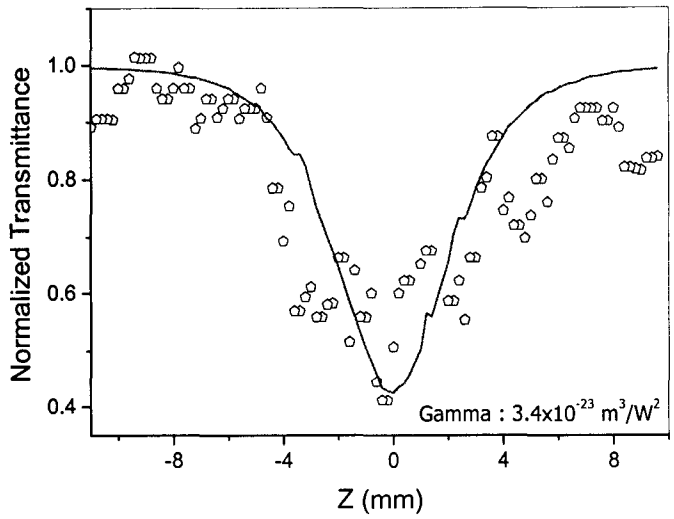

Fig 6.27 : Strontium Ferrite particles annealed at 900 ^{0}C excited with 130μJ laser pulses

It may be noted that the samples show an absorption at 266nm (two photon wavelength corresponding to the excitation wavelength). This absorption spectrum allows the possibilities for one photon, two photon and two-step absorptions to take place in the samples. Also, as the samples are metallic in nature, there is a high probability of additional photon absorption from the terminal level reached by the two-photon and two-step transitions. Hence the obtained three photon absorption seen in the samples can be described as an effective one, which arises from a combination of these processes.

In conclusion, the nonlinear optical transmission studies at 532 nm using 5 ns laser pulses on the amine coated Ag nanoparticles as well as on the strontium nanoparticles show the existence of an effective three-photon type absorption at this wavelength, which may be of potential application in fabricating optical limiting devices.

REFERENCES

1. Glass Science-Robert H.Doeremus,John Wiley and Sons Inc,1994.
2. Sol-Gel Technology For Thin Films,Fibers,Preforms,Electronics and Speciality Shapes,Lisa C.Klein,*Noyes publications.*
3. Sol-Gel Materials Chemistry and Applications – John D.Wright and Nico. A.J.M.Sommerdijk,*Gordon and Breach Science Publishers.*
4. Nano Scale Materials in Chemistry-kenneth j.Klabunde, *Wiley-Interscience*
5. Nanocomposite Science and Technology-Pilickel M.Ajayan,Linda S.Schadler, Paul.V.Braun,*Wiley-VCH verlag,(2003)*
6. Nano Materials:Synthesis,Properties and applications,A.S.Edelstein and R.C.Cmmarata,*Institute of Science Publishing*
7. Physics Of Nonlinear Optics-GuangS.He,Song H.Liu,*World Scientific.*
8. Kreibig,U; Vollumer.M,"optical Properties of Metal Clusters,Springer-verlag(1995).
9. Lee W.Tutt,Thomas F.Boggess,Prog.Quant Electr Vol.17,pp.299-338,(1993).
10. A.L.Stepnov,R.A.Ganeev,A.I.Ryasnyasky,t.Usmanov,Nucl.Instr.and Meth. In Phys.Rev.B 206,624-628(2003).
11. Brinker, C.J.; G.W. Scherer (1990). *Sol-Gel Science: The Physics and Chemistry of Sol-Gel Processing*. Academic Press.
12. Klein, L. (1994). *Sol-Gel Optics: Processing and Applications*. Springer Verlag.
13. Hench, L.L.; J.K. West (1990). "The Sol-Gel Process". *Chemical Reviews* **90**: 33.
14. *Sol-Gel Technologies for Glass Producers and Users* by Michel A. Aegerter and M. Mennig
15. *Sol-Gel Optics: Processing and Applications*, Lisa Klein, Springer Verlag (1994)
16. Askeland, Donald R.; Pradeep P. Phulé (2005). *The Science & Engineering of Materials* (5th ed.). Thomson-Engineering..
17. Mathews, F.L. & Rawlings, R.D. (1999). *Composite Materials: Engineering and Science*. Boca Raton: CRC Press. 18. Callister, Jr., William D. (2000).
18. *Materials Science and Engineering – An Introduction* (5th ed.). John Wiley and Sons.
19. Jerzy Chrusciel,ludomir Slusarski,Material Science,Vol.21.no.4(2004)
20. L.Stoch,M.S'roda,J.Molec.Struct.511.77,(1999).
21. U.Kreibig,L.Genzel.Sur.Sci.156,678,(1988)
22. Vinoy Thomas,Gijo Jose,Gin Jose,P.R.Biju,S.Rajagopal,N.V.Unnikrishnan,Sol-gel Sci.Tech.3,269(2005).
23. I.k.Battisha, Fizika.A11,2,61(70),(2002).
24. P.V.Kamat,M.Flumiani,G.V.Hartland,J.Phys.Chem B 102,3123,(1988).
25. Priya Saravanapavan,Larry L Hench ,J – Non Crystaline Solids 318,1-13(2003)
26. Maouro Epifani et al,J Material Chemistry 11,3326,(2001)
27. Ping Yang et al,Chemical Physical Letters,345,429, ,(2001).
28. J Serra et al,Journal Of Non Crystaline Solids332,20-27 (2003).
29. Cai Weiping and Zhang Lide J.Phys:Condens.Matter 9,7257-7267(1997).
30. Ying, Jackie. Nanostructured Materials. New York: Academic Press, 2001.
31. Aksay, I.A., Lange, F.F., Davis, B.I. (1983). "Uniformity of Al2O3-ZrO2 Composites by Colloidal Filtration". *J. Am. Ceram. Soc.* **66**: C-190.